6 RADIATION ANALYSIS AND NEUTRON DOSIMETRY

6.1 INTRODUCTION

This section describes a discrete ordinates (S_n) transport analysis performed for the Prairie Island Unit 2 reactor to determine the neutron radiation environment within the reactor pressure vessel and surveillance capsules. In this analysis, fast neutron exposure parameters in terms of fast neutron (E > 1.0 MeV) fluence and iron atom displacements (dpa) were established on a plant- and fuel-cycle-specific basis. An evaluation of the most recent dosimetry sensor set from Capsule N, withdrawn at the end of the 31st plant operating cycle, is provided. Comparison of the results from the dosimetry evaluations with the analytical predictions served to validate the plant-specific neutron transport calculations. These validated calculations subsequently form the basis for projections of the neutron exposure of the reactor pressure vessel for operating periods extending to 60 effective full-power years (EFPY).

The use of fast neutron (E > 1.0 MeV) fluence to correlate measured material property changes to the neutron exposure of the material has traditionally been accepted for the development of damage trend curves as well as for the implementation of trend curve data to assess the condition of the vessel. However, it has been suggested that an exposure model that accounts for differences in neutron energy spectra between surveillance capsule locations and positions within the vessel wall could lead to an improvement in the uncertainties associated with damage trend curves and improved accuracy in the evaluation of damage gradients through the reactor vessel wall.

Because of this potential shift away from a threshold fluence toward an energy-dependent damage function for data correlation, ASTM E853-18, "Standard Practice for Analysis and Interpretation of Light-Water Reactor Surveillance Neutron Exposure Results" [17], recommends reporting displacements per iron atom along with fluence (E > 1.0 MeV) to provide a database for future reference. The energy-dependent dpa function to be used for this evaluation is specified in ASTM E693-94, "Standard Practice for Characterizing Neutron Exposures in Iron and Low Alloy Steels in Terms of Displacements per Atom (DPA) , E706 (ID)" [18]. The application of the dpa parameter to the assessment of embrittlement gradients through the thickness of the reactor vessel wall has been promulgated in Revision 2 to Regulatory Guide 1.99, "Radiation Embrittlement of Reactor Vessel Materials" [1].

All of the calculations and dosimetry evaluations described in this section and in Appendix A were based on nuclear cross-section data derived from ENDF/B-VI. Furthermore, the neutron transport and dosimetry evaluation methodologies follow the guidance of Regulatory Guide 1.190, "Calculational and Dosimetry Methods for Determining Pressure Vessel Neutron Fluence" [19]. Additionally, the methods used to develop the calculated pressure vessel fluence are consistent with the NRC-approved methodology described in WCAP-18124-NP-A, "Fluence Determination with RAPTOR-M3G and FERRET" [20] and WCAP-18124-NP-A Revision 0 Supplement 1, "Fluence Determination with RAPTOR-M3G and FERRET – Supplement for Extended Beltline Materials" [21].

6.2 DISCRETE ORDINATES ANALYSIS

The arrangement of the surveillance capsules in the Prairie Island Unit 2 reactor vessel is shown in Figure 4-1. Six irradiation capsules attached to the thermal shield are included in the reactor design that constitutes the reactor vessel surveillance program. Capsules S, T, V, N, P, and R are located at azimuthal angles of

57°, 67°, 77°, 237°, 247°, and 257°, respectively. These full-core positions correspond to the following octant symmetric locations represented in Figure 6-1 and Figure 6-2: 13°, 23°, and 33° from the core cardinal axes. The stainless steel specimen containers are approximately 1-inch square in cross section and are approximately 63 inches in height. The containers are positioned axially such that the test specimens are centered on the core midplane, thus spanning the central five feet of the 12-foot high reactor core.

From a neutronic standpoint, the surveillance capsules and associated support structures are significant. The presence of these materials has a significant effect on both the spatial distribution of neutron exposure rate and the neutron spectrum in the vicinity of the capsules. However, the capsules are far enough apart that they do not interfere with one another. In order to determine the neutron environment at the test specimen location, the capsules themselves must be included in the analytical model.

In performing the fast neutron exposure evaluations for the Prairie Island Unit 2 reactor vessel and surveillance capsules, plant-specific 3D forward transport calculations were carried out to directly solve for the space- and energy-dependent neutron exposure rate, $\phi(r,\theta,z,E)$.

For the Prairie Island Unit 2 transport calculations, the model depicted in Figure 6-1 and Figure 6-2 was utilized. The model contained a representation of the reactor core, the reactor internals, the pressure vessel cladding and vessel wall, the insulation external to the pressure vessel, and the primary biological shield wall. This model formed the basis for the calculated results. In developing this analytical model, nominal design dimensions were generally employed for the various structural components. In addition, water temperatures, and hence, coolant densities in the reactor core and downcomer regions of the reactor were taken to be representative of full-power operating conditions. The coolant densities were treated on a fuel-cycle-specific basis. Table 6-10 contains the cycle-specific power levels, inlet coolant temperatures, and core average temperatures used in this analysis. The reactor core itself was treated as a homogeneous mixture of fuel, cladding, water, and miscellaneous core structures, such as fuel assembly grids, guide tubes, etc.

Section views of the model are shown in Figure 6-3 and Figure 6-4. The model extends radially from the centerline of the reactor core out to a location interior to the primary biological shield and over an axial span from an elevation more than five feet below the active fuel to more than five feet above the active fuel.

The RAPTOR-M3G model consisted of 186 radial mesh, 200 azimuthal mesh, and 435 axial mesh. Mesh sizes were chosen to assure that proper convergence of the inner iterations was achieved on a pointwise basis. The pointwise inner iteration flux convergence criterion utilized in the calculations was set at a value of 0.001.

The core power distributions used in the plant-specific transport analysis for the first 32 fuel cycles at Prairie Island Unit 2 included cycle-dependent fuel assembly initial enrichments, burnups, radial and axial power distributions. Actual operating characteristics through Cycle 32 have been evaluated; projections beyond Cycle 32 were based on Cycle 32 spatial power distributions, water temperatures, and reactor power level with a 10% bias on the peripheral and re-entrant corner relative powers as directed by Xcel Energy. The cycle-dependent fuel assembly initial enrichments, burnups, radial and axial power distributions were used to develop spatial- and energy-dependent core source distributions averaged over each individual fuel cycle. Therefore, the results from the neutron transport calculations provided data in terms of fuel-cycle-averaged neutron exposure rate, which when multiplied by the appropriate fuel cycle length, generated the

incremental fast neutron exposure for each fuel cycle. In constructing these core source distributions, the energy distribution of the source was based on an appropriate fission split for uranium and plutonium isotopes based on the initial enrichment and burnup history of individual fuel assemblies. From these assembly-dependent fission splits, composite values of energy release per fission, neutron yield per fission, and fission spectrum were determined.

All of the transport calculations supporting this analysis were carried out using the RAPTOR-M3G discrete ordinates code and the BUGLE-96 cross-section library, as described in Westinghouse Report WCAP-18124-NP-A [20]. The BUGLE-96 library provides a coupled 47-neutron, 20-gamma-group cross-section data set produced specifically for light-water reactor (LWR) applications. In these analyses, anisotropic scattering was treated with a P_3 Legendre expansion, and angular discretization was modeled with an S_{16} order of angular quadrature. Energy- and space-dependent core power distributions, as well as system operating temperatures, were treated on a fuel-cycle-specific basis.

Results of the discrete ordinates transport analyses pertinent to the surveillance capsule evaluations are provided in Table 6-1 through Table 6-3. In Table 6-1, the calculated fast neutron fluence rate and fluence (E > 1.0 MeV) are provided at the geometric center of the capsules, as a function of irradiation time for the Prairie Island Unit 2 reactor. Similar data presented in terms of iron atom displacement rate and integrated iron atom displacements are given in Table 6-2. Note that the fluence values for the surveillance capsules are different than the previous report. This is largely due to the updated methodology used in determining the fluence values. The previous values were determined using 2D adjoint transport methods. This analysis employed 3D forward transport methods.

In Table 6-3, lead factors associated with surveillance capsules are provided as a function of operating time for the Prairie Island Unit 2 reactor. The lead factor is defined as the ratio of the neutron fluence (E > 1.0 MeV) at the geometric center of the surveillance capsule to the maximum neutron fluence (E > 1.0 MeV) at the pressure vessel clad/base metal interface.

Neutron exposure data pertinent to the pressure vessel clad/base metal interface are given in Table 6-4 and Table 6-5 for neutron fluence (E > 1.0 MeV) rate and fluence (E > 1.0 MeV), respectively, and in Table 6-6 and Table 6-7 for dpa/s and dpa, respectively. In each case, the data are provided for each operating cycle of the Prairie Island Unit 2 reactor. Neutron fluence (E > 1.0 MeV) and dpa are also projected to future operating times extending to 60 EFPY. The vessel exposure data are presented in terms of the maximum exposure experienced by the pressure vessel at azimuthal angles of 0°, 15°, 30°, and 45°, and at the azimuthal location providing the maximum exposure relative to the core cardinal axes.

In Table 6-8 and Table 6-9, maximum projected fluences and dpa, respectively, of the various pressure vessel materials are given.

These data tabulations include both plant- and fuel-cycle-specific calculated neutron exposures at the end of Cycle 32 and projections to 60 EFPY. The projections beyond Cycle 32 were based on Cycle 32 spatial power distributions, water temperatures, and reactor power level with a 10% bias on the peripheral and re-entrant corner assemblies.

6.3 NEUTRON DOSIMETRY

The validity of the calculated neutron exposures reported in Section 6.2 is demonstrated by a direct comparison against the measured sensor reaction rates and a least-squares evaluation performed for each of the capsule dosimetry sets. However, since the neutron dosimetry measurement data merely serve to validate the calculated results, only the direct comparison of measured-to-calculated results for the most recent surveillance capsule removed from Prairie Island Unit 2, Capsule N, is provided in this section of the report. For completeness, the assessment of all measured dosimetry removed from Prairie Island Unit 2 up to date based on both direct and least-squares evaluation comparisons is documented in Appendix A.

The direct comparison of measured versus calculated fast neutron threshold reaction rates for the sensors from Capsule N, that was withdrawn from the reactor at the conclusion of Cycle 31, is summarized below.

Reaction	Reaction Rate (rps/atom)		M/C
	Measured	Calculated	
^{63}Cu (n,α) ^{60}Co	3.47E-17	4.23E-17	0.82
^{54}Fe (n,p) ^{54}Mn	3.56E-15	4.57E-15	0.78
^{58}Ni (n,p) ^{58}Co	6.28E-15	6.30E-15	1.00
^{238}U(Cd) (n,f) ^{137}Cs	2.23E-14	2.25E-14	0.99
^{237}Np(Cd) (n,f) ^{137}Cs	1.85E-13	1.82E-13	1.02
^{59}Co (n,γ) ^{60}Co	3.02E-12	3.98E-12	0.76
Average of M/C Results			0.92
Standard Deviation (%)			12.2

The measured-to-calculated (M/C) reaction rate ratios for the Capsule N threshold reactions range from 0.78 to 1.02, and the average M/C ratio is 0.92 ± 12.2% (1σ). This direct comparison falls within the ± 20% criterion specified in Regulatory Guide 1.190. This comparison validates the current analytical results described in Section 6.2; therefore, the calculations are deemed applicable for Prairie Island Unit 2.

6.4 CALCULATIONAL UNCERTAINTIES

The uncertainty associated with the calculated neutron exposure of the Prairie Island Unit 2 surveillance capsule and reactor pressure vessel is based on the recommended approach provided in Regulatory Guide 1.190. In particular, the qualification of the methodology was carried out in the following four stages:

1. **Simulator Benchmark Comparisons:** Comparisons of calculations with measurements from simulator benchmarks, including the Pool Critical Assembly (PCA) simulator at the Oak Ridge National Laboratory (ORNL) and the VENUS-1 Experiment.

2. **Operating Reactor and Calculational Benchmarks:** Comparisons of calculations with surveillance capsule and reactor cavity measurements from the H.B. Robinson power reactor

benchmark experiment. Also considered are comparisons of calculations to results published in the NRC fluence calculation benchmark.

3. **Analytic Uncertainty Analysis:** An analytical sensitivity study addressing the uncertainty components resulting from important input parameters applicable to the plant-specific transport calculations used in the neutron exposure assessments.

4. **Plant-Specific Benchmarking:** Comparisons of the plant-specific calculations with all available dosimetry results from the Prairie Island Unit 2 surveillance program.

The first phase of the methods qualification (simulator benchmark comparisons) addressed the adequacy of basic transport calculation and dosimetry evaluation techniques and associated cross-sections. This phase, however, did not test the accuracy of commercial core neutron source calculations nor did it address uncertainties in operational or geometric variables that impact power reactor calculations. The second phase of the qualification (operating reactor and calculational benchmark comparisons) addressed uncertainties in these additional areas that are primarily methods-related and would tend to apply generically to all fast neutron exposure evaluations. The third phase of the qualification (analytical sensitivity study) identified the potential uncertainties introduced into the overall evaluation due to calculational methods approximations, as well as to a lack of knowledge relative to various plant-specific input parameters. The overall calculational uncertainty applicable to the Prairie Island Unit 2 analysis was established from results of these three phases of the methods qualification.

The fourth phase of the uncertainty assessment (comparisons with Prairie Island Unit 2 measurements) was used solely to demonstrate the validity of the transport calculations and to confirm the uncertainty estimates associated with the analytical results. The comparison was used only as a check and was not used in any way to modify the calculated surveillance capsule and pressure vessel neutron exposures described in Section 6.2. As such, the validation of the Prairie Island Unit 2 analytical model based on the measured plant dosimetry is completely described in Appendix A.

The following summarizes the uncertainties developed from the first three phases of the methodology qualification. Additional information pertinent to these evaluations is provided in Westinghouse Report WCAP-18124-NP-A [20].

Description	**Capsule and Vessel IR**
Simulator Benchmark Comparisons	3%
Operating Reactor and Calculational Benchmarks	5%
Analytic Uncertainty Analysis	11%
Additional Uncertainty for Factors not Explicitly Evaluated	5%
Net Calculational Uncertainty	**13%**

The net calculational uncertainty was determined by combining the individual components in quadrature. Therefore, the resultant uncertainty was treated as random, and no systematic bias was applied to the analytical results. The plant-specific measurement comparisons described in Appendix A support these uncertainty assessments for Prairie Island Unit 2.

The NRC-issued Safety Evaluation for WCAP-18124-NP-A appears in Section A of [20]. The NRC identified two "Limitations and Conditions" associated with the application of RAPTOR-M3G and FERRET, which are reproduced here for convenience:

1. Applicability of WCAP-18124-NP, Revision 0 is limited to the RPV region near the active height of the core based on the uncertainty analysis performed and the measurement data provided. Additional justification should be provided via additional benchmarking, fluence sensitivity analysis to the response parameters of interest (e.g., pressure-temperature limits, material stress/strain), margin assessment, or a combination thereof, for applications of the method to components including, but not limited to, the RPV upper circumferential weld and the reactor coolant system inlet and outlet nozzles and reactor vessel internal components.

2. Least squares adjustment is acceptable if the adjustments to the M/C ratios and to the calculated spectra values are within the assigned uncertainties of the calculated spectra, the dosimetry measured reaction rates, and the dosimetry reaction cross sections. Should this not be the case, the user should re-examine both measured and calculated values for possible errors. If errors cannot be found, the particular values causing the discrepancy should be disqualified.

The neutron exposure values applicable to the surveillance capsules and the maximum reactor pressure vessel neutron exposure values used to derive the surveillance capsule lead factors are completely covered by the benchmarking and uncertainty analyses in WCAP-18124-NP-A. Note, however, that this report does contain neutron exposure values for materials that are outside the qualification basis of WCAP-18124-NP-A (i.e. "extended beltline" materials). For the materials considered to be located in the extended beltline region, a comprehensive analytical uncertainty analysis applicable to the Prairie Island Unit 2 RPV extended beltline region is summarized in WCAP-18124-NP-A, Revision 0, Supplement 1-NP-A [21]. All RPV extended beltline calculations for Prairie Island Unit 2 were performed using the WCAP-18124-NP-A, Revision 0, Supplement 1-NP-A methodology.

Limitation # 2 applies in situations where the least-squares analysis is used to *adjust* the calculated values of neutron exposure. In this report, the least-squares analysis is provided only as a supplemental check on the results of the dosimetry evaluation. The least-squares analysis was *not* used to modify the calculated surveillance capsule or reactor pressure vessel neutron exposure. Therefore, Limitation # 2 does not apply.

Table 6-1 Calculated Maximum Fast (E > 1.0 MeV) Neutron Fluence Rate and Fluence at Surveillance Capsule Locations

Cycle	Cycle Length (EFPY)	Total Time (EFPY)	Fluence Rate (n/cm^2-s)		
			13°	23°	33°
1	1.39	1.39	1.36E+11	7.79E+10	7.48E+10
2	0.87	2.26	1.45E+11	8.68E+10	8.40E+10
3	0.89	3.15	1.50E+11	8.91E+10	8.71E+10
4	0.98	4.13	1.51E+11	8.84E+10	8.46E+10
5	0.92	5.05	1.58E+11	9.03E+10	8.74E+10
6	0.99	6.04	1.49E+11	7.93E+10	7.12E+10
7	1.01	7.05	1.43E+11	8.20E+10	7.62E+10
8	0.90	7.95	1.25E+11	7.61E+10	7.06E+10
9	0.85	8.80	1.82E+11	9.43E+10	8.63E+10
10	0.92	9.71	1.58E+11	9.42E+10	9.12E+10
11	1.09	10.80	1.48E+11	8.63E+10	8.25E+10
12	1.08	11.88	1.26E+11	8.51E+10	8.57E+10
13	1.26	13.15	9.40E+10	6.46E+10	6.25E+10
14	1.33	14.47	8.76E+10	6.11E+10	6.11E+10
15	1.38	15.86	8.99E+10	5.67E+10	5.52E+10
16	1.38	17.24	9.43E+10	7.13E+10	6.69E+10
17	1.55	18.78	8.79E+10	6.56E+10	5.87E+10
18	1.48	20.27	8.37E+10	5.78E+10	5.47E+10
19	1.30	21.57	8.10E+10	6.50E+10	6.10E+10
20	1.56	23.13	9.53E+10	6.84E+10	6.04E+10
21	1.52	24.64	8.87E+10	6.30E+10	5.54E+10
22	1.48	26.12	8.86E+10	6.17E+10	5.81E+10
23	1.37	27.49	8.95E+10	6.00E+10	5.77E+10
24	1.72	29.21	8.69E+10	5.77E+10	5.48E+10
25	1.44	30.66	8.60E+10	5.94E+10	5.99E+10
26	1.68	32.34	8.87E+10	5.82E+10	5.74E+10
27	1.24	33.58	9.32E+10	6.10E+10	6.06E+10
28	1.65	35.24	9.35E+10	6.04E+10	5.70E+10
29	1.64	36.88	9.36E+10	6.14E+10	6.10E+10
30	1.85	38.73	8.86E+10	6.10E+10	6.21E+10
31	1.91	40.64	9.20E+10	5.91E+10	5.77E+10
32	1.95	42.59	9.15E+10	6.04E+10	6.01E+10

Table 6-1 Calculated Maximum Fast (E > 1.0 MeV) Neutron Fluence Rate and Fluence at Surveillance Capsule Locations (cont.)

Cycle	Total Time (EFPY)	Fluence (n/cm^2)					
		V (13°)	T (23°)	R (13°)	P (23°)	N (33°)	S (33°)
1	1.39	5.98E+18	3.42E+18	5.98E+18	3.42E+18	3.29E+18	3.29E+18
2	2.26		5.81E+18	9.97E+18	5.81E+18	5.59E+18	5.59E+18
3	3.15		8.30E+18	1.42E+19	8.30E+18	8.03E+18	8.03E+18
4	4.13		1.10E+19	1.88E+19	1.10E+19	1.06E+19	1.06E+19
5	5.05			2.34E+19	1.37E+19	1.32E+19	1.32E+19
6	6.04			2.81E+19	1.61E+19	1.54E+19	1.54E+19
7	7.05			3.26E+19	1.88E+19	1.78E+19	1.78E+19
8	7.95			3.62E+19	2.09E+19	1.98E+19	1.98E+19
9	8.80			4.11E+19	2.34E+19	2.22E+19	2.22E+19
10	9.71				2.62E+19	2.48E+19	2.48E+19
11	10.80				2.91E+19	2.76E+19	2.76E+19
12	11.88				3.20E+19	3.05E+19	3.05E+19
13	13.15				3.46E+19	3.30E+19	3.30E+19
14	14.47				3.72E+19	3.56E+19	3.56E+19
15	15.86				3.96E+19	3.80E+19	3.80E+19
16	17.24				4.27E+19	4.09E+19	4.09E+19
17	18.78					4.38E+19	4.38E+19
18	20.27					4.64E+19	4.64E+19
19	21.57					4.89E+19	4.89E+19
20	23.13					5.18E+19	5.18E+19
21	24.64					5.45E+19	5.45E+19
22	26.12					5.72E+19	5.72E+19
23	27.49					5.97E+19	5.97E+19
24	29.21					6.27E+19	6.27E+19
25	30.66					6.54E+19	6.54E+19
26	32.34					6.84E+19	6.84E+19
27	33.58					7.08E+19	7.08E+19
28	35.24					7.38E+19	7.38E+19
29	36.88					7.69E+19	7.69E+19
30	38.73					8.06E+19	8.06E+19
31	40.64					8.41E+19	8.41E+19
32	42.59						8.77E+19
	48						9.90E+19
	51						1.05E+20
	54						1.11E+20
	60						1.24E+20

Note:
1. Values beyond Cycle 32 are projected based on Cycle 32 with a 10% bias on the peripheral and re-entrant corner assemblies.

Table 6-2 Calculated Iron Atom Displacement Rate and Iron Atom Displacements at Surveillance Capsule Locations

Cycle	Cycle Length (EFPY)	Total Time (EFPY)	Iron Atom Displacement Rate (dpa/s)		
			13-degree	23-degree	33-degree
1	1.39	1.39	2.49E-10	1.37E-10	1.32E-10
2	0.87	2.26	2.66E-10	1.52E-10	1.48E-10
3	0.89	3.15	2.75E-10	1.56E-10	1.54E-10
4	0.98	4.13	2.77E-10	1.55E-10	1.49E-10
5	0.92	5.05	2.90E-10	1.58E-10	1.54E-10
6	0.99	6.04	2.73E-10	1.39E-10	1.25E-10
7	1.01	7.05	2.62E-10	1.44E-10	1.34E-10
8	0.90	7.95	2.29E-10	1.33E-10	1.24E-10
9	0.85	8.80	3.34E-10	1.66E-10	1.52E-10
10	0.92	9.71	2.89E-10	1.65E-10	1.61E-10
11	1.09	10.80	2.70E-10	1.51E-10	1.45E-10
12	1.08	11.88	2.30E-10	1.49E-10	1.51E-10
13	1.26	13.15	1.71E-10	1.13E-10	1.10E-10
14	1.33	14.47	1.59E-10	1.06E-10	1.07E-10
15	1.38	15.86	1.63E-10	9.88E-11	9.69E-11
16	1.38	17.24	1.71E-10	1.24E-10	1.17E-10
17	1.55	18.78	1.59E-10	1.14E-10	1.03E-10
18	1.48	20.27	1.52E-10	1.00E-10	9.59E-11
19	1.30	21.57	1.47E-10	1.13E-10	1.07E-10
20	1.56	23.13	1.73E-10	1.19E-10	1.06E-10
21	1.52	24.64	1.61E-10	1.09E-10	9.72E-11
22	1.48	26.12	1.61E-10	1.07E-10	1.02E-10
23	1.37	27.49	1.62E-10	1.04E-10	1.01E-10
24	1.72	29.21	1.58E-10	1.00E-10	9.61E-11
25	1.44	30.66	1.56E-10	1.03E-10	1.05E-10
26	1.68	32.34	1.61E-10	1.01E-10	1.01E-10
27	1.24	33.58	1.69E-10	1.06E-10	1.06E-10
28	1.65	35.24	1.70E-10	1.05E-10	9.99E-11
29	1.64	36.88	1.70E-10	1.07E-10	1.07E-10
30	1.85	38.73	1.61E-10	1.06E-10	1.09E-10
31	1.91	40.64	1.67E-10	1.03E-10	1.01E-10
32	1.95	42.59	1.66E-10	1.05E-10	1.05E-10

Table 6-2 Calculated Iron Atom Displacement Rate and Iron Atom Displacements at Surveillance Capsule Locations (cont.)

Cycle	Total Time (EFPY)	Iron Atom Displacements (dpa)					
		V (13°)	T (23°)	R (13°)	P (23°)	N (33°)	S (33°)
1	1.39	1.10E-02	6.00E-03	1.10E-02	6.00E-03	5.79E-03	5.79E-03
2	2.26		1.02E-02	1.83E-02	1.02E-02	9.86E-03	9.86E-03
3	3.15		1.46E-02	2.60E-02	1.46E-02	1.42E-02	1.42E-02
4	4.13		1.93E-02	3.45E-02	1.93E-02	1.88E-02	1.88E-02
5	5.05			4.29E-02	2.39E-02	2.32E-02	2.32E-02
6	6.04			5.15E-02	2.83E-02	2.72E-02	2.72E-02
7	7.05			5.98E-02	3.29E-02	3.14E-02	3.14E-02
8	7.95			6.63E-02	3.66E-02	3.50E-02	3.50E-02
9	8.80			7.53E-02	4.11E-02	3.90E-02	3.90E-02
10	9.71				4.58E-02	4.37E-02	4.37E-02
11	10.80				5.10E-02	4.87E-02	4.87E-02
12	11.88				5.61E-02	5.38E-02	5.38E-02
13	13.15				6.06E-02	5.82E-02	5.82E-02
14	14.47				6.50E-02	6.27E-02	6.27E-02
15	15.86				6.93E-02	6.69E-02	6.69E-02
16	17.24				7.47E-02	7.20E-02	7.20E-02
17	18.78					7.71E-02	7.71E-02
18	20.27					8.16E-02	8.16E-02
19	21.57					8.60E-02	8.60E-02
20	23.13					9.12E-02	9.12E-02
21	24.64					9.58E-02	9.58E-02
22	26.12					1.01E-01	1.01E-01
23	27.49					1.05E-01	1.05E-01
24	29.21					1.10E-01	1.10E-01
25	30.66					1.15E-01	1.15E-01
26	32.34					1.20E-01	1.20E-01
27	33.58					1.24E-01	1.24E-01
28	35.24					1.30E-01	1.30E-01
29	36.88					1.35E-01	1.35E-01
30	38.73					1.42E-01	1.42E-01
31	40.64					1.48E-01	1.48E-01
32	42.59						1.54E-01
	48						1.74E-01
	51						1.85E-01
	54						1.96E-01
	60						2.18E-01

Note:

1. Values beyond Cycle 32 are projected based on Cycle 32 with a 10% bias on the peripheral and re-entrant corner assemblies.

Table 6-3 Calculated Surveillance Capsule Lead Factors

Cycle	Cycle Length (EFPY)	Total Time (EFPY)	Lead Factor		
			13°	23°	33°
1	1.39	1.39	3.03[1]	1.73	1.66
2	0.87	2.26	3.06	1.78	1.72
3	0.89	3.15	3.08	1.80	1.74
4	0.98	4.13	3.08	1.80[2]	1.74
5	0.92	5.05	3.07	1.79	1.73
6	0.99	6.04	3.07	1.76	1.68
7	1.01	7.05	3.11	1.78	1.70
8	0.90	7.95	3.09	1.78	1.69
9	0.85	8.80	3.08[3]	1.76	1.66
10	0.92	9.71	3.08	1.77	1.68
11	1.09	10.80	3.07	1.76	1.67
12	1.08	11.88	3.08	1.80	1.71
13	1.26	13.15	3.09	1.82	1.74
14	1.33	14.47	3.09	1.84	1.76
15	1.38	15.86	3.09	1.85	1.77
16	1.38	17.24	3.11	1.88[4]	1.80
17	1.55	18.78	3.12	1.92	1.83
18	1.48	20.27	3.13	1.93	1.84
19	1.30	21.57	3.14	1.97	1.87
20	1.56	23.13	3.15	1.99	1.89
21	1.52	24.64	3.16	2.01	1.89
22	1.48	26.12	3.16	2.02	1.90
23	1.37	27.49	3.16	2.02	1.91
24	1.72	29.21	3.16	2.02	1.91
25	1.44	30.66	3.16	2.02	1.92
26	1.68	32.34	3.15	2.02	1.92
27	1.24	33.58	3.15	2.02	1.92
28	1.65	35.24	3.15	2.02	1.92
29	1.64	36.88	3.15	2.03	1.93
30	1.85	38.73	3.16	2.04	1.94
31	1.91	40.64	3.15	2.03	1.94[5]
32	1.95	42.59	3.15	2.04	1.95
		48	3.15	2.04	1.96
		51	3.15	2.04	1.97
		54	3.15	2.04	1.97
		60	3.15	2.04	1.98

Notes:

1. Capsule V was removed after Cycle 1.
2. Capsule T was removed after Cycle 4.
3. Capsule R was removed after Cycle 9.
4. Capsule P was removed after Cycle 16.
5. Capsule N was removed after Cycle 31.
6. The projections beyond Cycle 32 are based on Cycle 32 with a 10% bias on peripheral and re-entrant corner assemblies.

Table 6-4 Calculated Maximum Fast (E > 1.0 MeV) Neutron Fluence Rate at the Pressure Vessel Clad/Base Metal Interface

Cycle	Cycle Length (EFPY)	Total Time (EFPY)	Fluence Rate (n/cm^2-s)					
			0°	15°	30°	45°	Maximum	Elevation of Max. (cm)
1	1.39	1.39	4.49E+10	2.69E+10	1.77E+10	1.55E+10	4.49E+10	-9
2	0.87	2.26	4.75E+10	2.93E+10	2.01E+10	1.73E+10	4.75E+10	73
3	0.89	3.15	4.83E+10	2.97E+10	2.05E+10	1.80E+10	4.83E+10	-1
4	0.98	4.13	4.90E+10	3.00E+10	2.01E+10	1.72E+10	4.90E+10	5
5	0.92	5.05	5.19E+10	3.11E+10	2.06E+10	1.84E+10	5.19E+10	-3
6	0.99	6.04	5.03E+10	2.98E+10	1.74E+10	1.62E+10	5.03E+10	59
7	1.01	7.05	4.24E+10	2.84E+10	1.82E+10	1.75E+10	4.24E+10	-3
8	0.90	7.95	4.28E+10	2.53E+10	1.70E+10	1.47E+10	4.28E+10	-3
9	0.85	8.80	5.98E+10	3.53E+10	2.06E+10	1.92E+10	5.98E+10	-3
10	0.92	9.71	5.07E+10	3.13E+10	2.15E+10	1.85E+10	5.07E+10	5
11	1.09	10.80	5.06E+10	2.96E+10	1.95E+10	1.89E+10	5.06E+10	5
12	1.08	11.88	3.87E+10	2.60E+10	2.01E+10	1.89E+10	3.87E+10	5
13	1.26	13.15	2.96E+10	1.97E+10	1.50E+10	1.33E+10	2.96E+10	5
14	1.33	14.47	2.79E+10	1.84E+10	1.45E+10	1.29E+10	2.79E+10	73
15	1.38	15.86	2.95E+10	1.85E+10	1.32E+10	1.26E+10	2.95E+10	5
16	1.38	17.24	2.78E+10	2.02E+10	1.62E+10	1.41E+10	2.78E+10	5
17	1.55	18.78	2.61E+10	1.89E+10	1.45E+10	1.21E+10	2.61E+10	5
18	1.48	20.27	2.56E+10	1.76E+10	1.32E+10	1.19E+10	2.56E+10	5
19	1.30	21.57	2.27E+10	1.76E+10	1.48E+10	1.26E+10	2.27E+10	5
20	1.56	23.13	2.87E+10	2.03E+10	1.50E+10	1.19E+10	2.87E+10	67
21	1.52	24.64	2.69E+10	1.89E+10	1.38E+10	1.16E+10	2.69E+10	67
22	1.48	26.12	2.75E+10	1.86E+10	1.41E+10	1.24E+10	2.76E+10	67
23	1.37	27.49	2.87E+10	1.86E+10	1.38E+10	1.26E+10	2.87E+10	67
24	1.72	29.21	2.86E+10	1.80E+10	1.31E+10	1.14E+10	2.86E+10	3
25	1.44	30.66	2.76E+10	1.79E+10	1.41E+10	1.28E+10	2.76E+10	-73
26	1.68	32.34	2.93E+10	1.83E+10	1.36E+10	1.28E+10	2.93E+10	-73
27	1.24	33.58	3.02E+10	1.92E+10	1.44E+10	1.32E+10	3.02E+10	-73
28	1.65	35.24	2.97E+10	1.91E+10	1.36E+10	1.22E+10	2.97E+10	-3
29	1.64	36.88	2.88E+10	1.91E+10	1.44E+10	1.31E+10	2.88E+10	-3
30	1.85	38.73	2.76E+10	1.83E+10	1.46E+10	1.34E+10	2.76E+10	-73
31	1.91	40.64	2.96E+10	1.88E+10	1.37E+10	1.21E+10	2.96E+10	-73
32	1.95	42.59	2.93E+10	1.88E+10	1.42E+10	1.29E+10	2.93E+10	-3

Table 6-5 Calculated Maximum Fast (E > 1.0 MeV) Neutron Fluence at the Pressure Vessel Clad/Base Metal Interface

Cycle	Cycle Length (EFPY)	Total Time (EFPY)	Fluence (n/cm^2)					
			0°	15°	30°	45°	Maximum	Elevation of Max. (cm)
1	1.39	1.39	1.98E+18	1.18E+18	7.78E+17	6.81E+17	1.98E+18	-9
2	0.87	2.26	3.25E+18	1.97E+18	1.32E+18	1.15E+18	3.25E+18	-3
3	0.89	3.15	4.60E+18	2.81E+18	1.90E+18	1.65E+18	4.60E+18	-3
4	0.98	4.13	6.12E+18	3.73E+18	2.52E+18	2.18E+18	6.12E+18	-1
5	0.92	5.05	7.62E+18	4.63E+18	3.11E+18	2.72E+18	7.62E+18	-3
6	0.99	6.04	9.15E+18	5.55E+18	3.65E+18	3.22E+18	9.15E+18	-1
7	1.01	7.05	1.05E+19	6.45E+18	4.23E+18	3.78E+18	1.05E+19	-1
8	0.9	7.95	1.17E+19	7.17E+18	4.71E+18	4.19E+18	1.17E+19	-1
9	0.85	8.8	1.33E+19	8.12E+18	5.26E+18	4.71E+18	1.33E+19	-1
10	0.92	9.71	1.48E+19	9.02E+18	5.89E+18	5.24E+18	1.48E+19	-1
11	1.09	10.8	1.65E+19	1.00E+19	6.56E+18	5.89E+18	1.65E+19	-1
12	1.08	11.88	1.78E+19	1.09E+19	7.24E+18	6.54E+18	1.78E+19	1
13	1.26	13.15	1.90E+19	1.17E+19	7.84E+18	7.07E+18	1.90E+19	3
14	1.33	14.47	2.02E+19	1.25E+19	8.45E+18	7.61E+18	2.02E+19	3
15	1.38	15.86	2.15E+19	1.33E+19	9.02E+18	8.16E+18	2.15E+19	3
16	1.38	17.24	2.27E+19	1.42E+19	9.73E+18	8.77E+18	2.27E+19	3
17	1.55	18.78	2.39E+19	1.51E+19	1.04E+19	9.36E+18	2.39E+19	3
18	1.48	20.27	2.51E+19	1.59E+19	1.11E+19	9.92E+18	2.51E+19	3
19	1.3	21.57	2.61E+19	1.66E+19	1.17E+19	1.04E+19	2.61E+19	3
20	1.56	23.13	2.75E+19	1.76E+19	1.24E+19	1.10E+19	2.75E+19	5
21	1.52	24.64	2.88E+19	1.85E+19	1.31E+19	1.16E+19	2.88E+19	5
22	1.48	26.12	3.00E+19	1.94E+19	1.37E+19	1.22E+19	3.00E+19	5
23	1.37	27.49	3.13E+19	2.02E+19	1.43E+19	1.27E+19	3.13E+19	5
24	1.72	29.21	3.28E+19	2.12E+19	1.50E+19	1.33E+19	3.28E+19	5
25	1.44	30.66	3.41E+19	2.20E+19	1.57E+19	1.39E+19	3.41E+19	5
26	1.68	32.34	3.56E+19	2.29E+19	1.64E+19	1.46E+19	3.56E+19	5
27	1.24	33.58	3.68E+19	2.37E+19	1.69E+19	1.51E+19	3.68E+19	5
28	1.65	35.24	3.83E+19	2.47E+19	1.77E+19	1.57E+19	3.83E+19	3
29	1.64	36.88	3.98E+19	2.57E+19	1.84E+19	1.64E+19	3.98E+19	3
30	1.85	38.73	4.15E+19	2.68E+19	1.92E+19	1.72E+19	4.15E+19	3
31	1.91	40.64	4.32E+19	2.79E+19	2.01E+19	1.79E+19	4.32E+19	3
32	1.95	42.59	4.50E+19	2.90E+19	2.09E+19	1.87E+19	4.50E+19	3
		48	5.05E+19	3.25E+19	2.36E+19	2.11E+19	5.05E+19	3
		51	5.35E+19	3.45E+19	2.50E+19	2.24E+19	5.35E+19	3
		54	5.66E+19	3.64E+19	2.65E+19	2.38E+19	5.66E+19	3
		60	6.26E+19	4.03E+19	2.94E+19	2.64E+19	6.26E+19	3

Note:
1. Projections are based on Cycle 32 with a 10% bias on the peripheral and re-entrant corner assemblies.

Table 6-6 Calculated Maximum Iron Atom Displacement Rate at the Pressure Vessel Clad/Base Metal Interface

Cycle	Cycle Length (EFPY)	Total Time (EFPY)	Displacement Rate (dpa/s)					
			0°	15°	30°	45°	Maximum	Elevation of Max. (cm)
1	1.39	1.39	7.37E-11	4.44E-11	2.89E-11	2.52E-11	7.37E-11	-9
2	0.87	2.26	7.79E-11	4.84E-11	3.28E-11	2.82E-11	7.79E-11	73
3	0.89	3.15	7.92E-11	4.91E-11	3.35E-11	2.93E-11	7.92E-11	-1
4	0.98	4.13	8.04E-11	4.95E-11	3.27E-11	2.80E-11	8.04E-11	5
5	0.92	5.05	8.51E-11	5.14E-11	3.36E-11	3.00E-11	8.51E-11	-3
6	0.99	6.04	8.25E-11	4.93E-11	2.84E-11	2.64E-11	8.25E-11	57
7	1.01	7.05	6.95E-11	4.68E-11	2.97E-11	2.84E-11	6.95E-11	-3
8	0.90	7.95	7.01E-11	4.18E-11	2.77E-11	2.39E-11	7.01E-11	-3
9	0.85	8.80	9.82E-11	5.83E-11	3.37E-11	3.13E-11	9.82E-11	-3
10	0.92	9.71	8.32E-11	5.17E-11	3.51E-11	3.02E-11	8.32E-11	5
11	1.09	10.80	8.28E-11	4.88E-11	3.19E-11	3.07E-11	8.28E-11	5
12	1.08	11.88	6.34E-11	4.28E-11	3.28E-11	3.08E-11	6.34E-11	9
13	1.26	13.15	4.85E-11	3.23E-11	2.44E-11	2.16E-11	4.85E-11	5
14	1.33	14.47	4.56E-11	3.02E-11	2.36E-11	2.10E-11	4.56E-11	73
15	1.38	15.86	4.83E-11	3.05E-11	2.14E-11	2.05E-11	4.83E-11	9
16	1.38	17.24	4.55E-11	3.32E-11	2.64E-11	2.29E-11	4.55E-11	5
17	1.55	18.78	4.27E-11	3.10E-11	2.36E-11	1.97E-11	4.27E-11	5
18	1.48	20.27	4.18E-11	2.89E-11	2.15E-11	1.93E-11	4.18E-11	5
19	1.30	21.57	3.72E-11	2.89E-11	2.41E-11	2.05E-11	3.72E-11	5
20	1.56	23.13	4.70E-11	3.33E-11	2.44E-11	1.94E-11	4.70E-11	65
21	1.52	24.64	4.40E-11	3.10E-11	2.24E-11	1.89E-11	4.40E-11	65
22	1.48	26.12	4.50E-11	3.06E-11	2.29E-11	2.02E-11	4.52E-11	67
23	1.37	27.49	4.69E-11	3.05E-11	2.24E-11	2.05E-11	4.69E-11	67
24	1.72	29.21	4.67E-11	2.95E-11	2.13E-11	1.86E-11	4.67E-11	3
25	1.44	30.66	4.51E-11	2.94E-11	2.30E-11	2.08E-11	4.51E-11	-73
26	1.68	32.34	4.78E-11	3.01E-11	2.22E-11	2.07E-11	4.78E-11	-73
27	1.24	33.58	4.93E-11	3.16E-11	2.34E-11	2.15E-11	4.93E-11	-71
28	1.65	35.24	4.86E-11	3.14E-11	2.22E-11	1.98E-11	4.86E-11	61
29	1.64	36.88	4.71E-11	3.14E-11	2.34E-11	2.13E-11	4.71E-11	-3
30	1.85	38.73	4.51E-11	3.01E-11	2.37E-11	2.17E-11	4.51E-11	65
31	1.91	40.64	4.84E-11	3.09E-11	2.23E-11	1.97E-11	4.84E-11	-73
32	1.95	42.59	4.80E-11	3.09E-11	2.30E-11	2.09E-11	4.80E-11	63

Table 6-7 Calculated Maximum Iron Atom Displacements at the Pressure Vessel Clad/Base Metal Interface

Cycle	Cycle Length (EFPY)	Total Time (EFPY)	Displacements (dpa)					
			0°	15°	30°	45°	Maximum	Elevation of Max. (cm)
1	1.39	1.39	3.24E-03	1.95E-03	1.27E-03	1.11E-03	3.24E-03	-9
2	0.87	2.26	5.33E-03	3.26E-03	2.16E-03	1.87E-03	5.33E-03	-3
3	0.89	3.15	7.55E-03	4.63E-03	3.09E-03	2.69E-03	7.55E-03	-3
4	0.98	4.13	1.00E-02	6.16E-03	4.11E-03	3.56E-03	1.00E-02	-1
5	0.92	5.05	1.25E-02	7.65E-03	5.08E-03	4.43E-03	1.25E-02	-3
6	0.99	6.04	1.50E-02	9.16E-03	5.95E-03	5.24E-03	1.50E-02	-1
7	1.01	7.05	1.72E-02	1.07E-02	6.90E-03	6.15E-03	1.72E-02	-1
8	0.90	7.95	1.92E-02	1.18E-02	7.69E-03	6.83E-03	1.92E-02	-1
9	0.85	8.80	2.19E-02	1.34E-02	8.59E-03	7.67E-03	2.19E-02	-1
10	0.92	9.71	2.43E-02	1.49E-02	9.60E-03	8.54E-03	2.43E-02	-1
11	1.09	10.80	2.71E-02	1.66E-02	1.07E-02	9.59E-03	2.71E-02	-1
12	1.08	11.88	2.92E-02	1.80E-02	1.18E-02	1.06E-02	2.92E-02	-1
13	1.26	13.15	3.12E-02	1.93E-02	1.28E-02	1.15E-02	3.12E-02	3
14	1.33	14.47	3.31E-02	2.06E-02	1.38E-02	1.24E-02	3.31E-02	3
15	1.38	15.86	3.52E-02	2.19E-02	1.47E-02	1.33E-02	3.52E-02	3
16	1.38	17.24	3.72E-02	2.33E-02	1.59E-02	1.43E-02	3.72E-02	3
17	1.55	18.78	3.93E-02	2.49E-02	1.70E-02	1.52E-02	3.93E-02	3
18	1.48	20.27	4.12E-02	2.62E-02	1.80E-02	1.61E-02	4.12E-02	5
19	1.30	21.57	4.27E-02	2.74E-02	1.90E-02	1.70E-02	4.27E-02	5
20	1.56	23.13	4.50E-02	2.90E-02	2.02E-02	1.79E-02	4.50E-02	5
21	1.52	24.64	4.71E-02	3.05E-02	2.13E-02	1.88E-02	4.71E-02	5
22	1.48	26.12	4.92E-02	3.19E-02	2.24E-02	1.98E-02	4.92E-02	5
23	1.37	27.49	5.13E-02	3.33E-02	2.33E-02	2.07E-02	5.13E-02	5
24	1.72	29.21	5.38E-02	3.49E-02	2.45E-02	2.17E-02	5.38E-02	5
25	1.44	30.66	5.58E-02	3.62E-02	2.55E-02	2.26E-02	5.58E-02	5
26	1.68	32.34	5.84E-02	3.78E-02	2.67E-02	2.37E-02	5.84E-02	5
27	1.24	33.58	6.03E-02	3.90E-02	2.76E-02	2.45E-02	6.03E-02	5
28	1.65	35.24	6.28E-02	4.06E-02	2.88E-02	2.56E-02	6.28E-02	5
29	1.64	36.88	6.52E-02	4.23E-02	3.00E-02	2.67E-02	6.52E-02	5
30	1.85	38.73	6.79E-02	4.40E-02	3.13E-02	2.79E-02	6.79E-02	3
31	1.91	40.64	7.08E-02	4.59E-02	3.27E-02	2.91E-02	7.08E-02	3
32	1.95	42.59	7.37E-02	4.78E-02	3.41E-02	3.04E-02	7.37E-02	3
		48	8.27E-02	5.35E-02	3.84E-02	3.43E-02	8.27E-02	3
		51	8.76E-02	5.67E-02	4.08E-02	3.65E-02	8.76E-02	3
		54	9.26E-02	5.99E-02	4.32E-02	3.86E-02	9.26E-02	3
		60	1.02E-01	6.63E-02	4.79E-02	4.30E-02	1.02E-01	-1

Note(s):

1. Projections are based on Cycle 32 with a 10% bias on the peripheral and re-entrant corner assemblies.

Table 6-8 Calculated Maximum Fast Neutron Fluence (E > 1.0 MeV) at Pressure Vessel Welds and Shells

Material	Fast Neutron (E > 1.0 MeV) Fluence (n/cm^2)			
	42.6 EFPY	**48 EFPY**	**54 EFPY**	**60 EFPY**
Upper Shell Forging	2.63E+19	2.98E+19	3.37E+19	3.76E+19
Intermediate Shell Forging	4.50E+19	5.05E+19	5.66E+19	6.26E+19
Lower Shell Forging	4.43E+19	4.98E+19	5.58E+19	6.19E+19
Inlet Nozzle to Nozzle Shell Weld – Lowest Extent	2.64E+16	3.01E+16	3.42E+16	3.82E+16
Upper to Intermediate Shell Weld	2.82E+19	3.20E+19	3.61E+19	4.03E+19
Intermediate to Lower Shell Weld	4.43E+19	4.98E+19	5.58E+19	6.19E+19
Lower Shell to Lower Closure Head Weld	1.52E+16	1.73E+16	1.95E+16	2.18E+16

Note(s):

1. Projections are based on Cycle 32 with a 10% bias on the peripheral and re-entrant corner assemblies.

Table 6-9 Calculated Maximum Iron Atom Displacements at Pressure Vessel Welds and Shells

Material	Iron Atom Displacements (dpa)			
	42.6 EFPY	**48 EFPY**	**54 EFPY**	**60 EFPY**
Upper Shell Forging	4.32E-02	4.90E-02	5.54E-02	6.17E-02
Intermediate Shell Forging	7.37E-02	8.27E-02	9.26E-02	1.03E-01
Lower Shell Forging	7.25E-02	8.14E-02	9.13E-02	1.01E-01
Inlet Nozzle to Nozzle Shell Weld – Lowest Extent	1.26E-04	1.43E-04	1.62E-04	1.80E-04
Upper to Intermediate Shell Weld	4.65E-02	5.26E-02	5.94E-02	6.62E-02
Intermediate to Lower Shell Weld	7.25E-02	8.14E-02	9.13E-02	1.01E-01
Lower Shell to Lower Closure Head Weld	7.78E-05	8.82E-05	9.97E-05	1.11E-04

Note:

1. Projections are based on Cycle 32 with a 10% bias on the peripheral and re-entrant corner assemblies.

Table 6-10 Summary of Reactor Power and RCS Temperatures

Cycle	Core Power (MWth)	Core Average Coolant Temperature (°F)	Core Inlet Temperature (°F)
1	1650	571	536
2	1650	571	536
3	1650	571	536
4	1650	571	536
5	1650	571	536
6	1650	571	536
7	1650	571	536
8	1650	571	536
9	1650	571	536
10	1650	571	536
11	1650	571	536
12	1650	571	536
13	1650	571	536
14	1650	571	536
15	1650	571	536
16	1650	571	536
17	1650	571	536
18	1650	571	536
19	1650	571	536
20	1650	571	536
21	1650	571	536
22	1650	571	536
23	1650	563	531
24	1650	563	531
25	1650	562	530
26	1671[(1)]	563	530
27	1677	563	530
28	1677	562	531
29	1677	562	531
30	1677	562	531
31	1677	562	531
32	1677	562	531

Note(s):

1. There was a mid-cycle power uprate during Cycle 26 from 1650 MWth to 1677 MWth. This uprate was done at a burnup of 4,975 MWD/MTU. The burnup-weighted average thermal power of 1671 MWth was used for the Cycle 26 transport calculations.

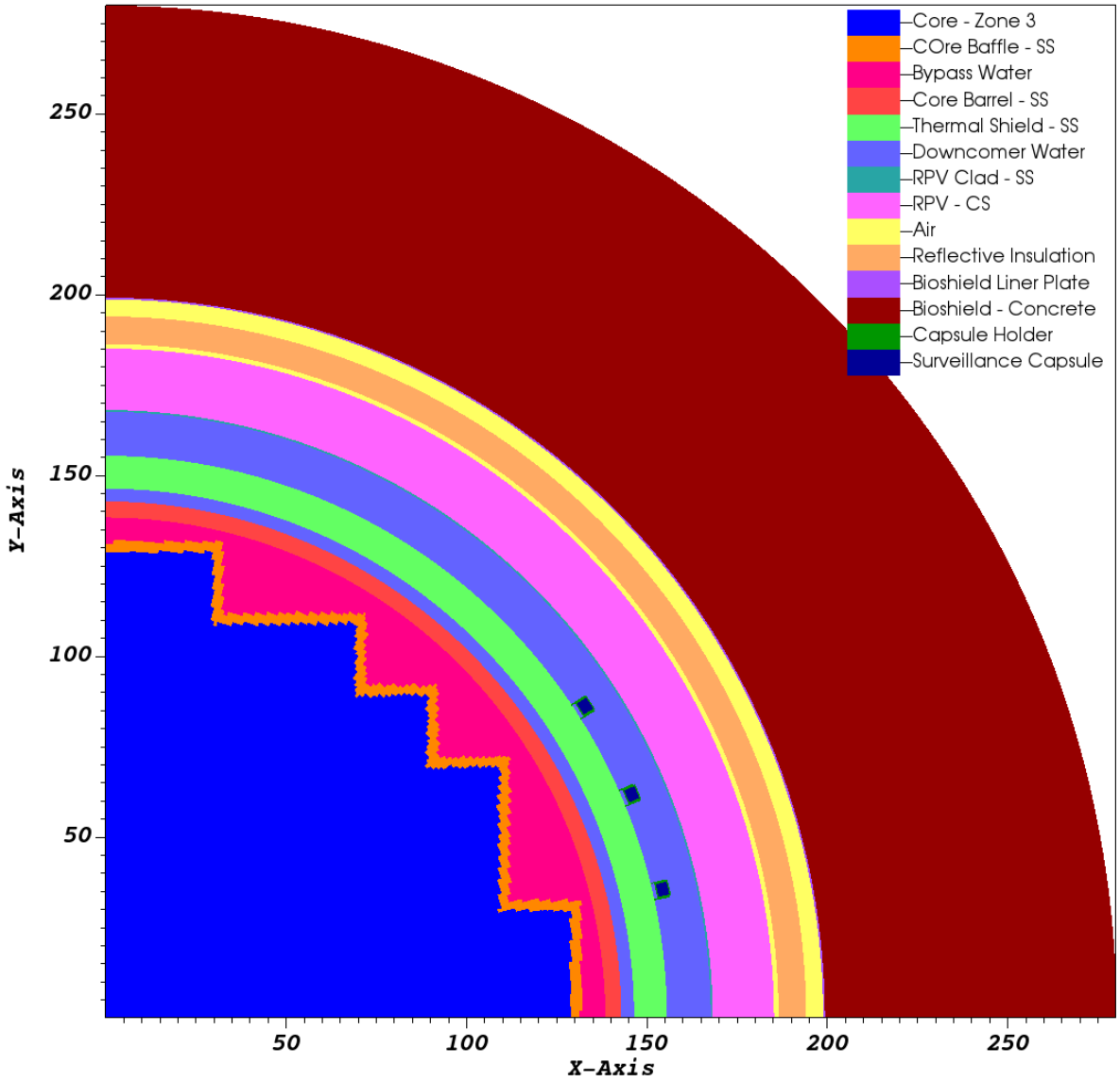

Figure 6-1 Prairie Island Unit 2 Plan View of the Reactor Geometry at the Core Midplane

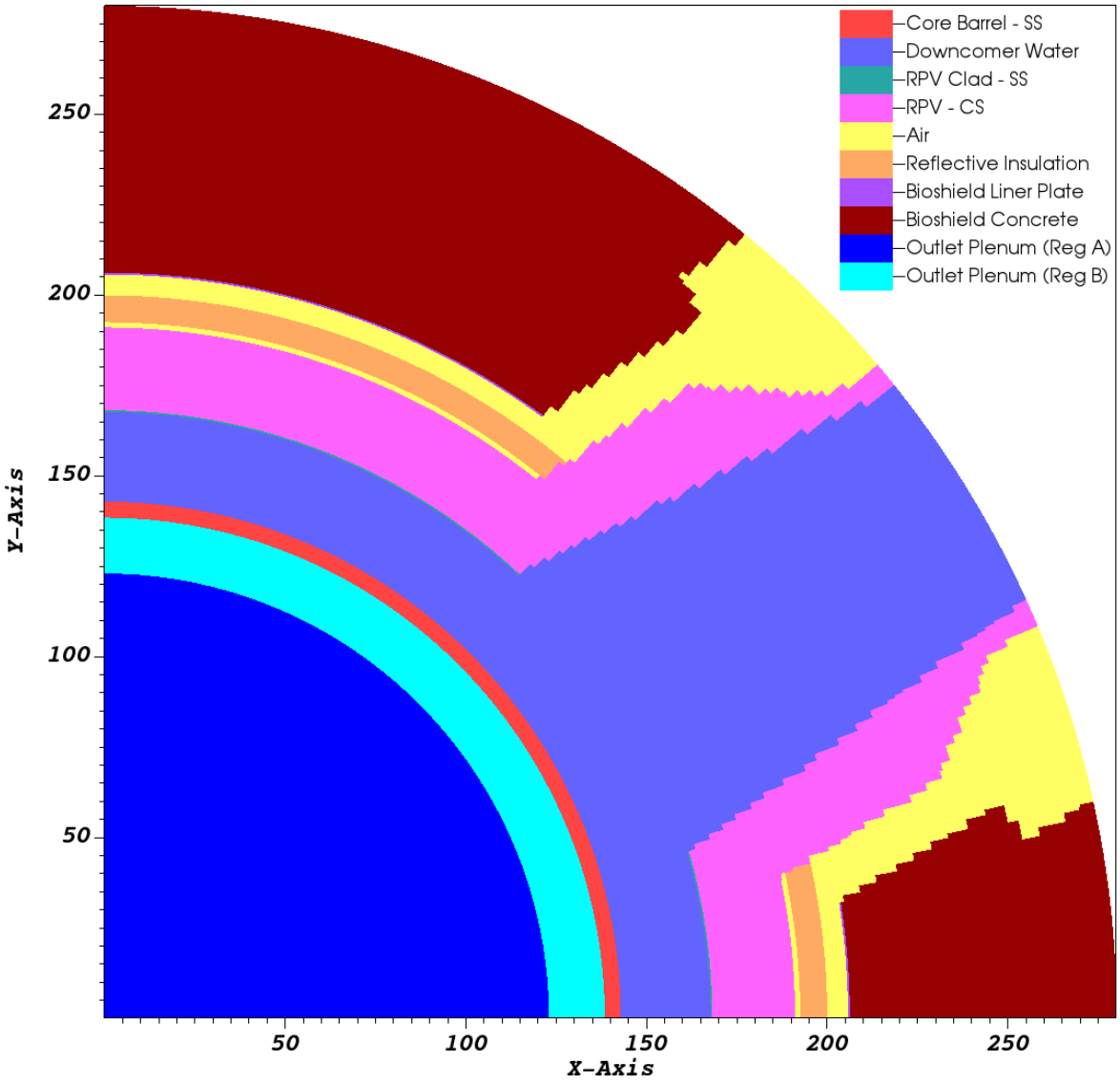

Figure 6-2 Prairie Island Unit 2 Plan View of the Reactor Geometry at the Nozzle Centerline

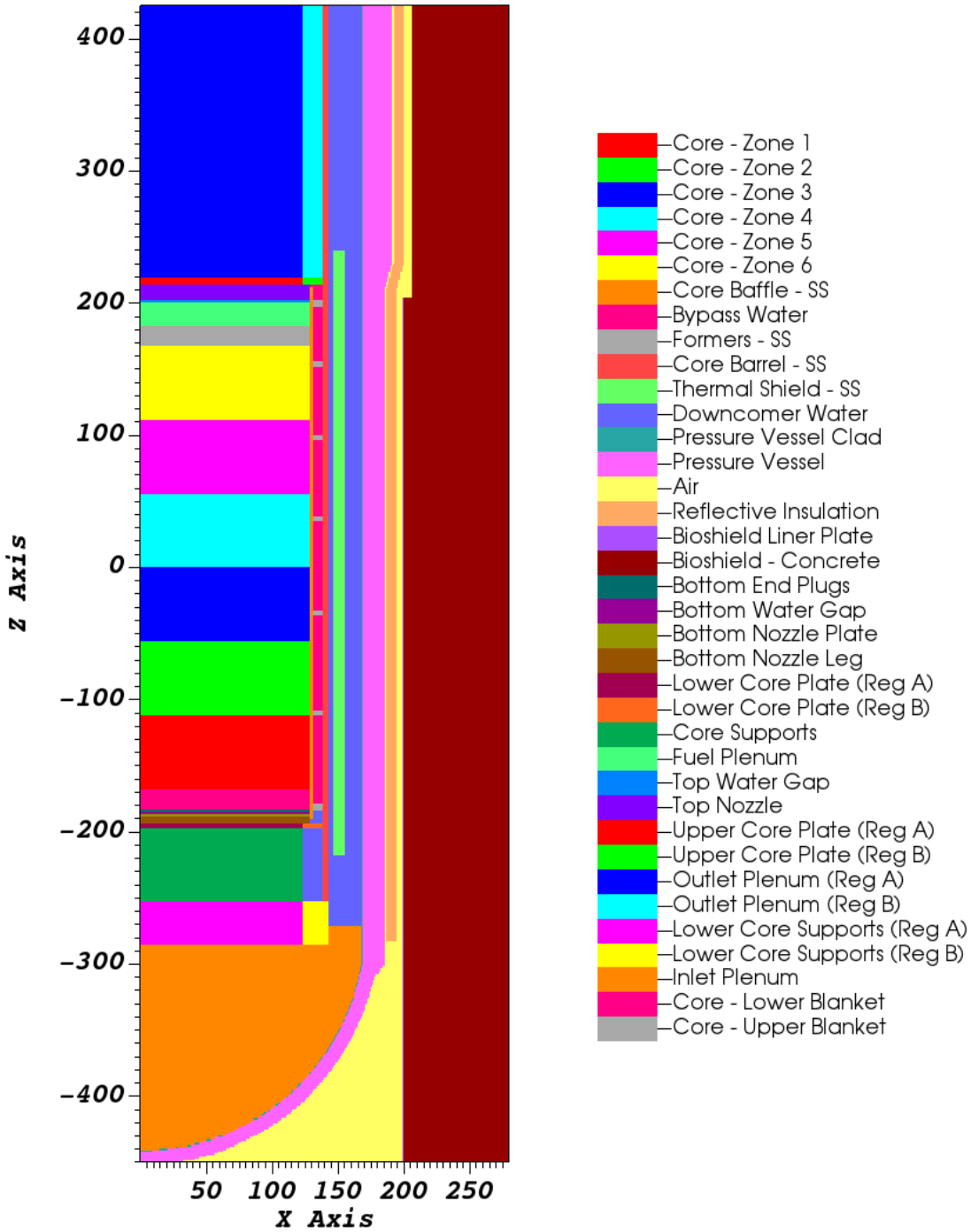

Figure 6-3 Prairie Island Unit 2 Section View of the Reactor Geometry at 0-Degrees

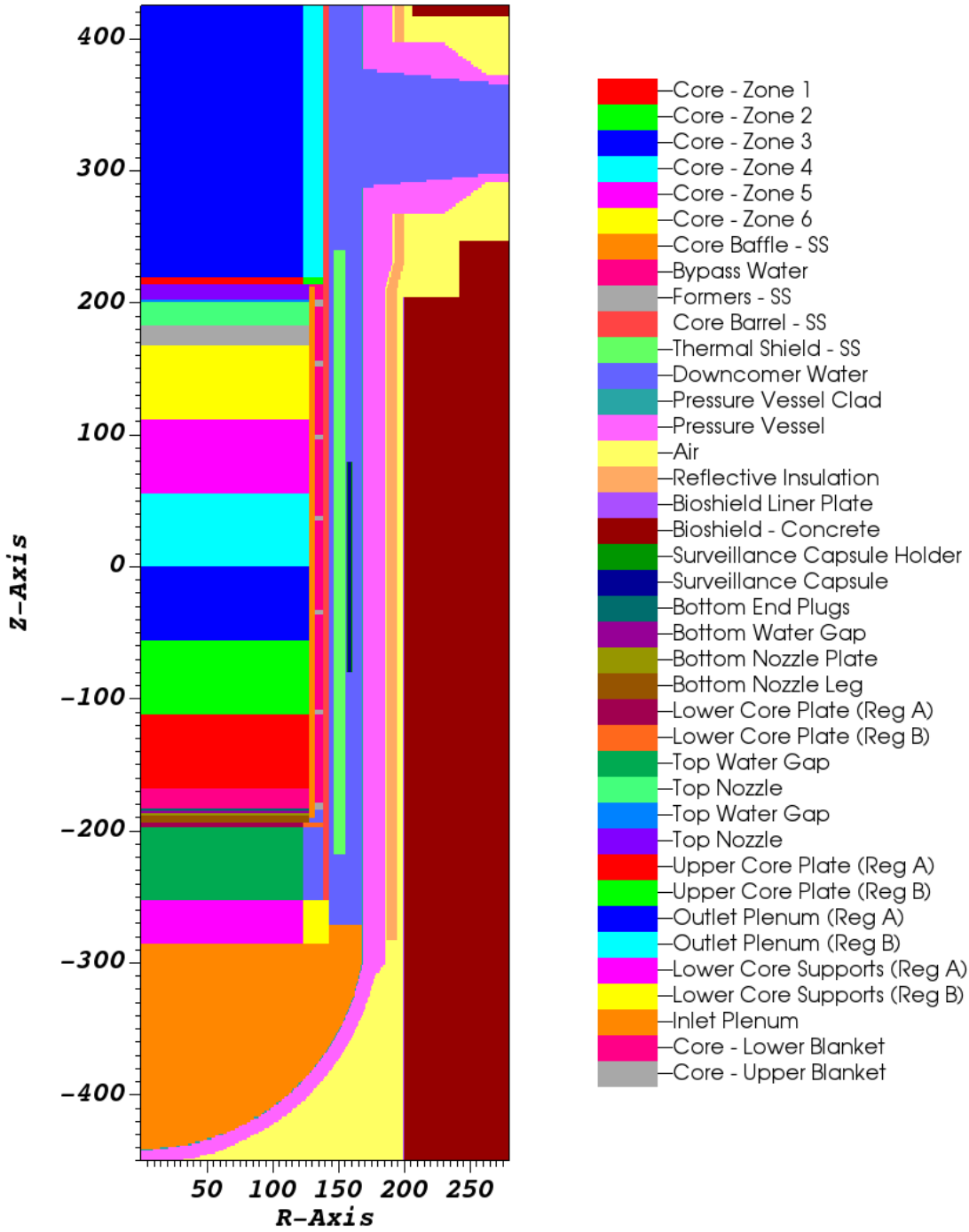

Figure 6-4 Prairie Island Unit 2 Section View of the Reactor Geometry at 33-Degrees

7 SURVEILLANCE CAPSULE REMOVAL SCHEDULE

The following surveillance capsule removal schedule (Table 7-1) meets the requirements of ASTM E185-82 [10] with consideration of NUREG-1801 [7] and NUREG-2191 [22]. It is noted that the Capsule N fluence bounds the projected fluence of the Prairie Island Unit 2 RV through 80 years of operation (peak vessel fluence of 7.46 x 10^{19} n/cm^2 at 72 EFPY).

Table 7-1 Prairie Island Unit 2 Surveillance Capsule Withdrawal Schedule

Capsule	Capsule Location	Lead Factor	Withdrawal EFPY(1)	Fluence (n/cm^2, E > 1.0 MeV)
V	77°	3.03	1.39 (EOC 1)	5.98E+18
T	67°	1.80	4.13 (EOC 4)	1.10E+19
R	257°	3.08	8.80 (EOC 9)	4.11E+19
P	247°	1.88	17.24 (EOC 16)	4.27E+19
N	237°	1.94	40.64 (EOC 31)	8.41E+19
S	57°	- - -	Standby(2)	- - -

Notes:
1. Effective full-power years (EFPY) from plant startup. EOC = end-of-cycle.
2. It is recommended that Capsule S be removed at approximately 54 EFPY, which is the projected peak reactor vessel fluence at 120 years (1.11 x 10^{20} n/cm^2 at 108 EFPY). The need for an alternative form of neutron dosimetry should be assessed when the last capsule is withdrawn.

8 REFERENCES

1. U.S. Nuclear Regulatory Commission, Office of Nuclear Regulatory Research, Regulatory Guide 1.99, Revision 2, "Radiation Embrittlement of Reactor Vessel Materials," May 1988. *[Agencywide Documents Access and Management System (ADAMS) Accession Number ML003740284]*

2. Westinghouse Report, WCAP-8193, Rev. 0, "Northern States Power Co. Prairie Island Unit No. 2 Reactor Vessel Radiation Surveillance Program," September 1973.

3. ASTM E185-70, "Standard Recommended Practice for Surveillance Tests for Nuclear Reactor Vessels," 1970.

4. Appendix G of the ASME Boiler and Pressure Vessel (B&PV) Code, Section XI, Division 1, Fracture Toughness Criteria for Protection Against Failure.

5. ASTM E208, Standard Test Method for Conducting Drop-Weight Test to Determine Nil-Ductility Transition Temperature of Ferritic Steels, ASTM.

6. ASTM E399, Standard Test Method for Linear-Elastic Plane-Strain Fracture Toughness K_{Ic} of Metallic Materials, ASTM.

7. NUREG-1801, Rev. 2, "Generic Aging Lessons Learned (GALL) Report," December 2010, U.S. Nuclear Regulatory Commission Report. *[ADAMS Accession Number ML103490041]*

8. Westinghouse Report RT-TR-22-26, Rev. 0, "Prairie Island Unit 2 Surveillance Capsule Test Report," September 29, 2022.

9. 10 CFR 50, Appendix H, "Reactor Vessel Material Surveillance Program Requirements," U.S. Nuclear Regulatory Commission, Federal Register, October 2, 2020.

10. ASTM E185-82, "Standard Practice for Conducting Surveillance Tests for Light-Water Cooled Nuclear Power Reactor Vessels," American Society for Testing and Materials, 1982.

11. ASTM E23-18, Standard Test Methods for Notched Bar Impact Testing of Metallic Materials, 2018.

12. ASTM E2298-18, Standard Test Method for Instrumented Impact Testing of Metallic Materials, 2018.

13. ASTM A370-18, Standard Test Methods and Definitions for Mechanical Testing of Steel Products, 2018.

14. ASTM E8/E8M-16a, Standard Test Methods for Tension Testing of Metallic Materials, 2016.

15. ASTM E21-17, Standard Test Methods for Elevated Temperature Tension Tests of Metallic Materials, 2017.

16. Westinghouse Report, WCAP-14613, Rev. 2, "Analysis of Capsule P from the Northern States Power Company Prairie Island Unit 2 Reactor Vessel Radiation Surveillance Program," February 1998.

17. ASTM E853-18, Standard Practice for Analysis and Interpretation of Light-Water Reactor Surveillance Neutron Exposure Results, 2018.

18. ASTM E693-94, Standard Practice for Characterizing Neutron Exposures in Iron and Low Alloy Steels in Terms of Displacements Per Atom (DPA), E706 (ID), 1994.

19. U.S. Nuclear Regulatory Commission, Office of Nuclear Regulatory Research, Regulatory Guide 1.190, "Calculational and Dosimetry Methods for Determining Pressure Vessel Neutron Fluence," March 2001. *[ADAMS Accession Number ML010890301]*

20. Westinghouse Report, WCAP-18124-NP-A, Rev. 0, "Fluence Determination with RAPTOR-M3G and FERRET," July 2018. *[ADAMS Accession Number ML18204A010]*

21. Westinghouse Report, WCAP-18124-NP-A, Rev. 0, Supplement 1 NP-A, "Fluence Determination with RAPTOR-M3G and FERRET – Supplement for Extended Beltline Materials," May 2022. *[ADAMS Accession Number ML22153A139]*

22. NUREG-2191, Volume 2, "Generic Aging Lessons Learned for Subsequent License Renewal (GALL-SLR) Report," July 2017, U.S. Nuclear Regulatory Commission Report. *[ADAMS Accession Number ML17187A204]*

APPENDIX A VALIDATION OF THE RADIATION TRANSPORT MODELS BASED ON NEUTRON DOSIMETRY MEASUREMENTS

A.1 NEUTRON DOSIMETRY

Comparisons of measured dosimetry results to both the calculated and least-squares adjusted values for Capsules V, T, R, P, and N are provided in this appendix. The sensor sets have been analyzed in accordance with the current dosimetry evaluation methodology described in Regulatory Guide 1.190, "Calculational and Dosimetry Methods for Determining Pressure Vessel Neutron Fluence" [A-1]. One of the main purposes for providing this material is to demonstrate that the overall measurements agree with the calculated and least-squares adjusted values to within ± 20% as specified by Regulatory Guide 1.190, thus serving to validate the calculated neutron exposures reported in Section 6.2.

A.1.1 Sensor Reaction Rate Determinations

In this section, the results of the evaluations of Capsules V, T, R, P, and N are presented. The capsules designation, locations within the reactor, and time of withdrawal are as follows:

Capsule	Azimuthal Location	Withdrawal Time	Irradiation Time (EFPY)
V	77º	End of Cycle 1	1.39
T	67º	End of Cycle 4	4.13
R	257º	End of Cycle 9	8.80
P	247º	End of Cycle 16	17.24
N	237º	End of Cycle 31	40.64
S	57º	Standby	---

The passive neutron sensors included in these evaluations are summarized as follows:

Sensor Material	Reaction of Interest	Capsule V	Capsule T	Capsule R	Capsule P	Capsule N
Copper	Cu-63 (n,α) Co-60	X	X	X	X	X
Iron	Fe-54 (n,p) Mn-54	X	X	X	X	X
Nickel	Ni-58 (n,p) Co-58	X	X	X	X	X
Uranium-238	U-238 (n,f) Cs-137	X	X	X	X	X
Neptunium-237	Np-237 (n,f) Cs-137	X	X	X	X	X
Cobalt-Aluminum(1)	Co-59 (n,γ) Co-60	X	X	X	X	X

Notes:

1. The cobalt-aluminum sensors include only bare sensors. For all the capsules withdrawn to-date, none of the cadmium shielded cobalt-aluminum wires have been recovered.

The design of the in-vessel surveillance capsules places the individual neutron sensors at several radial locations within the test specimen array. As a result of the various radial locations, gradient correction factors are applied to the measured reaction rates to index all of the neutron sensor measurements to a common geometric location (the center of the capsule) prior to use in the least-squares adjustment procedure. Pertinent physical and nuclear characteristics of the passive neutron sensors analyzed are listed in Table A-1.

The use of passive monitors does not yield a direct measure of the energy-dependent neutron exposure rate at the point of interest. Rather, the activation or fission process is a measure of the integrated effect that the time- and energy-dependent neutron exposure rate has on the target material over the course of the irradiation period. An accurate assessment of the average neutron exposure rate incident on the various monitors may be derived from the activation measurements only if the irradiation parameters are well known. In particular, the following variables are of interest:

- The measured specific activity of each monitor.
- The physical characteristics of each monitor.
- The operating history of the reactor.
- The energy response of each monitor.
- The neutron energy spectrum at the monitor location.

The radiometric counting of the sensors from Capsule N was carried out by Pace Analytical Services, Inc. The radiometric counting followed established ASTM procedures. The previously withdrawn in-vessel Capsules V, T, R, and P were re-evaluated using the current calculational model.

The operating history of the reactor over the irradiation periods was based on the monthly power generation of Prairie Island Unit 2 from initial reactor criticality through the end of the dosimetry evaluation period. For the sensor sets utilized in the surveillance capsules, the half-lives of the product isotopes are long enough that a monthly histogram describing reactor operation has proven to be an adequate representation for use in radioactive decay corrections for the reactions of interest in the exposure evaluations. The irradiation history for Cycle 1 through Cycle 16 is in [A-2]. The monthly thermal generation data for Cycle 17 through Cycle 31 were provided by Xcel Energy.

The irradiation history for Cycle 17 through Cycle 31 is summarized in Table A-2.

Having the measured specific activities, the physical characteristics of the sensors, and the operating history of the reactor, reaction rates referenced to full-power operation were determined from the following equation:

$$R = \frac{A}{N_0 F Y \sum \frac{P_j}{P_{ref}} C_j \left[1 - e^{-\lambda t_j}\right]\left[e^{-\lambda t_{d,j}}\right]}$$

where:

R	=	Reaction rate averaged over the irradiation period and referenced to operation at a core power level of P_{ref} (rps/nucleus).
A	=	Measured specific activity (dps/g).
N_0	=	Number of target element atoms per gram of sensor.
F	=	Atom fraction of the target isotope in the target element.
Y	=	Number of product atoms produced per reaction.
P_j	=	Average core power level during irradiation Period j (MW).
P_{ref}	=	Maximum or reference power level of the reactor (MW).
C_j	=	Calculated ratio of ϕ (E > 1.0 MeV) during irradiation Period j to the time weighted average ϕ (E > 1.0 MeV) over the entire irradiation period.
λ	=	Decay constant of the product isotope (1/sec).
t_j	=	Length of irradiation Period j (sec).
$t_{d,j}$	=	Decay time following irradiation Period j (sec).

The summation is carried out over the total number of monthly intervals comprising the irradiation period.

In the equation describing the reaction rate calculation, the Ratio $[P_j]/[P_{ref}]$ accounts for month-by-month variation of reactor core power level within any given fuel cycle as well as over multiple fuel cycles. The Ratio C_j, which was calculated for each fuel cycle using the transport methodology discussed in Section 6.2, accounts for the change in sensor reaction rates caused by variations in exposure rate level induced by changes in core spatial power distributions from fuel cycle to fuel cycle. For a single-cycle irradiation, C_j is normally taken to be 1.0. However, for multiple-cycle irradiations, the additional C_j term should be employed. The impact of changing exposure rate levels for constant power operation can be quite significant for sensor sets that have been irradiated for many cycles in a reactor that has transitioned from

non-low-leakage to low-leakage fuel management or for sensor sets contained in surveillance capsules that have been moved from one capsule location to another. The fuel-cycle-specific neutron exposure rate values are used to compute cycle-dependent values for C_j values at the radial and azimuthal center of the respective capsules at core midplane.

Prior to using the measured reaction rates in the least-squares evaluations of the dosimetry sensor sets, additional corrections were made to the U-238 measurements to account for the presence of ^{235}U impurities in the sensors, as well as to adjust for the build-in of plutonium isotopes over the course of the irradiation. Corrections were also made to the U-238 and Np-237 sensor reaction rates to account for gamma-ray-induced fission reactions that occurred over the course of the surveillance capsule irradiations. The correction factors corresponding to the Prairie Island Unit 2 fission sensor reaction rates are summarized as follows:

Correction	Capsule V	Capsule T	Capsule R	Capsule P	Capsule N
U-235 Impurity/Pu Build-in	0.8611	0.8417	0.7389	0.7332	0.6213
U-238 (γ,f)	0.9548	0.9596	0.9548	0.9603	0.9599
Net U-238 Correction	0.8222	0.8077	0.7055	0.7041	0.5964
Np-237 (γ,f)	0.9851	0.9855	0.9851	0.9856	0.9858

The correction factors were applied in a multiplicative fashion to the decay-corrected cadmium-covered fission sensor reaction rates.

Results of the sensor reaction rate determinations for the in-vessel Capsules V, T, R, P, and N are given in Table A-3 through Table A-7, where the measured specific activities, decay-corrected saturated specific activities, and computed reaction rates for each sensor are listed.

A.1.2 Least-Squares Evaluation of Sensor Sets

Least-squares adjustment methods provide the capability of combining the measurement data with the corresponding neutron transport calculations resulting in a best-estimate neutron energy spectrum with associated uncertainties. Best-estimates for key exposure parameters such as fluence rate (E > 1.0 MeV) or dpa/s along with their uncertainties are then easily obtained from the adjusted spectrum. In general, the least-squares method, as applied to dosimetry evaluations, act to reconcile the measured sensor reaction rate data, dosimetry reaction cross-sections, and the calculated neutron energy spectrum within their respective uncertainties. For example,

$$R_i \pm \delta_{R_i} = \sum_g (\sigma_{ig} \pm \delta_{\sigma_{ig}})(\varphi_g \pm \delta_{\varphi_g})$$

relates a set of measured reaction rates, R_i, to a single neutron spectrum, ϕ_g, through the multigroup dosimeter reaction cross-sections, σ_{ig}, each with an uncertainty δ. The primary objective of the least-squares evaluation is to produce unbiased estimates of the neutron exposure parameters at the location of the measurement.

For the least-squares evaluation of the Prairie Island Unit 2 dosimetry, the FERRET code [A-3] was employed to combine the results of the plant-specific neutron transport calculations and sensor set reaction rate measurements to determine the best-estimate values of exposure parameters (fluence rate (E > 1.0 MeV) and dpa) and their associated uncertainties.

The application of the least-squares methodology requires the following input:

1. The calculated neutron energy spectrum and associated uncertainties at the measurement location.
2. The measured reaction rates and associated uncertainty for each sensor contained in the multiple sensor set.
3. The energy-dependent dosimetry reaction cross-sections and associated uncertainties for each sensor contained in the multiple sensor set.

For the Prairie Island Unit 2, the calculated neutron spectrum was obtained from the results of plant-specific neutron transport calculations described in Section 6.2. The sensor reaction rates were derived from the measured specific activities using the procedures described in Section A.1.1. The dosimetry reaction cross-sections and uncertainties were obtained from the SNLRML dosimetry cross-section library [A-4].

The uncertainties associated with the measured reaction rates, dosimetry cross-sections, and calculated neutron spectrum were input to the least-squares procedure in the form of variances and covariances. The assignment of the input uncertainties followed the guidance provided in ASTM E944, "Standard Guide for Application of Neutron Spectrum Adjustment Methods in Reactor Surveillance" [A-5].

The following provides a summary of the uncertainties associated with the least-squares evaluation of the Prairie Island Unit 2 surveillance capsule sensor sets.

Reaction Rate Uncertainties

The overall uncertainty associated with the measured reaction rates includes components due to the basic measurement process, irradiation history corrections, and corrections for competing reactions. A high level of accuracy in the reaction rate determinations is ensured by utilizing laboratory procedures that conform to the ASTM National Consensus Standards for reaction rate determinations for each sensor type.

After combining all of these uncertainty components, the sensor reaction rates derived from the counting and data evaluation procedures were assigned the following net uncertainties for input to the least-squares evaluation:

Reaction	Uncertainty (1σ)
^{63}Cu (n,α) ^{60}Co	5%
^{54}Fe (n,p) ^{54}Mn	5%
^{58}Ni (n,p) ^{58}Co	5%
^{59}Co (n,γ) ^{60}Co	5%
^{238}U (n,f) FP	10%
^{237}Np (n,f) FP	10%

In the case of Capsule N, two sets of data are provided. The Case 1 data set was based on the use of the nominal uncertainties for the measured reaction rates. However, as seen in Table A-12, the value of χ^2 per degree of freedom associated with this evaluation was 1.128. A value of χ^2/DOF greater than 1.0 indicates that the uncertainties associated with the input parameters may have been underestimated. Since the same transport calculations and dosimetry reaction cross-sections were used in all five capsule evaluations with no issue arising with respect to capsules V, T, R, and P, it is not likely that the uncertainties associated with these input parameters caused the inconsistency noted in the Capsule N evaluation. Additionally, a comparison of the Capsule N normalized reaction rates with the database of 2-Loop Thermal Shield plant in-vessel capsules at 33 degrees was completed. This comparison showed that all normalized measured reaction rates fall within three standard deviations of the normalized reaction rates in the database. As such, they are all judged to be credible. Therefore, based on the assumption that the uncertainties associated with the Capsule N measured reaction rates were too small, the Case 2 least-squares analysis was performed using larger input uncertainties for the measured reaction rates. The reaction rate uncertainties used in the two least squares evaluations for Capsule N are summarized as follows:

Reaction	Uncertainty (1σ)	
	Case 1	Case 2
^{63}Cu (n,α) ^{60}Co	5%	10%
^{54}Fe (n,p) ^{54}Mn	5%	10%
^{58}Ni (n,p) ^{58}Co	5%	10%
^{59}Co (n,γ) ^{60}Co	5%	10%
^{238}U (n,f) FP	10%	15%
^{237}Np (n,f) FP	10%	15%

From Table A-13, it is noted that the used of the larger reaction rate uncertainties reduced the value of χ^2/DOF to 0.512. Therefore, for Capsule N, the Case 2 least squares evaluation was taken as the final result.

Dosimetry Cross-Section Uncertainties

The reaction rate cross-sections used in the least-squares evaluations were taken from the SNLRML library. This data library provides reaction cross-sections and associated uncertainties, including covariances, for

66 dosimetry sensors in common use. Both cross-sections and uncertainties are provided in a fine multigroup structure for use in least-squares adjustment applications. These cross-sections were compiled from recent cross-section evaluations, and they have been tested for accuracy and consistency for least-squares evaluations. Further, the library has been empirically tested for use in fission spectra determination, as well as in the fluence and energy characterization of 14 MeV neutron sources.

For sensors included in the Prairie Island Unit 2 surveillance program, the following uncertainties in the fission spectrum averaged cross-sections are provided in the SNLRML documentation package:

Reaction	Uncertainty
Cu-63 (n,α) Co-60	4.08–4.16%
Fe-54 (n,p) Mn-54	3.05–3.11%
Ni-58 (n,p) Co-58	4.49–4.56%
Co-59 (n,γ) Co-60	0.79–3.59%
U-238 (n,f)	0.54–0.64%
Np-237 (n,f)	10.32-10.97%

These tabulated ranges provide an indication of the dosimetry cross-section uncertainties associated with the sensor sets used in LWR irradiations.

Calculated Neutron Spectrum

The neutron spectra inputs to the least-squares adjustment procedure were obtained directly from the results of plant-specific transport calculations for each surveillance capsule irradiation period and location. The spectrum for each capsule was input in an absolute sense (rather than as simply a relative spectral shape). Therefore, within the constraints of the assigned uncertainties, the calculated data were treated equally with the measurements.

While the uncertainties associated with the reaction rates were obtained from the measurement procedures and counting benchmarks and the dosimetry cross-section uncertainties were supplied directly with the SNLRML library, the uncertainty matrix for the calculated spectrum was constructed from the following relationship:

$$M_{gg'} = R_n^2 + R_g * R_{g'} * P_{gg'}$$

where R_n specifies an overall fractional normalization uncertainty and the fractional uncertainties R_g and $R_{g'}$ specify additional random groupwise uncertainties that are correlated with a correlation matrix given by:

$$P_{gg'} = [1 - \theta]\delta_{gg'} + \theta\, e^{-H}$$

where:

$$H = \frac{(g - g')^2}{2\gamma^2}$$

The first term in the correlation matrix equation specifies purely random uncertainties, while the second term describes the short-range correlations over a group range γ (θ specifies the strength of the latter term). The value of δ is 1.0 when $g = g'$, and is 0.0 otherwise.

The set of parameters defining the input covariance matrix for the Prairie Island Unit 2 calculated spectra was as follows:

Exposure Rate Normalization Uncertainty (R_n)	15%
Exposure Rate Group Uncertainties (R_g, $R_{g'}$)	
(E > 0.0055 MeV)	15%
(0.68 eV < E < 0.0055 MeV)	25%
(E < 0.68 eV)	50%
Short Range Correlation (θ)	
(E > 0.0055 MeV)	0.9
(0.68 eV < E < 0.0055 MeV)	0.5
(E < 0.68 eV)	0.5
Exposure Rate Group Correlation Range (γ)	
(E > 0.0055 MeV)	6
(0.68 eV < E < 0.0055 MeV)	3
(E < 0.68 eV)	2

A.1.3 Comparisons of Measurements and Calculations

Results of the least-squares evaluations are provided in Table A-8 through Table A-13. In these tables, measured, calculated, and best-estimate values for sensor reaction rates are given. Also provided in these tabulations are ratios of the measured reaction rates to both the calculated and least-squares adjusted reaction rates. These ratios of measured-to-calculated (M/C) and measured-to-best estimate (M/BE) illustrate the consistency of the fit of the calculated neutron energy spectra to the measured reaction rates both before and after adjustment. Additionally, comparisons of the calculated and best-estimate values of neutron fluence rate (E > 1.0 MeV) and iron atom displacement rate are tabulated along with the best-estimate-to-calculated (BE/C) ratios observed for each of the capsules.

The data comparisons provided in Table A-8 through Table A-13 show that the adjustments to the calculated spectra are relatively small and within the assigned uncertainties for the calculated spectra, measured sensor reaction rates, and dosimetry reaction cross-sections. Further, these results indicate that the use of the least-squares evaluation results in a reduction in the uncertainties associated with the exposure of the surveillance capsules. From Section 6.4, the calculational uncertainty is specified as 13% at the 1σ level.

Further comparisons of the measurement results with calculations are given in Table A-14 and Table A-15. In Table A-14, calculations of individual threshold sensor reaction rates are compared directly with the corresponding measurements. These threshold reaction rate comparisons provide a good evaluation of the accuracy of the fast neutron portion of the calculated energy spectra. In Table A-15, calculations of fast neutron exposure rates in terms of fast neutron (E > 1.0 MeV) fluence rate and dpa/s are compared with the best-estimate results obtained from the least-squares evaluation of the capsule dosimetry results. These comparisons yield consistent and similar results with all measurement-to-calculation comparisons falling within the 20% limits specified as the acceptance criteria in Regulatory Guide 1.190.

In the case of the direct comparison of the measured and calculated sensor reaction rates, for the individual threshold sensors considered in the least-squares analysis, the M/C comparisons of the fast neutron threshold reactions range from 0.90 to 1.09. The overall average M/C ratio is 0.98 with an associated standard deviation of 9.8%.

In the case of the comparison of the best-estimate and calculated fast neutron exposure parameters, the BE/C comparisons are 0.97 and 0.98 for fast neutron (E > 1.0 MeV) fluence rate and iron atom displacement rate, respectively.

Based on these comparisons, it is concluded that the calculated fast neutron exposures provided in Section 6.2 are valid for use in the assessment of the condition of the materials comprising the beltline region of the Prairie Island Unit 2 reactor pressure vessel.

Table A-1 Nuclear Parameters Used in the Evaluation of Neutron Sensors

Reaction of Interest	Atomic Weight (g/g-atom)	Target Atom Fraction	Product Half-life (days)	Fission Yield (%)	90% Response Range[(1)] (MeV)
Cu-63 (n,α) Co-60	63.546	0.6917	1925.28	-	4.53–11.0
Fe-54 (n,p) Mn-54	55.845	0.05845	312.13	-	2.27–7.54
Ni-58 (n,p) Co-58	58.693	0.68077	70.86	-	1.98–7.51
Co-59 (n,γ) Co-60	58.933	0.0015	1925.28	-	Non-threshold
U-238 (n,f) Cs-137	238.051	1.00	10975.76	6.02	1.44–6.69
Np-237 (n,f) Cs-137	237.048	1.00	10975.76	6.27	0.68-5.61

Note:

1. Energies between which 90% of activity is produced (U-235 fission spectrum) [A-6]

Table A-2 Monthly Thermal Generation at Prairie Island Unit 2 Cycles 17 through 31

Cycle 17		Cycle 18		Cycle 19		Cycle 20	
Month	**Thermal Generation [MW-Hr]**	**Month**	**Thermal Generation [MW-Hr]**	**Month**	**Thermal Generation [MW-Hr]**	**Month**	**Thermal Generation [MW-Hr]**
6/27/1995	75988	3/30/1997	26012	1/1/1999	1069376	6/7/2000	854709
7/1/1995	1218591	4/1/1997	1040736	2/1/1999	1036346	7/1/2000	1230424
8/1/1995	1227600	5/1/1997	1191043	3/1/1999	1229905	8/1/2000	1230622
9/1/1995	1180266	6/1/1997	1191090	4/1/1999	1191542	9/1/2000	1184198
10/1/1995	1227600	7/1/1997	1196001	5/1/1999	1232232	10/1/2000	1231043
11/1/1995	1168654	8/1/1997	1231031	6/1/1999	1173590	11/1/2000	1191652
12/1/1995	1231175	9/1/1997	1190525	7/1/1999	1231528	12/1/2000	1229784
1/1/1996	1218525	10/1/1997	1230313	8/1/1999	1231668	1/1/2001	1225145
2/1/1996	1121189	11/1/1997	1191028	9/1/1999	1072708	2/1/2001	1106582
3/1/1996	1154299	12/1/1997	1231287	10/1/1999	1221341	3/1/2001	1222419
4/1/1996	1137599	1/1/1998	939213	11/1/1999	1188948	4/1/2001	1158990
5/1/1996	1229222	2/1/1998	0	12/1/1999	1217110	5/1/2001	354077
6/1/1996	1143478	3/1/1998	1056451	1/1/2000	1231319	6/1/2001	962014
7/1/1996	1103500	4/1/1998	1190681	2/1/2000	1152886	7/1/2001	1191567
8/1/1996	1219943	5/1/1998	1232133	3/1/2000	1230836	8/1/2001	1225305
9/1/1996	1191672	6/1/1998	1167691	4/1/2000	1098309	9/1/2001	1185794
10/1/1996	1207935	7/1/1998	1231407	5/1/2000	0	10/1/2001	1210389
11/1/1996	1188085	8/1/1998	1231786			11/1/2001	1059661
12/1/1996	1228990	9/1/1998	1148852			12/1/2001	1224856
1/1/1997	906076	10/1/1998	1230748			1/1/2002	1196794
2/1/1997	0	11/1/1998	317705			2/1/2002	28116
		12/1/1998	0				
Total	22380386	**Total**	21465733	**Total**	18809643	**Total**	22504141
EFPS	4.883E+07	**EFPS**	4.683E+07	**EFPS**	4.104E+07	**EFPS**	4.910E+07
EFPD	565.16	**EFPD**	542.06	**EFPD**	474.99	**EFPD**	568.29
EFPY	1.55	**EFPY**	1.48	**EFPY**	1.30	**EFPY**	1.56

Table A-2 Monthly Thermal Generation at Prairie Island Unit 2 Cycles 17 through 31 (cont.)

Cycle 21		Cycle 22		Cycle 23		Cycle 24	
Month	**Thermal Generation [MW-Hr]**	**Month**	**Thermal Generation [MW-Hr]**	**Month**	**Thermal Generation [MW-Hr]**	**Month**	**Thermal Generation [MW-Hr]**
3/2/2002	1141963	10/10/2003	711673	6/11/2005	741210	12/15/2006	633256
4/1/2002	1166946	11/1/2003	1185786	7/1/2005	1224846	1/1/2007	1229041
5/1/2002	1225500	12/1/2003	1224823	8/1/2005	1224904	2/1/2007	1106467
6/1/2002	1185858	1/1/2004	1225381	9/1/2005	1184999	3/1/2007	846054
7/1/2002	1221635	2/1/2004	1146123	10/1/2005	1223543	4/1/2007	1043592
8/1/2002	1225458	3/1/2004	1225203	11/1/2005	1177296	5/1/2007	1227888
9/1/2002	1185913	4/1/2004	1155295	12/1/2005	1224848	6/1/2007	1187991
10/1/2002	1222094	5/1/2004	1225074	1/1/2006	1223916	7/1/2007	1227957
11/1/2002	1185952	6/1/2004	1185771	2/1/2006	487714	8/1/2007	1228169
12/1/2002	1225505	7/1/2004	1224369	3/1/2006	1224694	9/1/2007	1130705
1/1/2003	1206856	8/1/2004	1222124	4/1/2006	1176371	10/1/2007	1227781
2/1/2003	1106655	9/1/2004	1185565	5/1/2006	1228916	11/1/2007	1188861
3/1/2003	1224708	10/1/2004	1219475	6/1/2006	1189157	12/1/2007	1229147
4/1/2003	1165336	11/1/2004	1099413	7/1/2006	1188995	1/1/2008	1229835
5/1/2003	1225142	12/1/2004	1223666	8/1/2006	1228897	2/1/2008	1150644
6/1/2003	1185302	1/1/2005	1224633	9/1/2006	1165170	3/1/2008	1206182
7/1/2003	1224683	2/1/2005	1105536	10/1/2006	1216823	4/1/2008	1187368
8/1/2003	1207972	3/1/2005	1122097	11/1/2006	544083	5/1/2008	1226011
9/1/2003	407081	4/1/2005	471606			6/1/2008	1185834
		5/1/2005	0			7/1/2008	1225203
						8/1/2008	1224236
						9/1/2008	727472
						10/1/2008	0
Total	21940558	**Total**	21383613	**Total**	19876382	**Total**	24869695
EFPS	4.787E+07	**EFPS**	4.666E+07	**EFPS**	4.337E+07	**EFPS**	5.426E+07
EFPD	554.05	**EFPD**	539.99	**EFPD**	501.93	**EFPD**	628.02
EFPY	1.52	**EFPY**	1.48	**EFPY**	1.37	**EFPY**	1.72

Table A-2 Monthly Thermal Generation at Prairie Island Unit 2 Cycles 17 through 31 (cont.)

Cycle 25		Cycle 26		Cycle 27		Cycle 28	
Month	**Thermal Generation [MW-Hr]**	**Month**	**Thermal Generation [MW-Hr]**	**Month**	**Thermal Generation [MW-Hr]**	**Month**	**Thermal Generation [MW-Hr]**
11/1/2008	1043453	5/26/2010	181340	5/29/2012	32064	1/3/2014	973614
12/1/2008	1228706	6/1/2010	1183890	6/1/2012	1174547	2/1/2014	1128408
1/1/2009	1228724	7/1/2010	1226471	7/1/2012	1247728	3/1/2014	1236797
2/1/2009	1109454	8/1/2010	1226649	8/1/2012	1246540	4/1/2014	1207937
3/1/2009	1229385	9/1/2010	1183241	9/1/2012	1206440	5/1/2014	1001225
4/1/2009	1189241	10/1/2010	1227610	10/1/2012	1207071	6/1/2014	1203966
5/1/2009	1206648	11/1/2010	1206766	11/1/2012	1207742	7/1/2014	1247880
6/1/2009	1188775	12/1/2010	1246099	12/1/2012	1247012	8/1/2014	1247821
7/1/2009	1223052	1/1/2011	1246011	1/1/2013	1211658	9/1/2014	1205353
8/1/2009	1222790	2/1/2011	1126465	2/1/2013	1127094	10/1/2014	1083893
9/1/2009	1184118	3/1/2011	1247370	3/1/2013	1247860	11/1/2014	1207978
10/1/2009	1227379	4/1/2011	1202166	4/1/2013	1207453	12/1/2014	1247969
11/1/2009	1185142	5/1/2011	1181954	5/1/2013	1198727	1/1/2015	1248353
12/1/2009	1226266	6/1/2011	1203939	6/1/2013	1033796	2/1/2015	1127999
1/1/2010	1225975	7/1/2011	1244062	7/1/2013	1007918	3/1/2015	342250
2/1/2010	1110106	8/1/2011	1245244	8/1/2013	1008484	4/1/2015	1103690
3/1/2010	1229268	9/1/2011	1206628	9/1/2013	642402	5/1/2015	1233108
4/1/2010	602761	10/1/2011	585661	10/1/2013	0	6/1/2015	937272
		11/1/2011	1207636	11/1/2013	0	7/1/2015	1247623
		12/1/2011	1248018	12/1/2013	0	8/1/2015	1247039
		1/1/2012	1248637			9/1/2015	1209080
		2/1/2012	781320			10/1/2015	638708
		3/1/2012	0			11/1/2015	0
		4/1/2012	0				
Total	20861244	**Total**	24657176	**Total**	18254534	**Total**	24327965
EFPS	4.552E+07	**EFPS**	5.312E+07	**EFPS**	3.919E+07	**EFPS**	5.222E+07
EFPD	526.80	**EFPD**	614.81	**EFPD**	453.55	**EFPD**	604.45
EFPY	1.44	**EFPY**	1.68	**EFPY**	1.24	**EFPY**	1.65

Table A-2 Monthly Thermal Generation at Prairie Island Unit 2 Cycles 17 through 31 (cont.)

Cycle 29		Cycle 30		Cycle 31	
Month	**Thermal Generation [MW-Hr]**	**Month**	**Thermal Generation [MW-Hr]**	**Month**	**Thermal Generation [MW-Hr]**
12/5/2015	310537	11/21/2017	353040	10/28/2019	92447
1/1/2016	0	12/1/2017	1251387	11/1/2019	1211100
2/1/2016	211718	1/1/2018	1251004	12/1/2019	1251473
3/1/2016	1249663	2/1/2018	1130125	1/1/2020	1251331
4/1/2016	1209451	3/1/2018	1251040	2/1/2020	1169142
5/1/2016	1250183	4/1/2018	1206955	3/1/2020	1249699
6/1/2016	1208231	5/1/2018	1250965	4/1/2020	1208979
7/1/2016	1247211	6/1/2018	1210003	5/1/2020	1237156
8/1/2016	1247986	7/1/2018	1251370	6/1/2020	1183794
9/1/2016	1204150	8/1/2018	1251177	7/1/2020	1250514
10/1/2016	1247704	9/1/2018	1210055	8/1/2020	1250946
11/1/2016	1207974	10/1/2018	1251124	9/1/2020	1120784
12/1/2016	1249217	11/1/2018	1207350	10/1/2020	1252048
1/1/2017	1182008	12/1/2018	1250374	11/1/2020	1205131
2/1/2017	1130755	1/1/2019	1252476	12/1/2020	1252794
3/1/2017	1250940	2/1/2019	1131344	1/1/2021	1253136
4/1/2017	1147542	3/1/2019	1252656	2/1/2021	1131808
5/1/2017	1252118	4/1/2019	1211916	3/1/2021	1250685
6/1/2017	1211399	5/1/2019	1247839	4/1/2021	1212547
7/1/2017	1251833	6/1/2019	1211475	5/1/2021	1252614
8/1/2017	1250924	7/1/2019	1251166	6/1/2021	1211746
9/1/2017	1124021	8/1/2019	1237465	7/1/2021	1251771
10/1/2017	517064	9/1/2019	1009021	8/1/2021	1239063
		10/1/2019	109665	9/1/2021	1015179
				10/1/2021	11128
Total	24162628	**Total**	27240994	**Total**	28017016
EFPS	5.187E+07	**EFPS**	5.848E+07	**EFPS**	6.014E+07
EFPD	600.34	**EFPD**	676.83	**EFPD**	696.11
EFPY	1.64	**EFPY**	1.85	**EFPY**	1.91

Table A-3 Measured Sensor Activities and Reaction Rates for Surveillance Capsule V

Sample	Target Isotope	Measured Activity (dps/g)	Saturated Activity (dps/g)	Reaction Rate (rps/atom)	Average Reaction Rate (rps/atom)	Corrected Average Reaction Rate (rps/atom)
77-918	Cu-63	5.900E+04	4.320E+05	6.591E-17		
77-919	Cu-63	6.460E+04	4.730E+05	7.216E-17	6.903E-17	6.903E-17
77-921	Fe-54	2.370E+06	5.045E+06	8.004E-15		
77-922	Fe-54	2.210E+06	4.704E+06	7.464E-15		
77-923	Fe-54	2.340E+06	4.981E+06	7.903E-15		
77-924	Fe-54	2.430E+06	5.173E+06	8.207E-15		
77-925	Fe-54	2.490E+06	5.300E+06	8.409E-15	7.997E-15	7.997E-15
77-920	Ni-58	1.397E+07	7.543E+07	1.080E-14	1.080E-14	1.080E-14
77-926	U-238 (Cd)	2.620E+05	8.394E+06	5.512E-14	5.512E-14	4.532E-14
77-927	Np-237 (Cd)	2.250E+06	7.209E+07	4.526E-13	4.526E-13	4.459E-13
77-914	Co-59	2.150E+07	1.277E+08	8.334E-12		
77-916	Co-59	2.020E+07	1.200E+08	7.830E-12	8.082E-12	8.082E-12

Note(s):

1. Measured activity is decay corrected to 3/14/1977.

Table A-4 Measured Sensor Activities and Reaction Rates for Surveillance Capsule T

Sample	Target Isotope	Measured Activity (dps/g)	Saturated Activity (dps/g)	Reaction Rate (rps/atom)	Average Reaction Rate (rps/atom)	Corrected Average Reaction Rate (rps/atom)
80-2999	Cu-63	1.040E+05	3.315E+05	5.058E-17		
80-2003	Cu-63	1.160E+05	3.698E+05	5.641E-17	5.350E-17	5.350E-17
80-2997	Fe-54	1.650E+06	3.647E+06	5.786E-15		
80-2998	Fe-54	1.470E+06	3.249E+06	5.155E-15		
80-3000	Fe-54	1.650E+06	3.647E+06	5.786E-15		
80-3002	Fe-54	1.610E+06	3.559E+06	5.646E-15		
80-3006	Fe-54	1.720E+06	3.802E+06	6.032E-15	5.681E-15	5.681E-15
80-3001	Ni-58	1.790E+06	5.732E+07	8.206E-15	8.206E-15	8.206E-15
80-3007	U-238 (Cd)	4.840E+05	5.471E+06	3.592E-14	3.592E-14	2.901E-14
80-3008	Np-237 (Cd)	4.090E+06	4.623E+07	2.902E-13	2.902E-13	2.860E-13
80-2995	Co-59	2.650E+07	6.682E+07	4.360E-12		
80-3004	Co-59	2.600E+07	6.556E+07	4.277E-12	4.319E-12	4.319E-12

Note(s):

1. Measured activity is decay corrected to 12/2/1980.

Table A-5 Measured Sensor Activities and Reaction Rates for Surveillance Capsule R

Sample	Target Isotope	Measured Activity (dps/g)	Saturated Activity (dps/g)	Reaction Rate (rps/atom)	Average Reaction Rate (rps/atom)	Corrected Average Reaction Rate (rps/atom)
86-2035	Cu-63	2.380E+05	4.768E+05	7.274E-17		
86-2037	Cu-63	2.560E+05	5.129E+05	7.824E-17	7.549E-17	7.549E-17
86-2028	Fe-54	2.642E+06	5.404E+06	8.574E-15		
86-2036	Fe-54	2.431E+06	4.973E+06	7.889E-15		
86-2030	Fe-54	2.602E+06	5.322E+06	8.444E-15		
86-2038	Fe-54	2.525E+06	5.165E+06	8.194E-15		
86-2032	Fe-54	2.851E+06	5.832E+06	9.252E-15		
86-2033	Fe-54	2.789E+06	5.705E+06	9.051E-15	8.567E-15	8.567E-15
86-2031	Ni-58	3.320E+06	8.237E+07	1.179E-14	1.179E-14	1.179E-14
86-2025	U-238 (Cd)	2.165E+06	1.222E+07	8.025E-14	8.025E-14	5.661E-14
86-2026	Np-237 (Cd)	1.282E+07	7.237E+07	4.543E-13	4.543E-13	4.475E-13
86-2029	Co-59	6.924E+07	1.126E+08	7.343E-12		
86-2034	Co-59	7.604E+07	1.236E+08	8.064E-12	7.703E-12	7.703E-12

Note(s):

1. Measured activity is decay corrected to 7/22/1986.

Table A-6 Measured Sensor Activities and Reaction Rates for Surveillance Capsule P

Sample	Target Isotope	Measured Activity (dps/g)	Saturated Activity (dps/g)	Reaction Rate (rps/atom)	Average Reaction Rate (rps/atom)	Corrected Average Reaction Rate (rps/atom)
95-2274	Cu-63	1.980E+05	3.226E+05	4.921E-17		
95-2278	Cu-63	2.140E+05	3.487E+05	5.319E-17	5.120E-17	5.120E-17
95-2273	Fe-54	1.930E+06	3.312E+06	5.254E-15		
95-2275	Fe-54	1.650E+06	2.831E+06	4.492E-15		
95-2277	Fe-54	1.850E+06	3.174E+06	5.036E-15		
95-2279	Fe-54	1.780E+06	3.054E+06	4.846E-15		
95-2282	Fe-54	2.070E+06	3.552E+06	5.635E-15	5.053E-15	5.053E-15
95-2276	Ni-58	7.830E+06	4.984E+07	7.135E-15	7.135E-15	7.135E-15
95-2269	U-238 (Cd)	1.690E+06	5.421E+06	3.560E-14	3.560E-14	2.507E-14
95-2270	Np-237 (Cd)	1.160E+07	3.721E+07	2.336E-13	2.336E-13	2.302E-13
95-2271	Co-59	3.930E+07	5.065E+07	3.304E-12		
95-2280	Co-59	4.030E+07	5.193E+07	3.388E-12	3.346E-12	3.346E-12

Note(s):

1. Measured activity is decay corrected to 10/20/1995.

Table A-7 Measured Sensor Activities and Reaction Rates for Surveillance Capsule N

Sample	Target Isotope	Measured Activity (dps/g)	Saturated Activity (dps/g)	Reaction Rate (rps/atom)	Average Reaction Rate (rps/atom)	Corrected Average Reaction Rate (rps/atom)
30490505006	Cu-63	1.420E+05	2.202E+05	3.360E-17		
30490505009	Cu-63	1.510E+05	2.342E+05	3.572E-17	3.466E-17	3.466E-17
30490505004	Fe-54	1.320E+06	2.410E+06	3.823E-15		
30490505005	Fe-54	1.150E+06	2.099E+06	3.331E-15		
30490505008	Fe-54	1.220E+06	2.227E+06	3.533E-15		
30490505010	Fe-54	1.210E+06	2.209E+06	3.505E-15		
30490505011	Fe-54	1.240E+06	2.264E+06	3.591E-15	3.557E-15	3.557E-15
30490505007	Ni-58	3.430E+06	4.385E+07	6.279E-15	6.279E-15	6.279E-15
30490505001	U-238 (Cd)	3.130E+06	5.685E+06	3.733E-14	3.733E-14	2.226E-14
30490505002	Np-237 (Cd)	1.650E+07	2.997E+07	1.881E-13	1.881E-13	1.854E-13
30490505003	Co-59	3.780E+07	4.632E+07	3.022E-12	3.022E-12	3.022E-12

Note(s):

1. Measured activity is decay corrected to 5/15/2022.

Table A-8 Least-Squares Evaluation of Dosimetry in Surveillance Capsule V (13° Position, Core Midplane, Irradiated During Cycle 1)

χ^2/DOF = 0.199	Reaction Rate (rps/atom)					
Reaction	Measured (M)	Calculated (C)	Best-Estimate (BE)	M/C	M/BE	BE/C
^{63}Cu (n,α) ^{60}Co	6.90E-17	7.02E-17	6.78E-17	0.98	1.02	0.97
^{54}Fe (n,p) ^{54}Mn	8.00E-15	8.47E-15	8.06E-15	0.94	0.99	0.95
^{58}Ni (n,p) ^{58}Co	1.08E-14	1.18E-14	1.12E-14	0.91	0.97	0.94
^{238}U(Cd) (n,f) ^{137}Cs	4.53E-14	4.50E-14	4.36E-14	1.01	1.04	0.97
^{237}Np(Cd) (n,f) ^{137}Cs	4.46E-13	3.95E-13	4.18E-13	1.13	1.06	1.06
^{59}Co (n,γ) ^{60}Co	8.08E-12	1.01E-11	8.13E-12	0.80	0.99	0.80
Average of Fast Energy Threshold Reactions				0.99	1.02	0.98
Percent Standard Deviation				8.6	3.6	4.9

Integral Quantity	Calculated (C)	% Unc.	Best-Estimate (BE)	% Unc.	BE/C
Neutron Fluence Rate (E > 1.0 MeV) (n/cm^2-s)	1.37E+11	13	1.34E+11	6	0.98
Displacement Rate (dpa/s)	2.46E-10	13	2.44E-10	7	0.99

Table A-9 Least-Squares Evaluation of Dosimetry in Surveillance Capsule T (23° Position, Core Midplane, Irradiated During Cycles 1 through 4)

χ^2/DOF = 0.176	Reaction Rate (rps/atom)					
Reaction	Measured (M)	Calculated (C)	Best-Estimate (BE)	M/C	M/BE	BE/C
^{63}Cu (n,α) ^{60}Co	5.35E-17	5.62E-17	5.34E-17	0.95	1.00	0.95
^{54}Fe (n,p) ^{54}Mn	5.68E-15	6.04E-15	5.83E-15	0.94	0.97	0.96
^{58}Ni (n,p) ^{58}Co	8.21E-15	8.30E-15	8.14E-15	0.99	1.01	0.98
^{238}U(Cd) (n,f) ^{137}Cs	2.90E-14	2.93E-14	2.93E-14	0.99	0.99	1.00
^{237}Np(Cd) (n,f) ^{137}Cs	2.86E-13	2.34E-13	2.63E-13	1.22	1.09	1.12
^{59}Co (n,γ) ^{60}Co	4.32E-12	5.16E-12	4.34E-12	0.84	1.00	0.84
Average of Fast Energy Threshold Reactions				1.02	1.01	1.00
Percent Standard Deviation				11.3	4.5	6.9

Integral Quantity	Calculated (C)	% Unc.	Best-Estimate (BE)	% Unc.	BE/C
Neutron Fluence Rate (E > 1.0 MeV) (n/cm^2-s)	8.49E+10	13	8.68E+10	6	1.02
Displacement Rate (dpa/s)	1.46E-10	13	1.51E-10	7	1.03

Table A-10 Least-Squares Evaluation of Dosimetry in Surveillance Capsule R (13° Position, Core Midplane, Irradiated During Cycles 1 through 9)

χ^2/DOF = 0.684	Reaction Rate (rps/atom)					
Reaction	Measured (M)	Calculated (C)	Best-Estimate (BE)	M/C	M/BE	BE/C
^{63}Cu (n,α) ^{60}Co	7.55E-17	7.62E-17	7.39E-17	0.99	1.02	0.97
^{54}Fe (n,p) ^{54}Mn	8.57E-15	9.19E-15	8.80E-15	0.93	0.97	0.96
^{58}Ni (n,p) ^{58}Co	1.18E-14	1.28E-14	1.22E-14	0.92	0.96	0.95
^{238}U(Cd) (n,f) ^{137}Cs	5.66E-14	4.89E-14	4.82E-14	1.16	1.18	0.99
^{237}Np(Cd) (n,f) ^{137}Cs	4.47E-13	4.30E-13	4.39E-13	1.04	1.02	1.02
^{59}Co (n,γ) ^{60}Co	7.70E-12	1.10E-11	7.78E-12	0.70	0.99	0.71
Average of Fast Energy Threshold Reactions				1.01	1.03	0.98
Percent Standard Deviation				9.7	8.6	2.8

Integral Quantity	Calculated (C)	% Unc.	Best-Estimate (BE)	% Unc.	BE/C
Neutron Fluence Rate (E > 1.0 MeV) (n/cm^2-s)	1.48E+11	13	1.48E+11	6	1.00
Displacement Rate (dpa/s)	2.67E-10	13	2.67E-10	7	1.00

Table A-11 Least-Squares Evaluation of Dosimetry in Surveillance Capsule P (33° Position, Core Midplane, Irradiated During Cycles 1 through 16)

χ^2/DOF = 0.139	Reaction Rate (rps/atom)					
Reaction	Measured (M)	Calculated (C)	Best-Estimate (BE)	M/C	M/BE	BE/C
^{63}Cu (n,α) ^{60}Co	5.12E-17	5.36E-17	5.03E-17	0.96	1.02	0.94
^{54}Fe (n,p) ^{54}Mn	5.05E-15	5.68E-15	5.18E-15	0.89	0.97	0.91
^{58}Ni (n,p) ^{58}Co	7.13E-15	7.79E-15	7.16E-15	0.92	1.00	0.92
^{238}U(Cd) (n,f) ^{137}Cs	2.51E-14	2.73E-14	2.53E-14	0.92	0.99	0.93
^{237}Np(Cd) (n,f) ^{137}Cs	2.30E-13	2.17E-13	2.17E-13	1.06	1.06	1.00
^{59}Co (n,γ) ^{60}Co	3.35E-12	4.73E-12	3.38E-12	0.71	0.99	0.71
Average of Fast Energy Threshold Reactions				0.95	1.01	0.94
Percent Standard Deviation				7.0	3.4	3.8

Integral Quantity	Calculated (C)	% Unc.	Best-Estimate (BE)	% Unc.	BE/C
Neutron Fluence Rate (E > 1.0 MeV) (n/cm^2-s)	7.88E+10	13	7.37E+10	6	0.93
Displacement Rate (dpa/s)	1.35E-10	13	1.28E-10	7	0.95

Table A-12 Least-Squares Evaluation of Dosimetry in Surveillance Capsule N (33° Position, Core Midplane, Irradiated During Cycles 1 through 31) – Case 1

χ^2/DOF = 1.128	Reaction Rate (rps/atom)					
Reaction	Measured (M)	Calculated (C)	Best-Estimate (BE)	M/C	M/BE	BE/C
^{63}Cu (n,α) ^{60}Co	3.47E-17	4.23E-17	3.52E-17	0.82	0.98	0.83
^{54}Fe (n,p) ^{54}Mn	3.56E-15	4.57E-15	3.92E-15	0.78	0.91	0.86
^{58}Ni (n,p) ^{58}Co	6.28E-15	6.30E-15	5.80E-15	1.00	1.09	0.92
^{238}U(Cd) (n,f) ^{137}Cs	2.23E-14	2.25E-14	2.09E-14	0.99	1.06	0.93
^{237}Np(Cd) (n,f) ^{137}Cs	1.85E-13	1.82E-13	1.81E-13	1.02	1.02	0.99
^{59}Co (n,γ) ^{60}Co	3.02E-12	3.98E-12	3.04E-12	0.76	0.99	0.76
Average of Fast Energy Threshold Reactions				0.92	1.01	0.91
Percent Standard Deviation				12.2	7.0	6.9

Integral Quantity	Calculated (C)	% Unc.	Best-Estimate (BE)	% Unc.	BE/C
Neutron Fluence Rate (E > 1.0 MeV) (n/cm^2-s)	6.57E+10	13	6.27E+10	6	0.95
Displacement Rate (dpa/s)	1.13E-10	13	1.09E-10	7	0.96

Table A-13 Least-Squares Evaluation of Dosimetry in Surveillance Capsule N (33° Position, Core Midplane, Irradiated During Cycles 1 through 31) – Case 2

χ^2/DOF = 0.512	Reaction Rate (rps/atom)					
Reaction	Measured (M)	Calculated (C)	Best-Estimate (BE)	M/C	M/BE	BE/C
^{63}Cu (n,α) ^{60}Co	3.47E-17	4.23E-17	3.64E-17	0.82	0.95	0.86
^{54}Fe (n,p) ^{54}Mn	3.56E-15	4.57E-15	4.04E-15	0.78	0.88	0.88
^{58}Ni (n,p) ^{58}Co	6.28E-15	6.30E-15	5.71E-15	1.00	1.10	0.91
^{238}U(Cd) (n,f) ^{137}Cs	2.23E-14	2.25E-14	2.07E-14	0.99	1.08	0.92
^{237}Np(Cd) (n,f) ^{137}Cs	1.85E-13	1.82E-13	1.76E-13	1.02	1.05	0.97
^{59}Co (n,γ) ^{60}Co	3.02E-12	3.98E-12	3.09E-12	0.76	0.98	0.78
Average of Fast Energy Threshold Reactions				0.92	1.01	0.91
Percent Standard Deviation				12.2	9.3	4.6

Integral Quantity	Calculated (C)	% Unc.	Best-Estimate (BE)	% Unc.	BE/C
Neutron Fluence Rate (E > 1.0 MeV) (n/cm^2-s)	6.57E+10	13	6.16E+10	7	0.94
Displacement Rate (dpa/s)	1.13E-10	13	1.07E-10	8	0.94

Table A-14 Measured-to-Calculated (M/C) Reaction Rates – In-Vessel Capsules

Reaction	Capsule					Average	% Std. Dev.
	V	T	R	P	N		
^{63}Cu (n,α) ^{60}Co	0.98	0.95	0.99	0.96	0.82	0.94	7.3
^{54}Fe (n,p) ^{54}Mn	0.94	0.94	0.93	0.89	0.78	0.90	7.6
^{58}Ni (n,p) ^{58}Co	0.91	0.99	0.92	0.92	1.00	0.95	4.6
^{238}U(Cd) (n,f) ^{137}Cs	1.01	0.99	1.16	0.92	0.99	1.01	8.7
^{237}Np(Cd) (n,f) ^{137}Cs	1.13	1.22	1.04	1.06	1.02	1.09	7.5
Average of M/C Results						0.98	9.8

Table A-15 Best-Estimate-to-Calculated (BE/C) Exposure Rates – In-Vessel Capsules

Capsule	Neutron Fluence (E > 1.0 MeV) Rate BE/C	Iron Atom Displacement Rate BE/C
V	0.98	0.99
T	1.02	1.03
R	1.00	1.00
P	0.93	0.95
N	0.94	0.94
Average	0.97	0.98
% Std. Dev.	3.9	3.8

A.2 REFERENCES

A-1 U.S. Nuclear Regulatory Commission Regulatory Guide 1.190, "Calculational and Dosimetry Methods for Determining Pressure Vessel Neutron Fluence," March 2001. *[ADAMS Accession Number ML010890301]*

A-2 Westinghouse Report, WCAP-14613, Rev. 2, "Analysis of Capsule P from the Northern States Power Company Prairie Island Unit 2 Reactor Vessel Radiation Surveillance Program," February 1998.

A-3 A. Schmittroth, FERRET Data Analysis Core, HEDL-TME 79-40, Hanford Engineering Development Laboratory, Richland, WA, September 1979.

A-4 RSICC Data Library Collection DLC-178, SNLRML Recommended Dosimetry Cross-Section Compendium, July 1994.

A-5 ASTM Standard E944-19, Standard Guide for Application of Neutron Spectrum Adjustment Methods in Reactor Surveillance, 2019.

A-6 ASTM Standard E844-18, Standard Guide for Sensor Set Design and Irradiation for Reactor Surveillance, 2018.

APPENDIX B LOAD-TIME RECORDS FOR CHARPY SPECIMEN TESTS FROM CAPSULE N

- "NLXX" denotes Lower Shell Forging D (Heat # 22642), Tangential Orientation
- "NTXX" denotes Lower Shell Forging D (Heat # 22642), Axial Orientation
- "NWXX" denotes Surveillance Weld material
- "NHXX" denotes Heat-Affected Zone (HAZ) material
- "RXX" denotes Correlation Monitor material

Note that the instrumented Charpy data is not required per ASTM Standards E185-82 or E23-18.

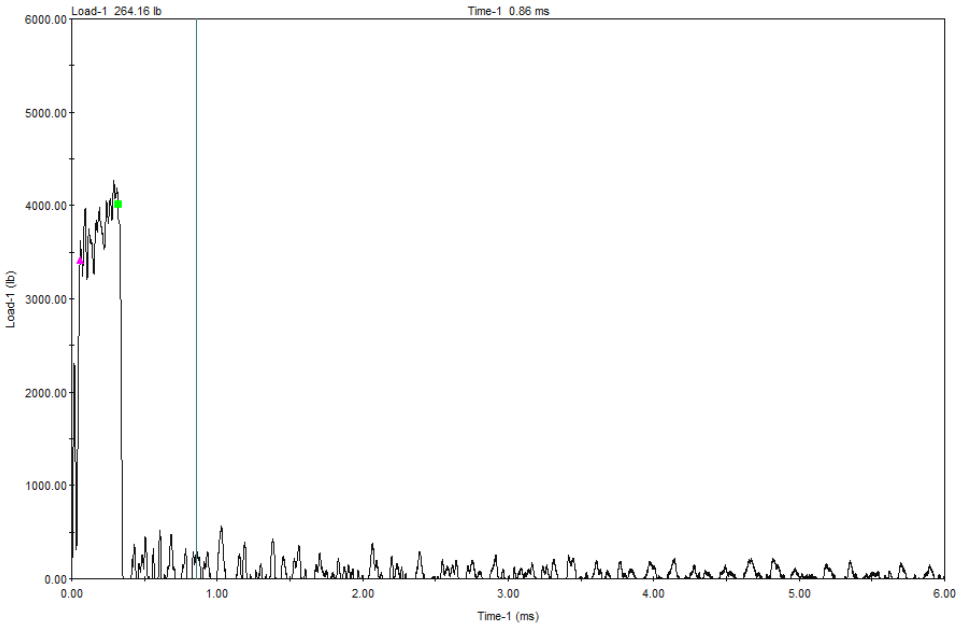

NL59: Tested at 73°F

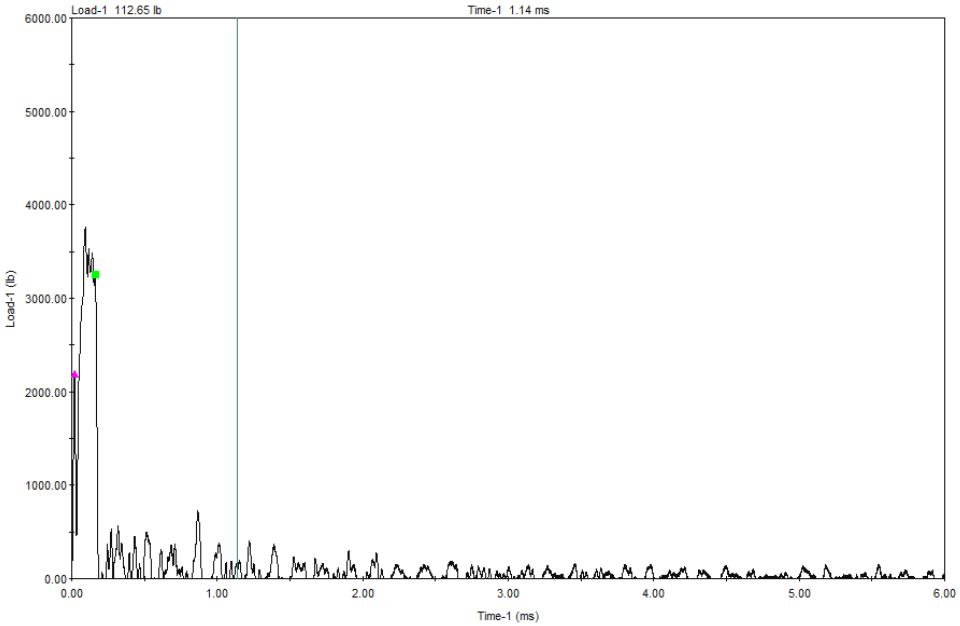

NL56: Tested at 120°F

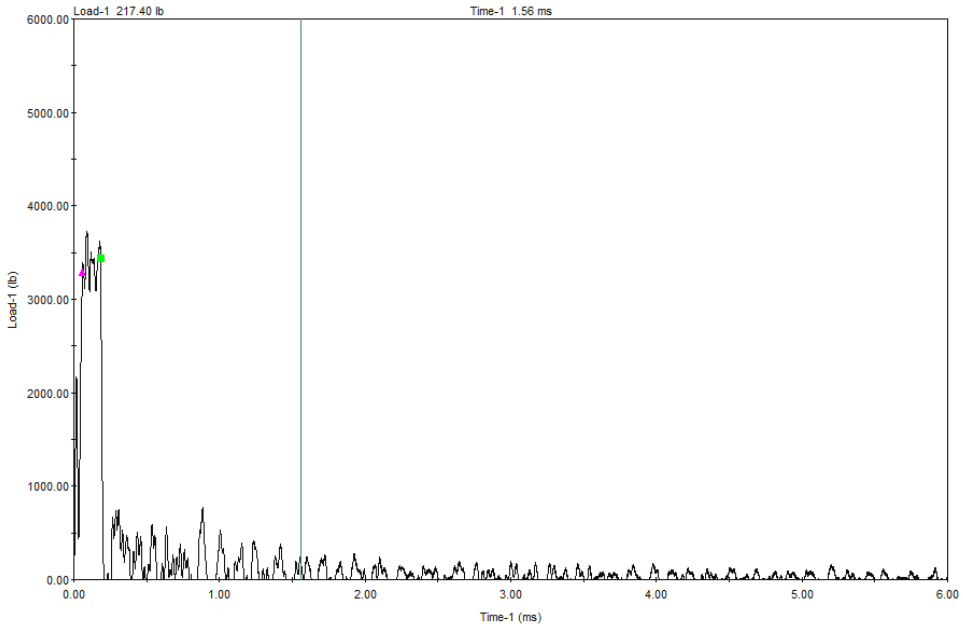

NL53: Tested at 130°F

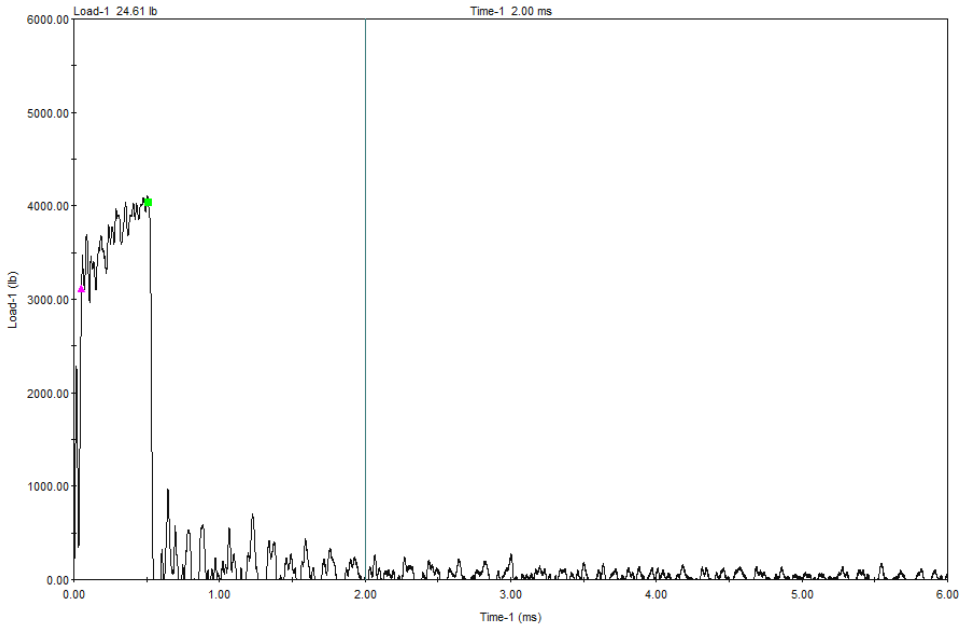

NL57: Tested at 140°F

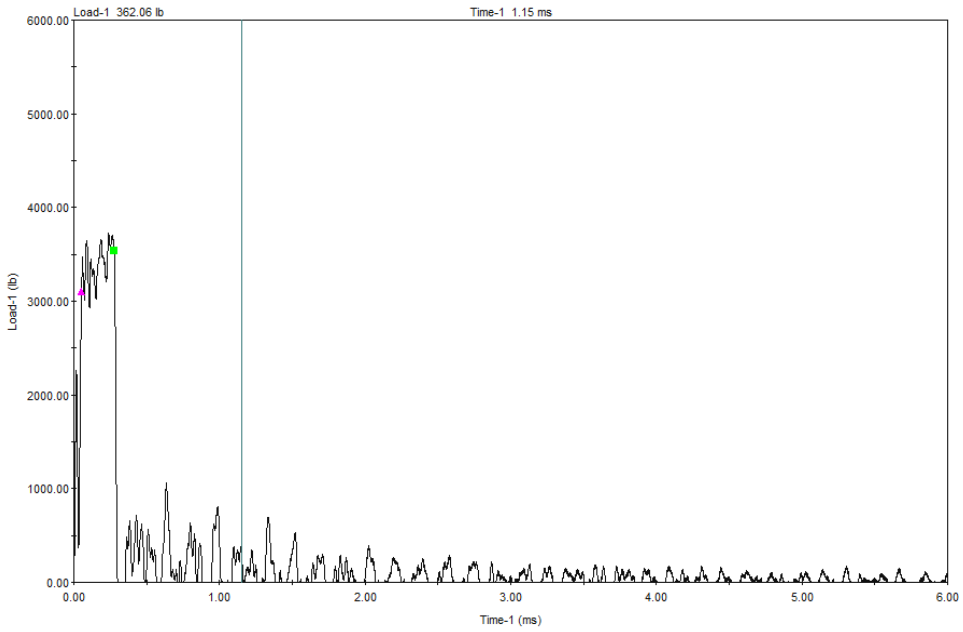

NL51: Tested at 155°F

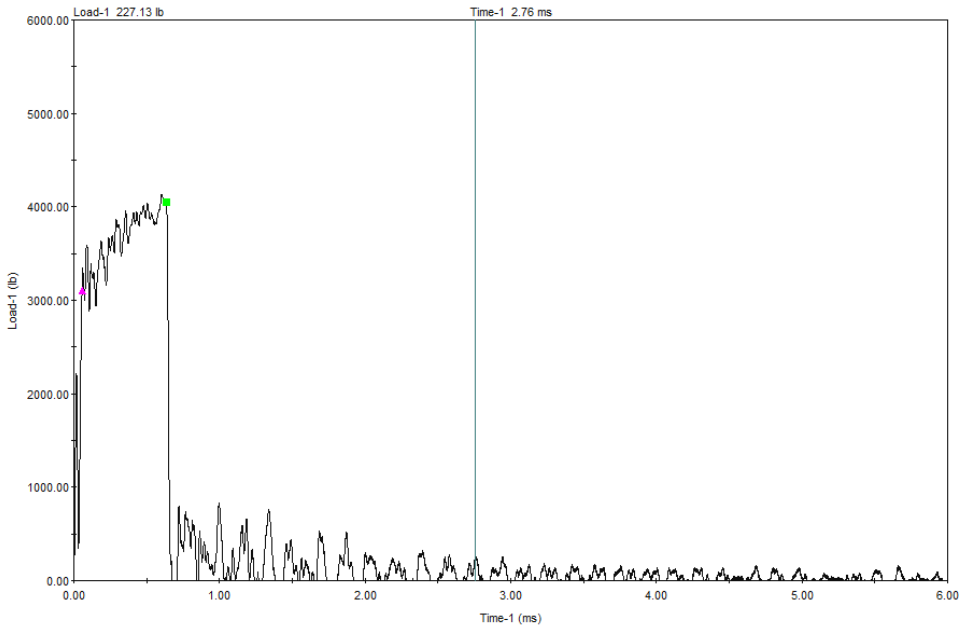

NL49: Tested at 165°F

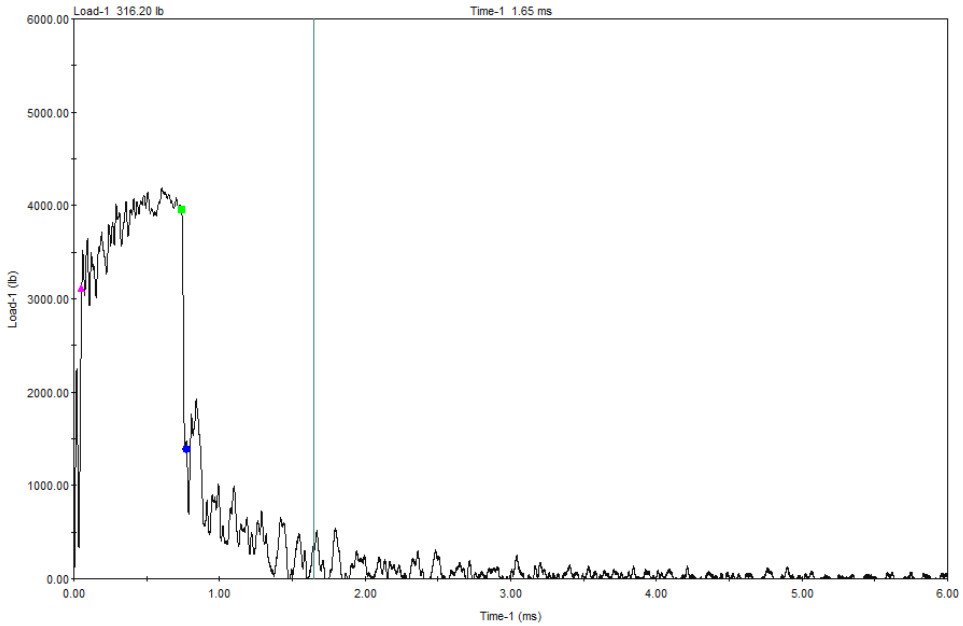

NL58: Tested at 175°F

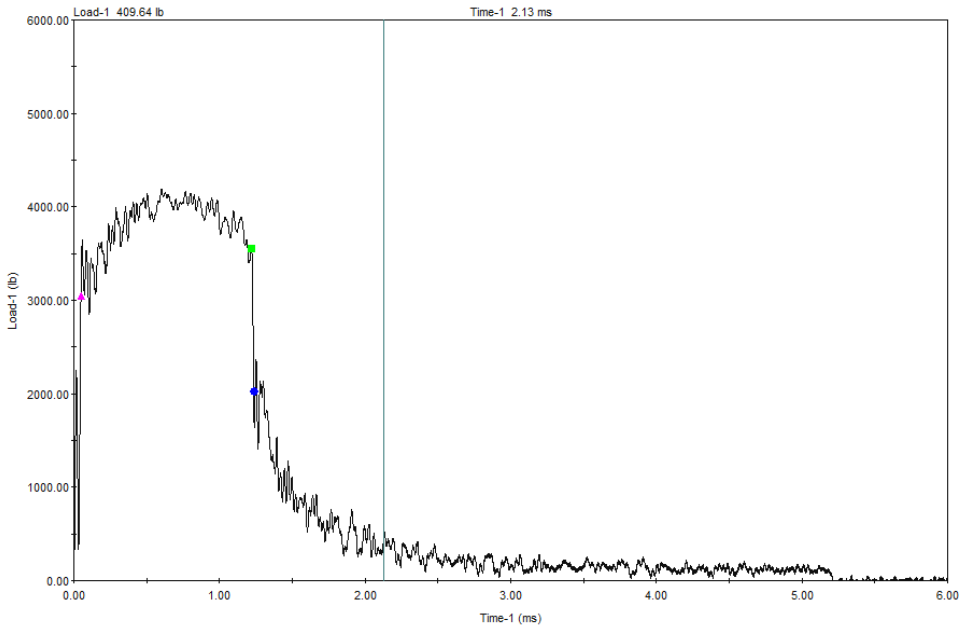

NL55: Tested at 200°F

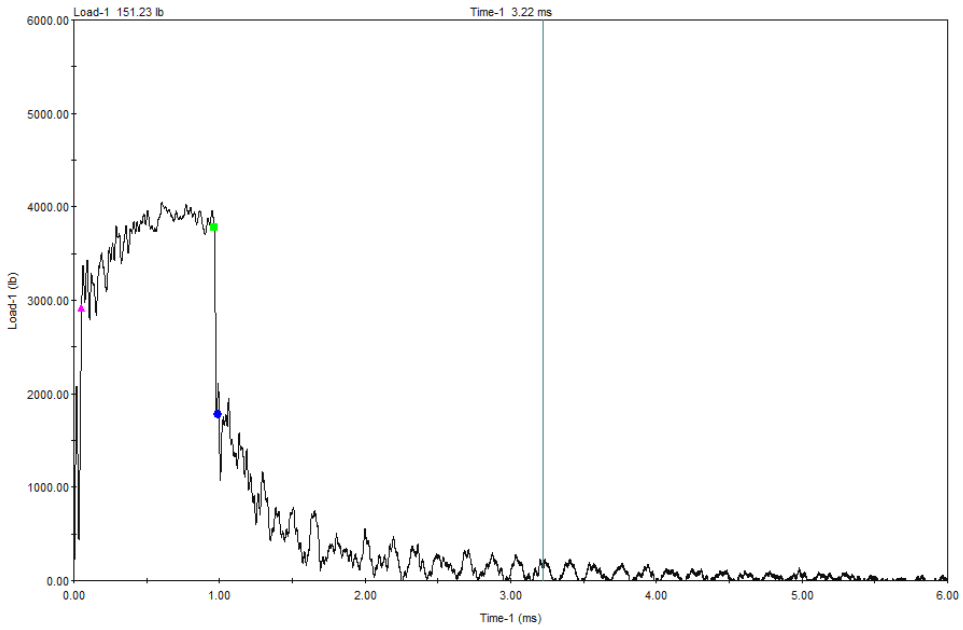

NL60: Tested at 225°F

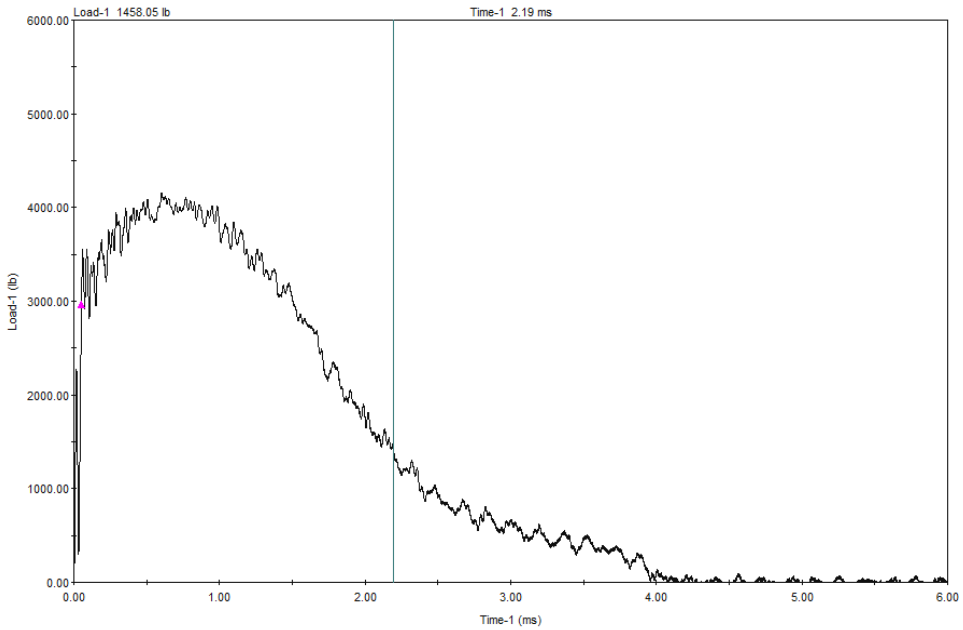

NL52: Tested at 250°F

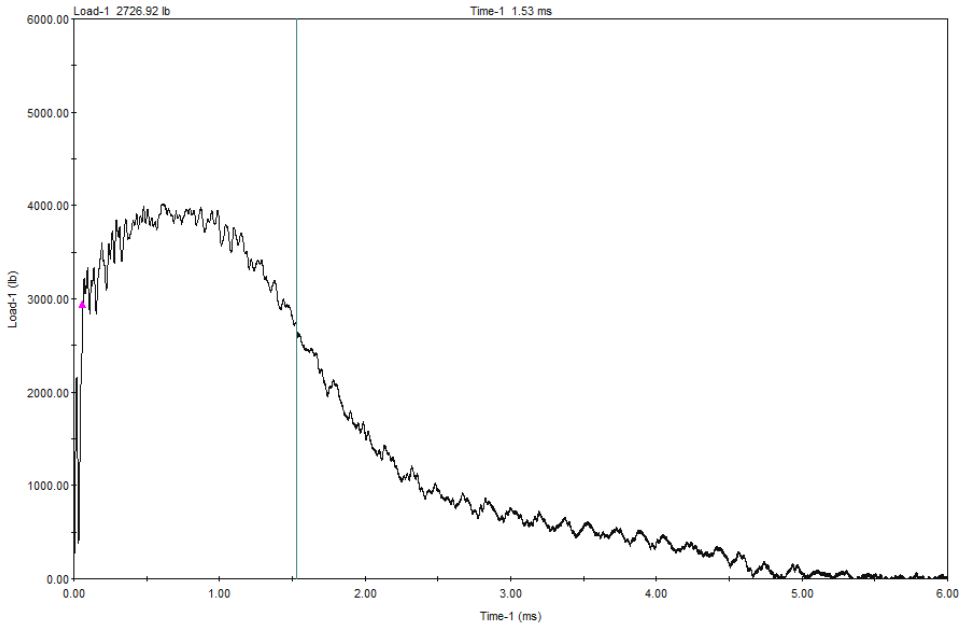

NL54: Tested at 300°F

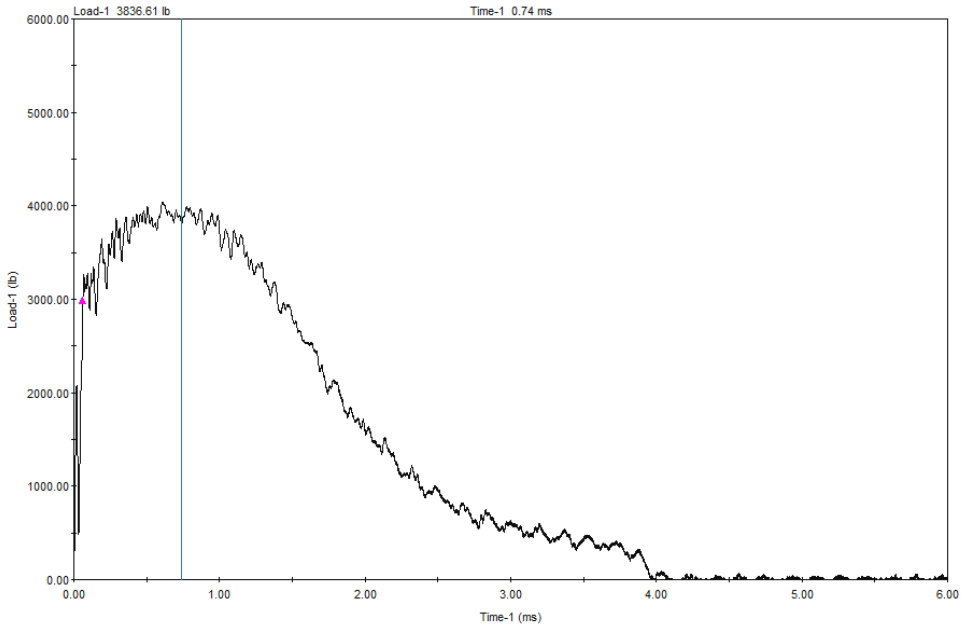

NL50: Tested at 325°F

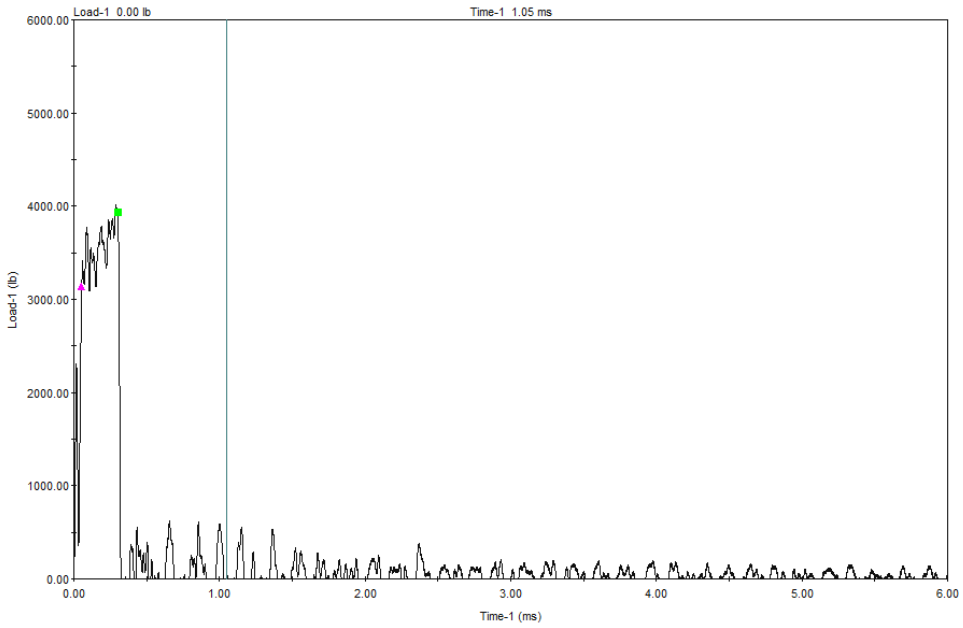

NT54: Tested at 100°F

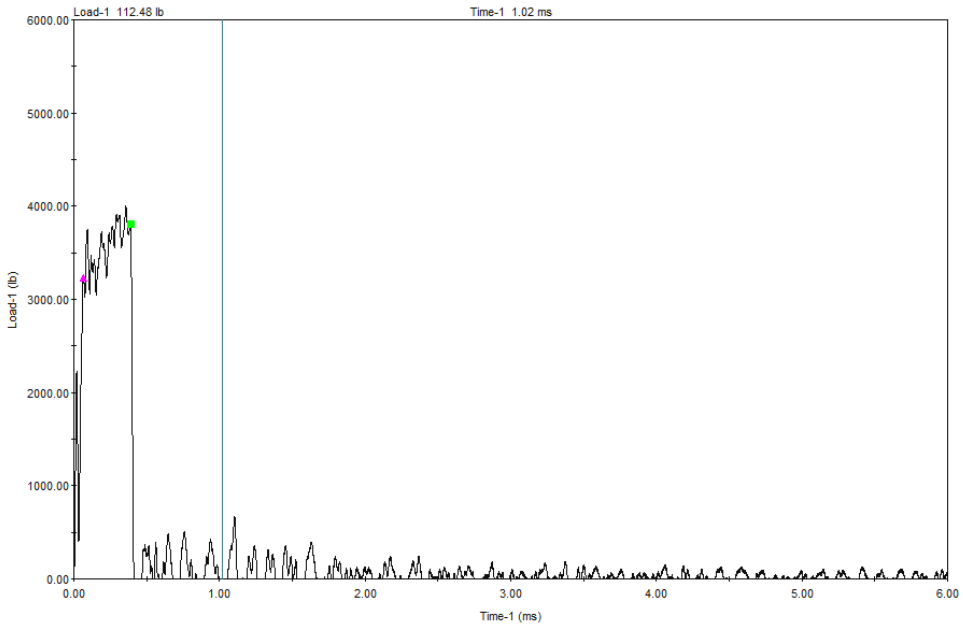

NT56: Tested at 120°F

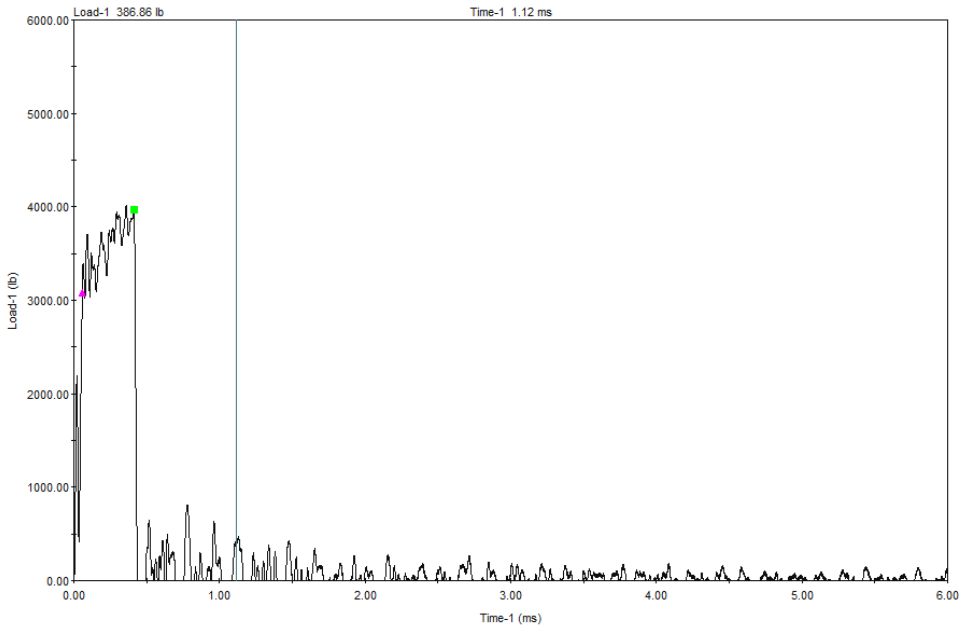

NT49: Tested at 140°F

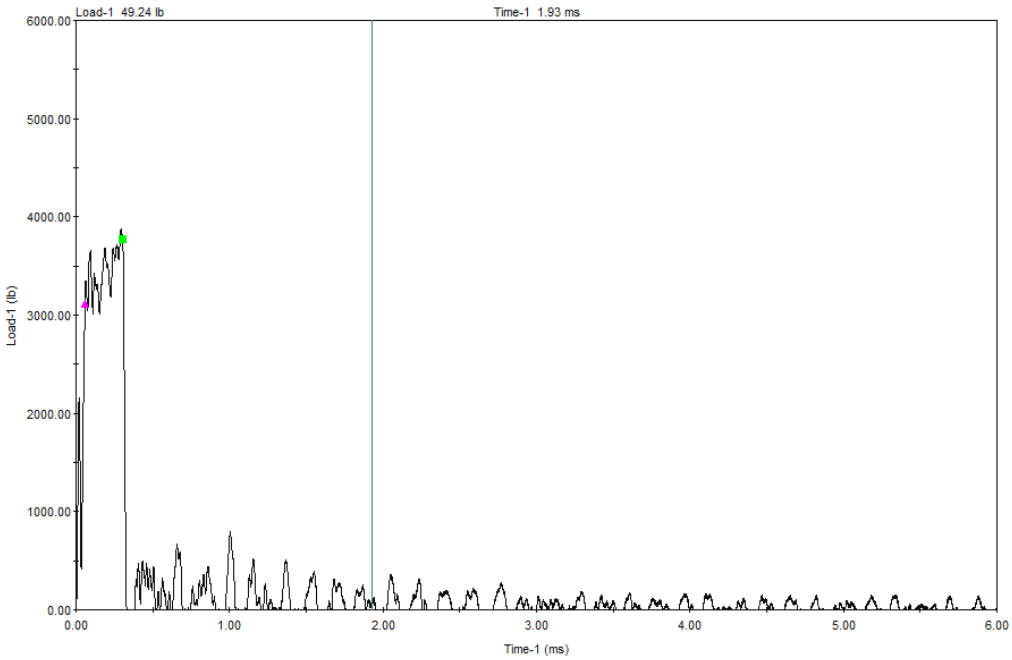

NT59: Tested at 155°F

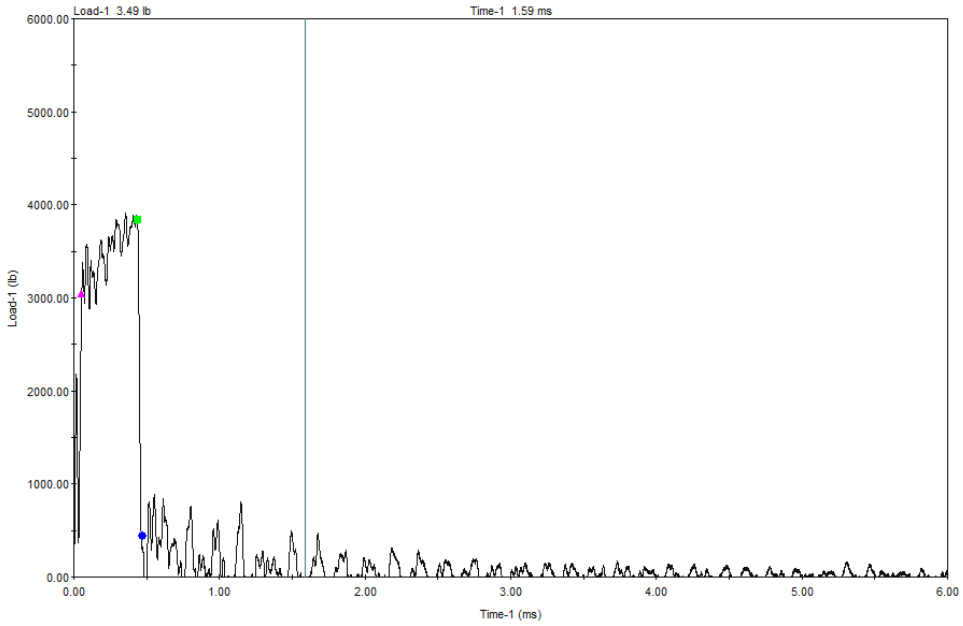

NT58: Tested at 165°F

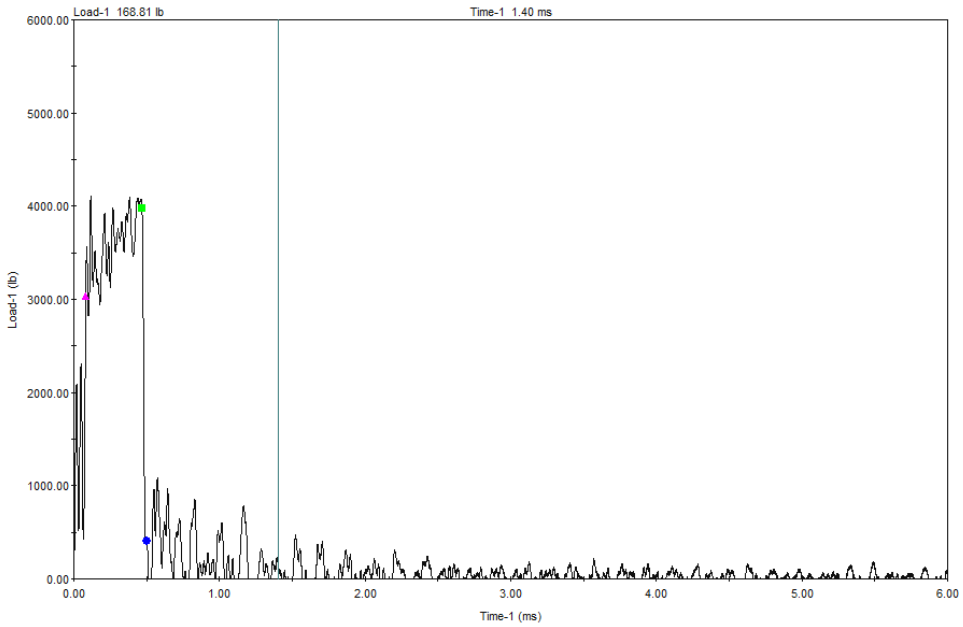

NT53: Tested at 170°F

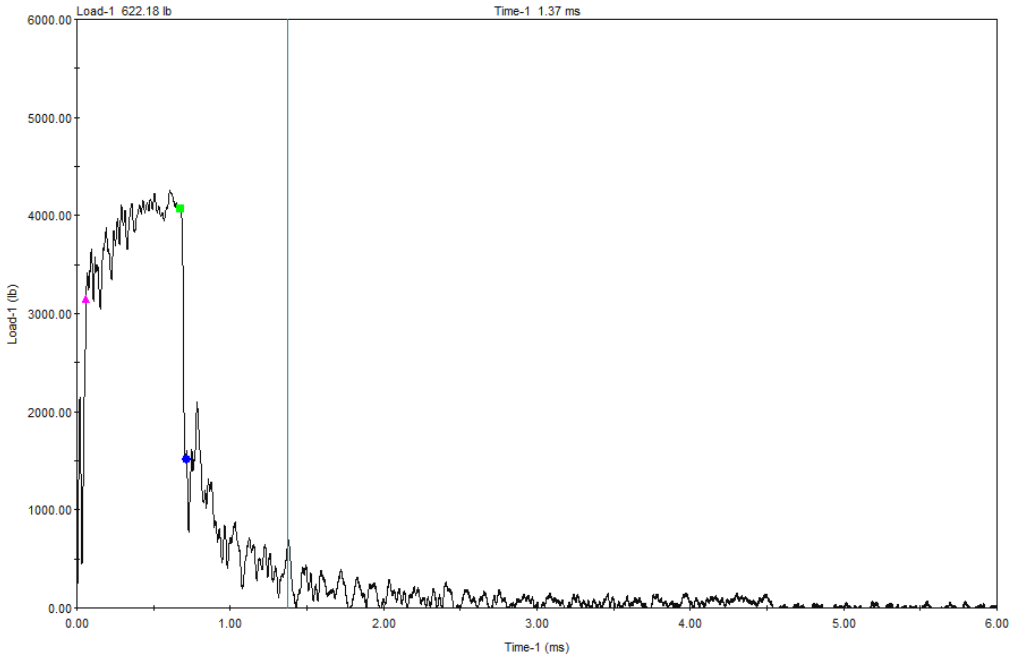

NT60: Tested at 175°F

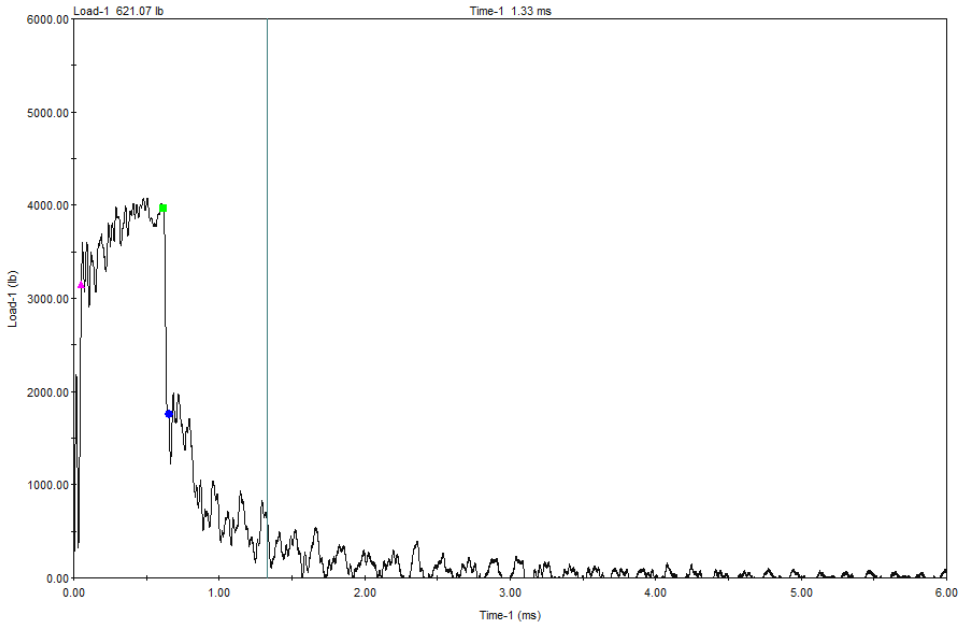

NT57: Tested at 200°F

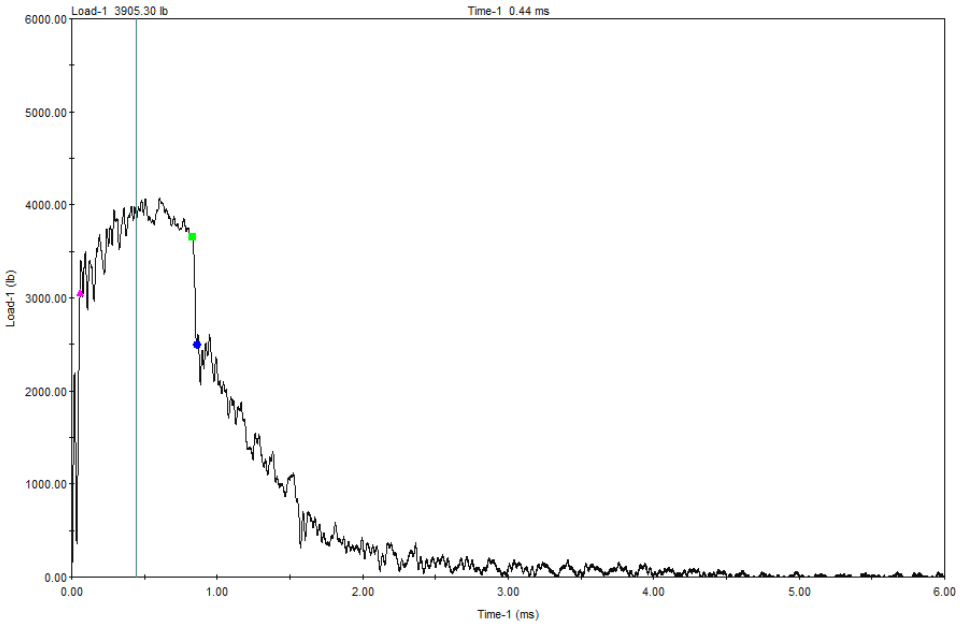

NT55: Tested at 225°F

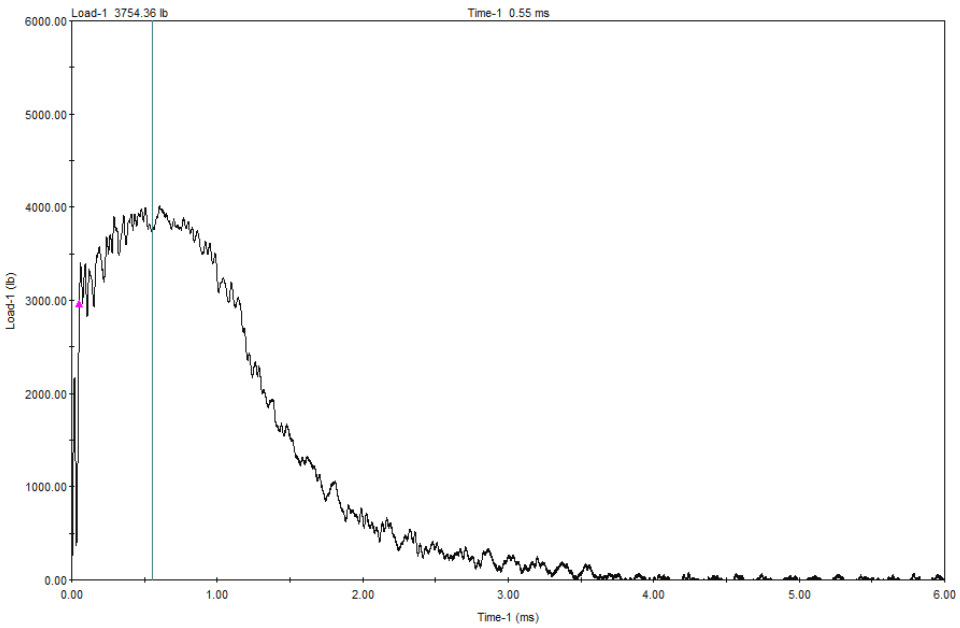

NT51: Tested at 275°F

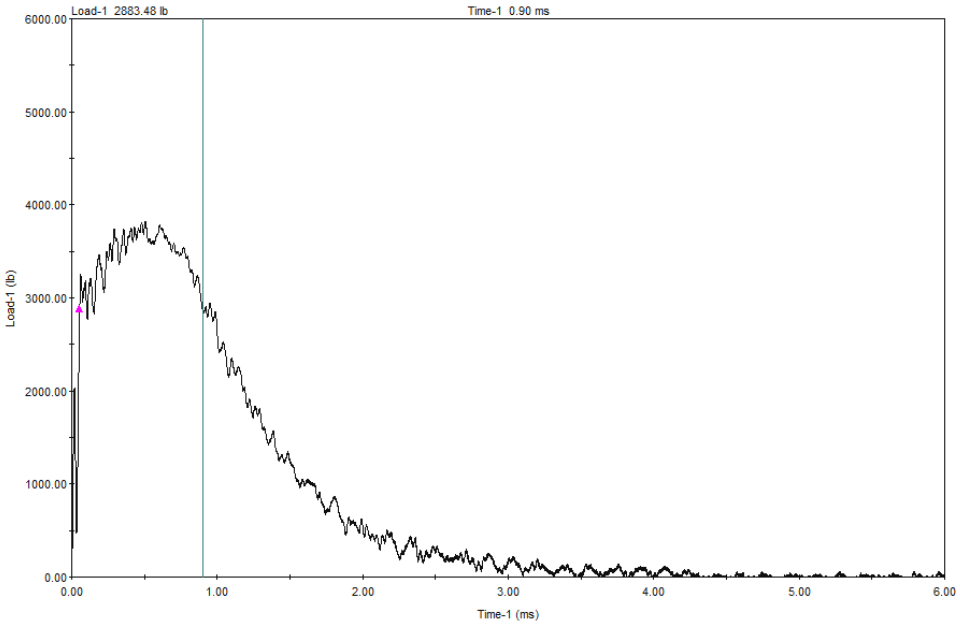

NT50: Tested at 300°F

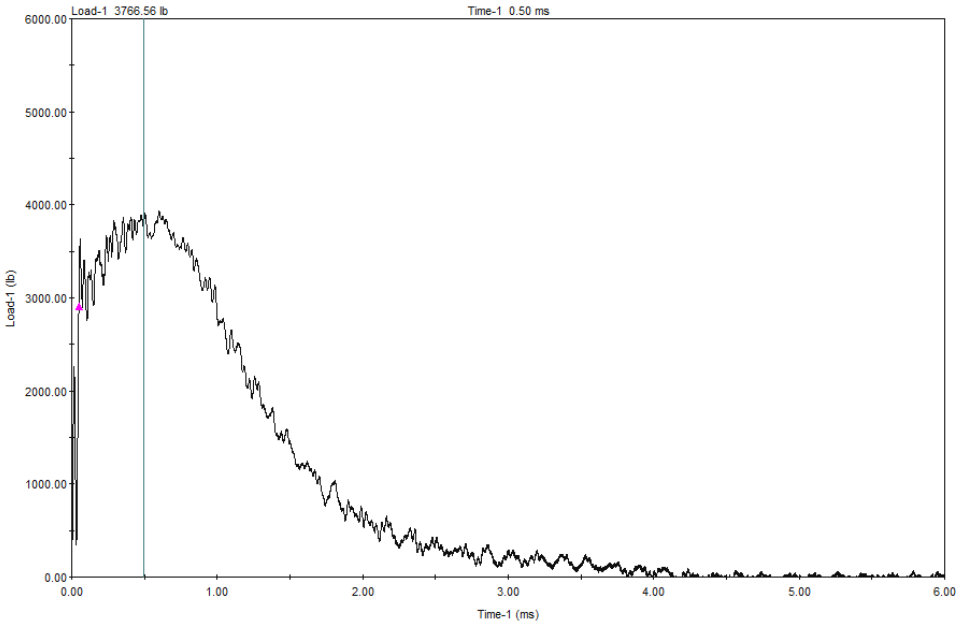

NT52: Tested at 325°F

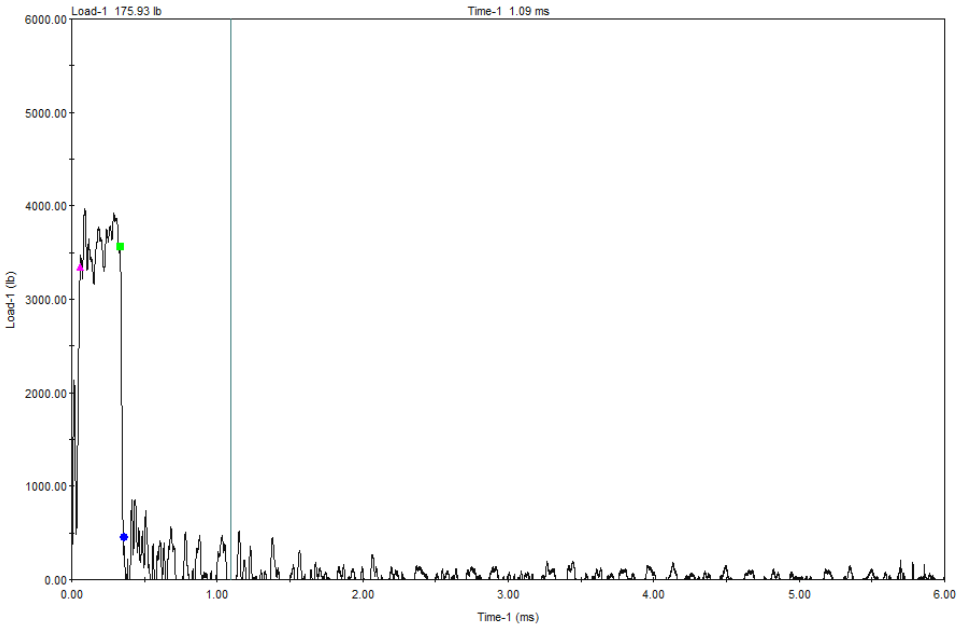

NW36: Tested at 30°F

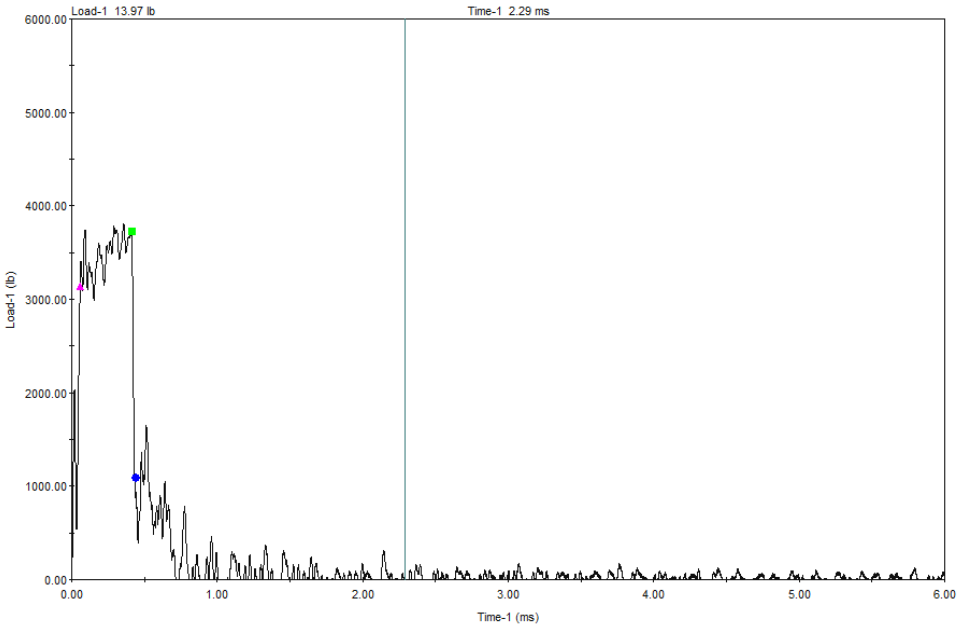

NW39: Tested at 50°F

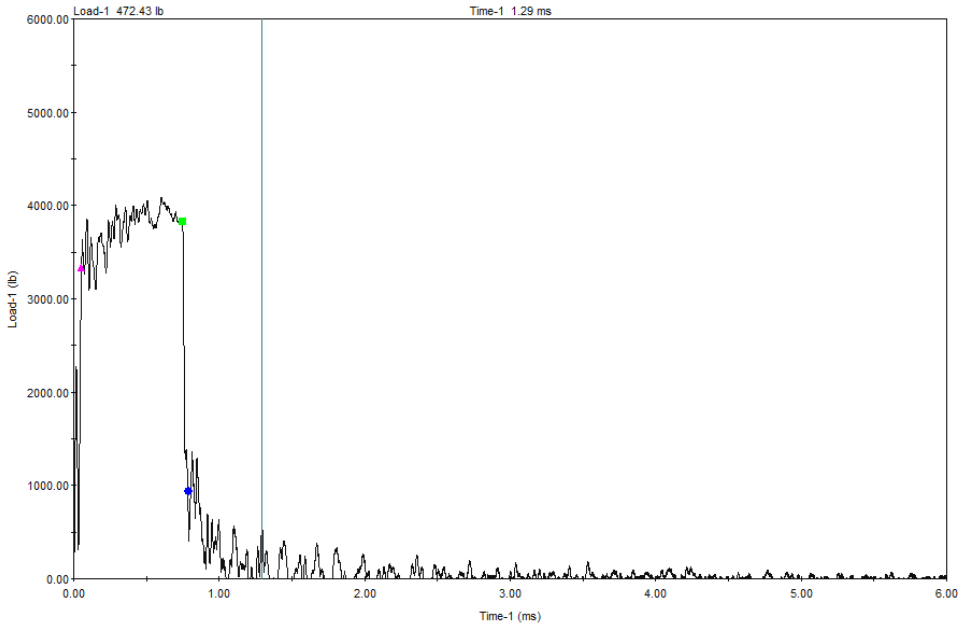

NW38: Tested at 73°F

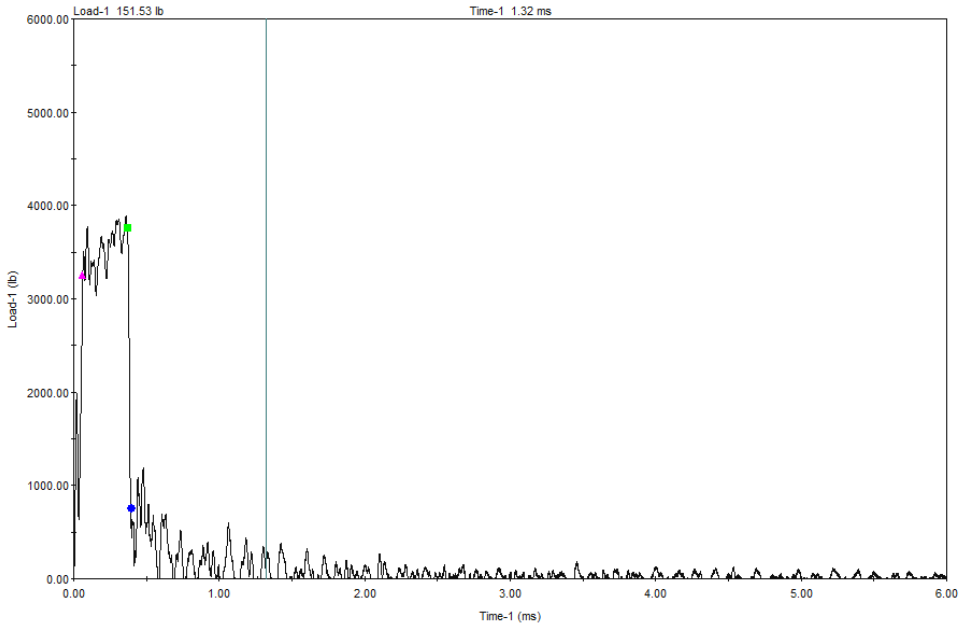

NW40: Tested at 100°F

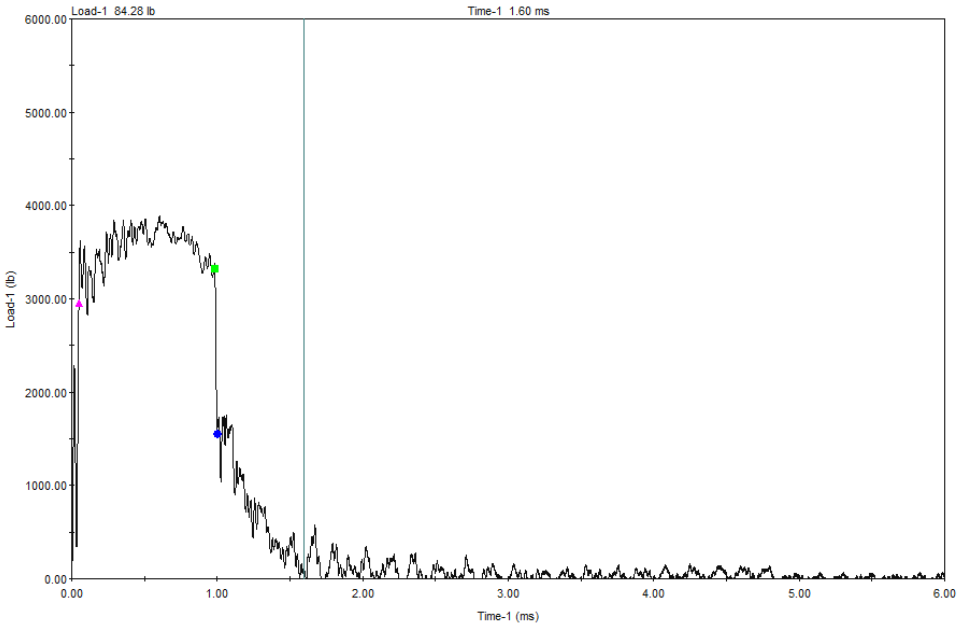

NW37: Tested at 175°F

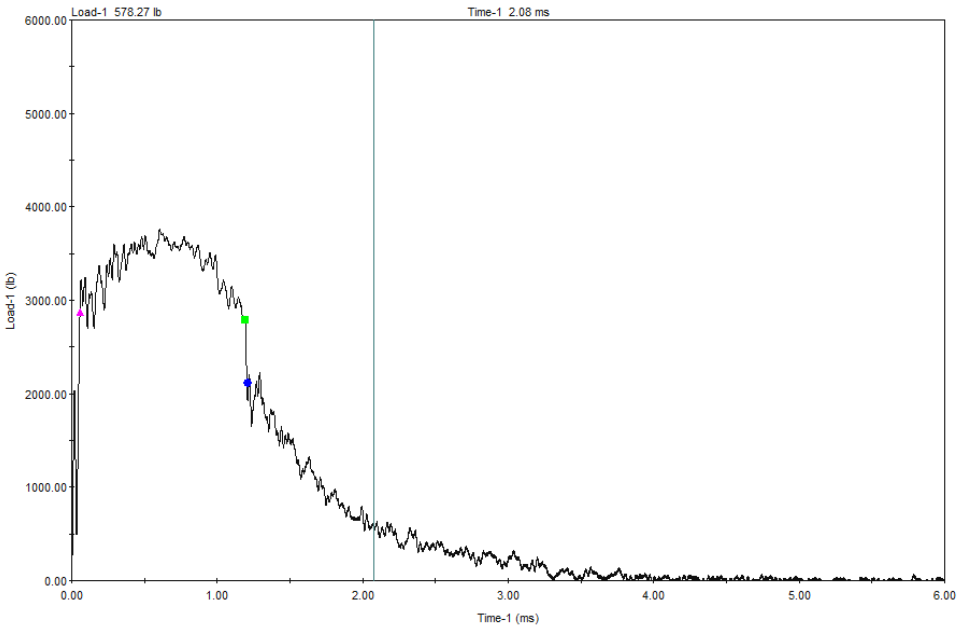

NW35: Tested at 225°F

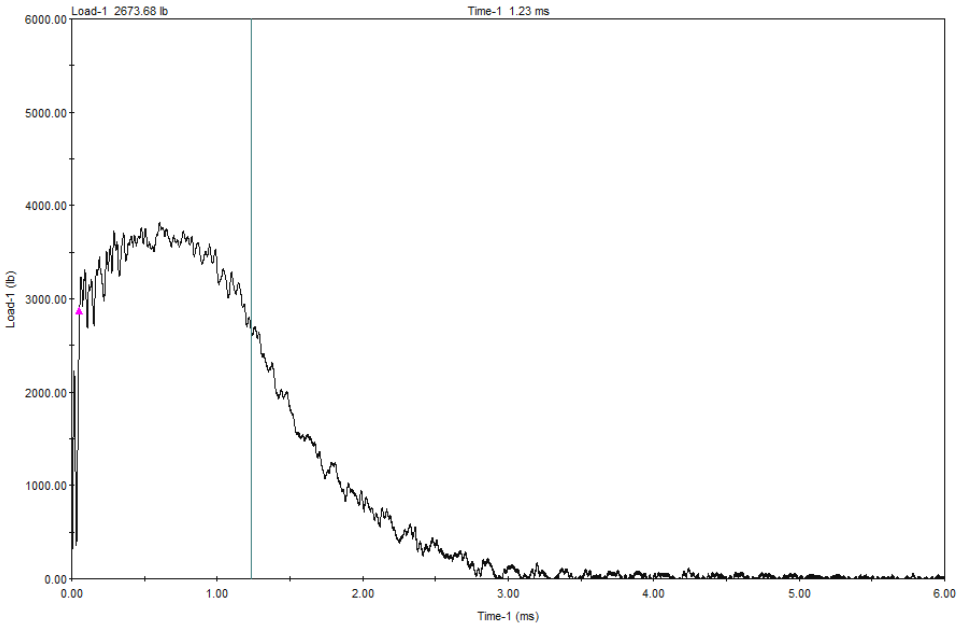

NW33: Tested at 275°F

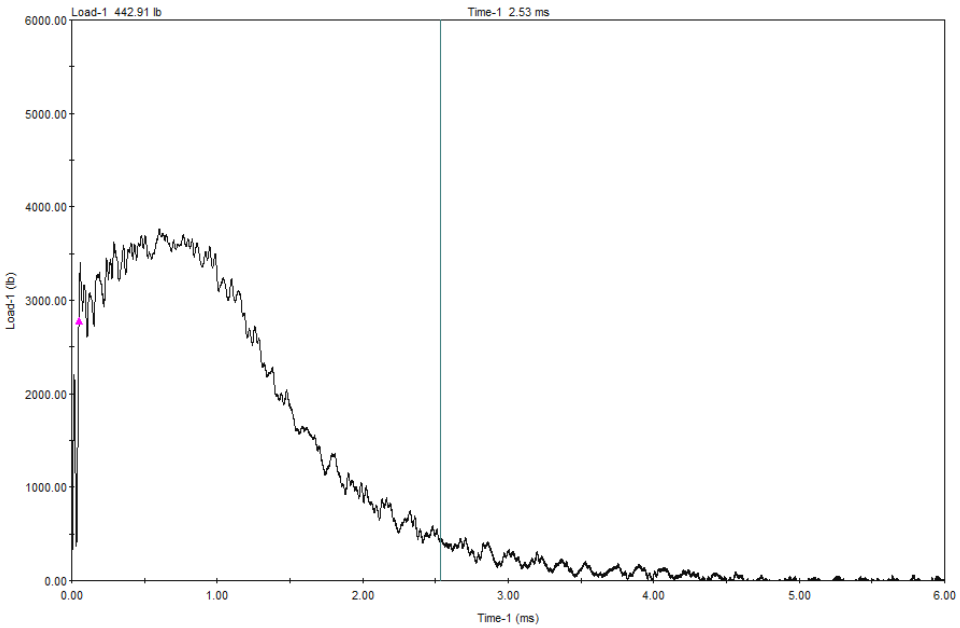

NW34: Tested at 300°F

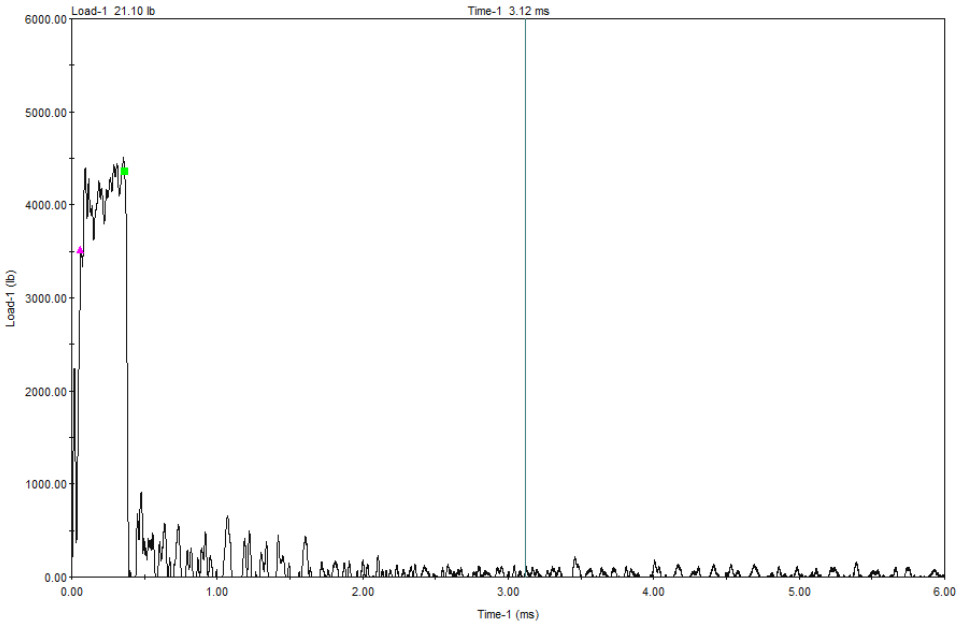

NH39: Tested at -25°F

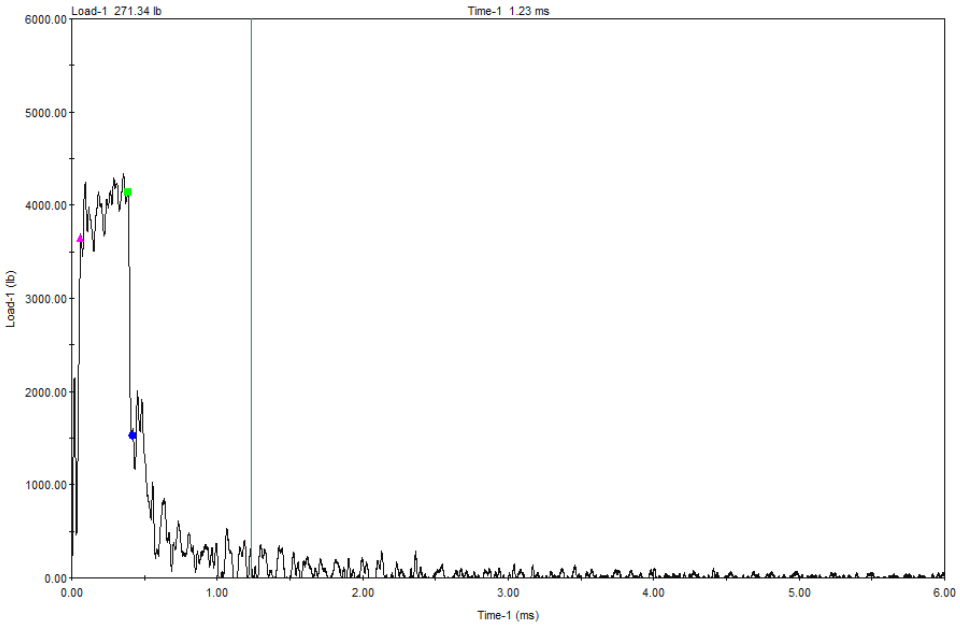

NH33: Tested at 25°F

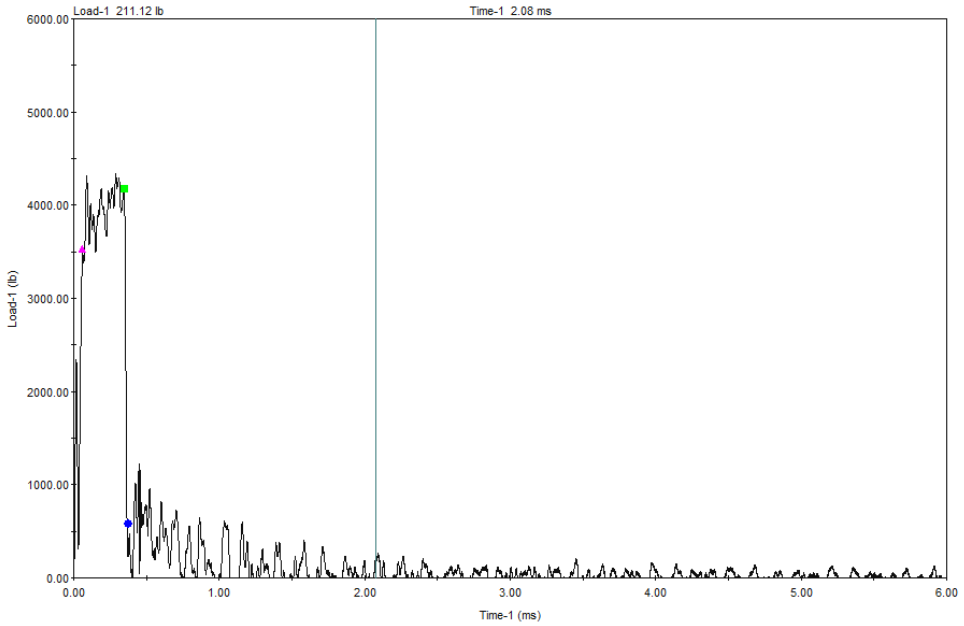

NH36: Tested at 30°F

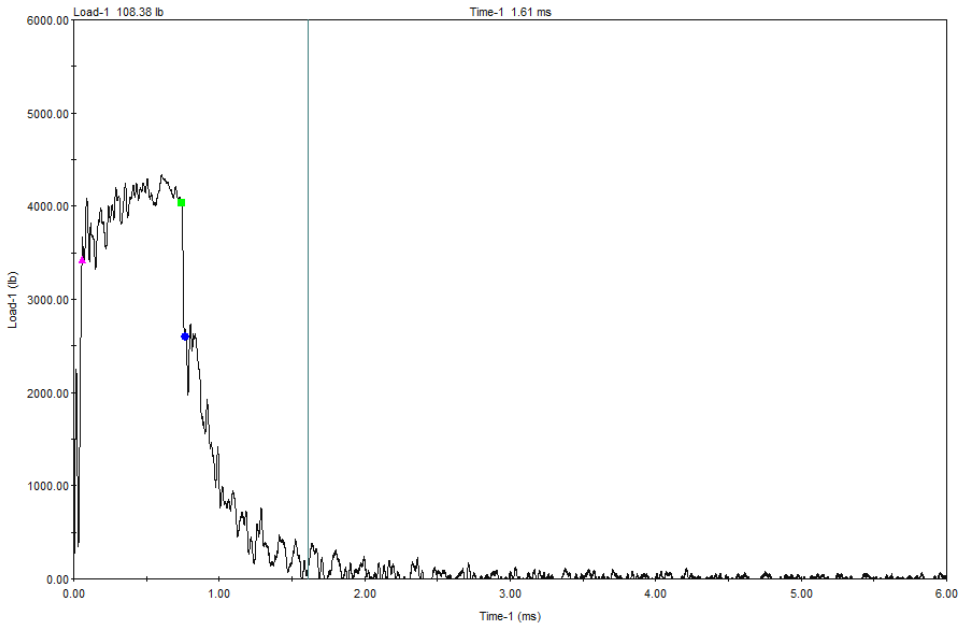

NH40: Tested at 60°F

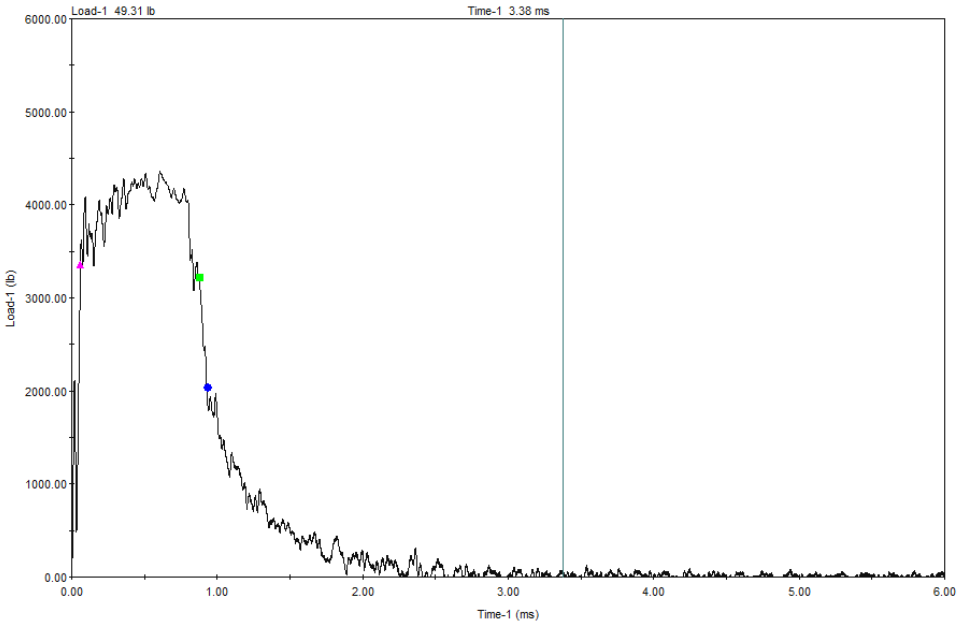

NH37: Tested at 90°F

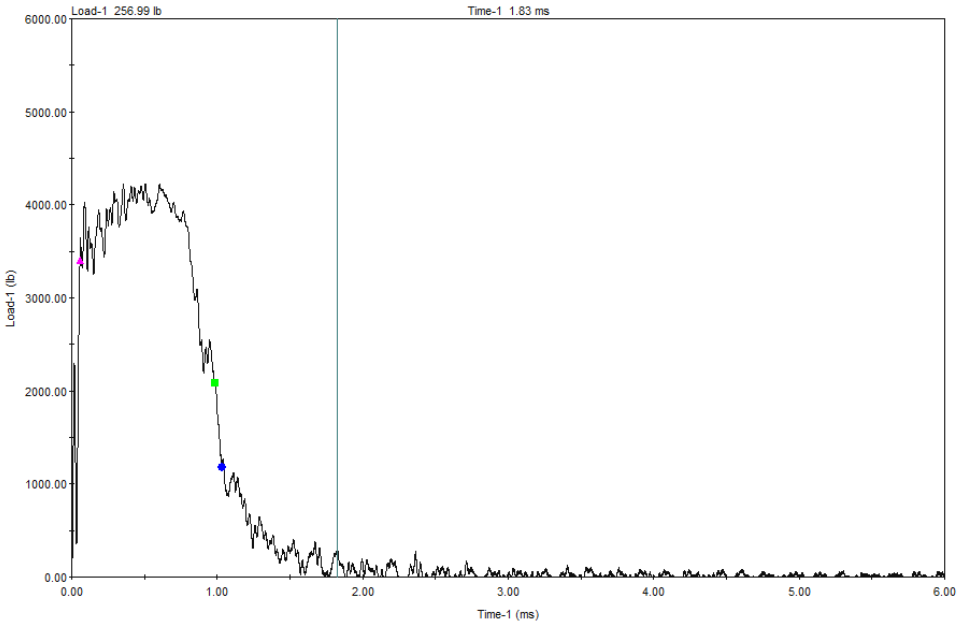

NH34: Tested at 120°F

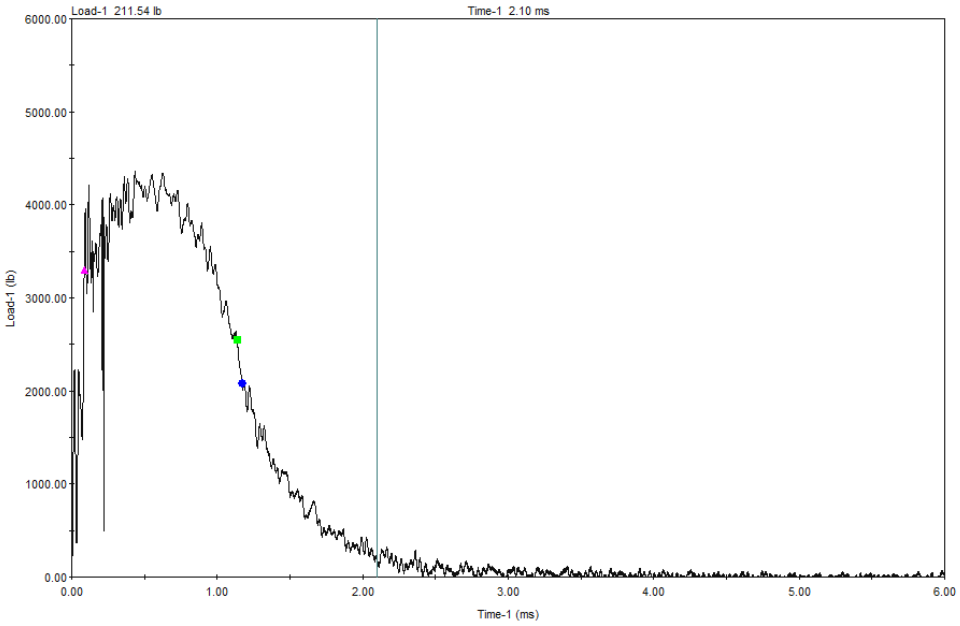

NH35: Tested at 175°F

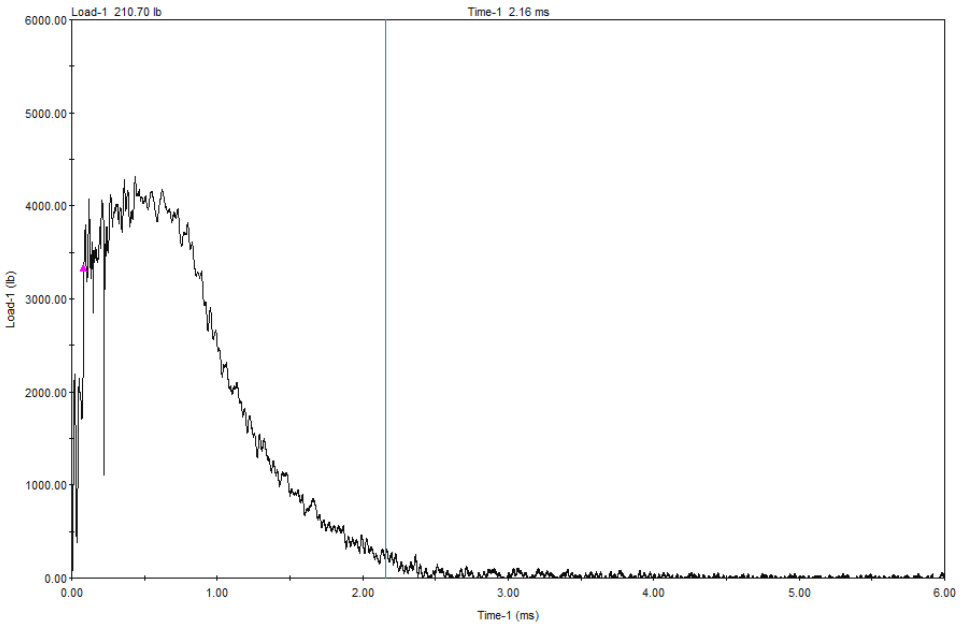

NH38: Tested at 275°F

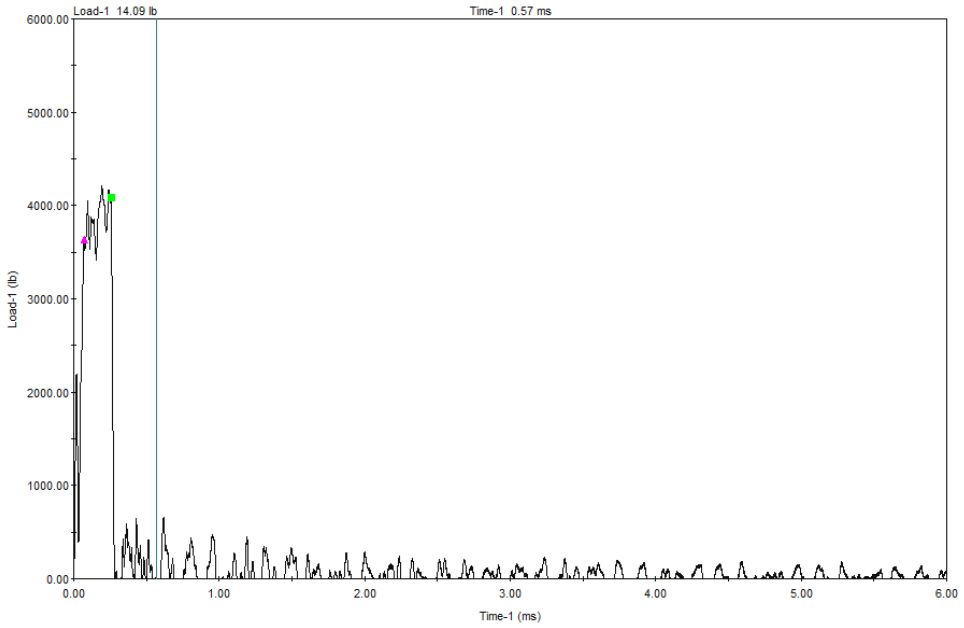

R37: Tested at 200°F

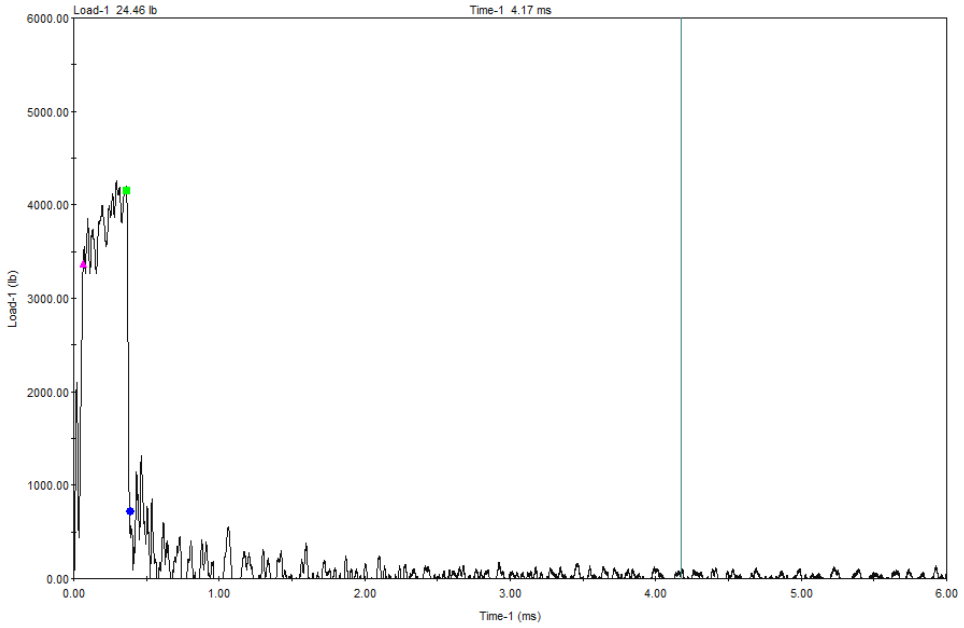

R35: Tested at 225°F

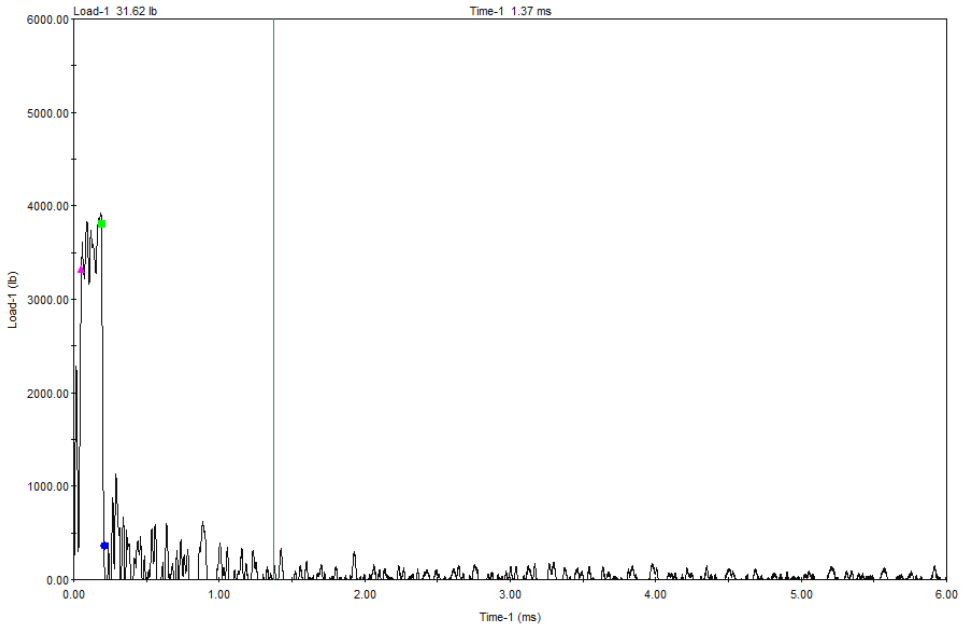

R34: Tested at 240°F

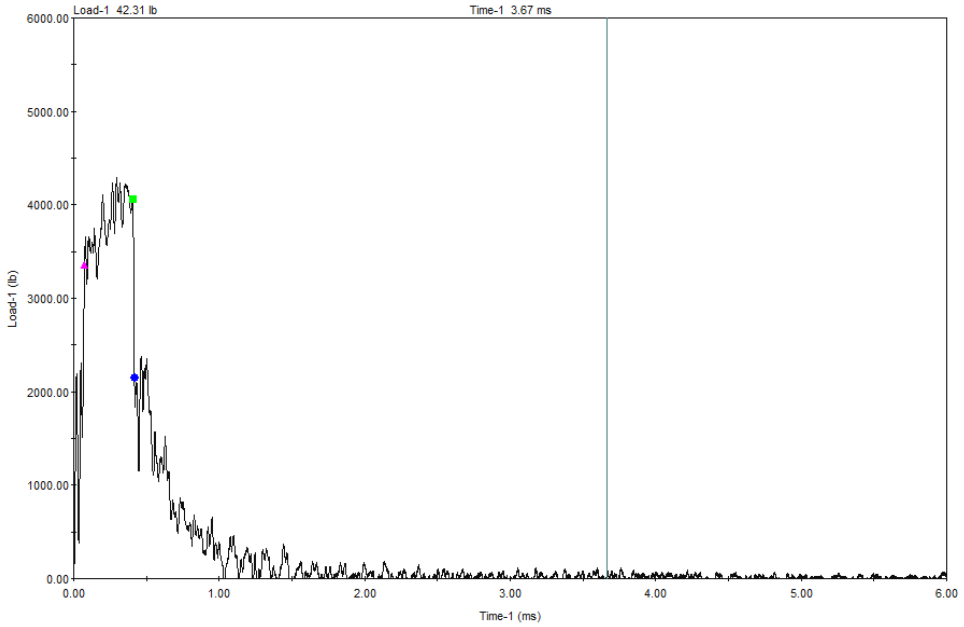

R33: Tested at 275°F

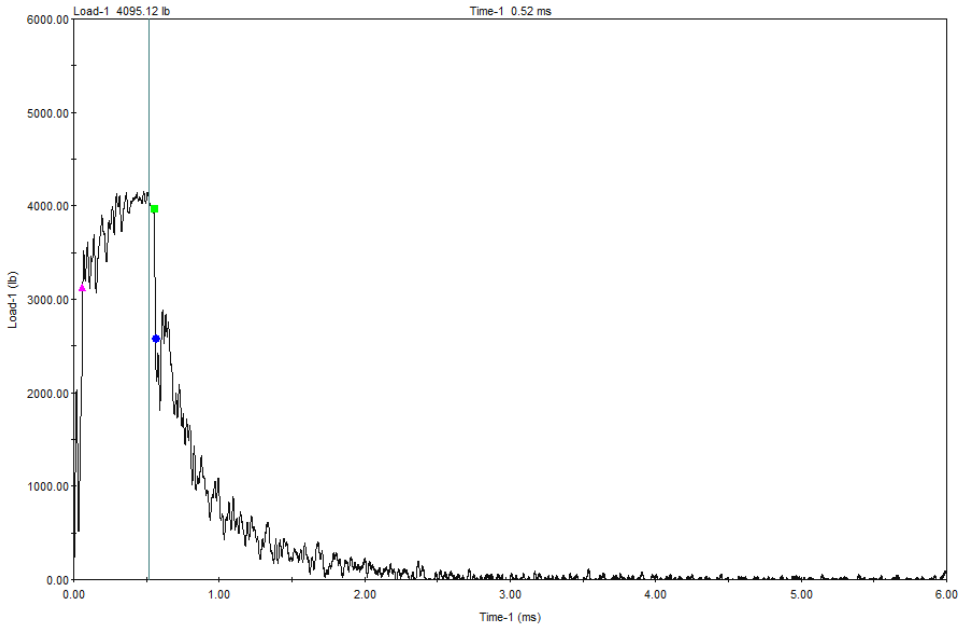

R36: Tested at 320°F

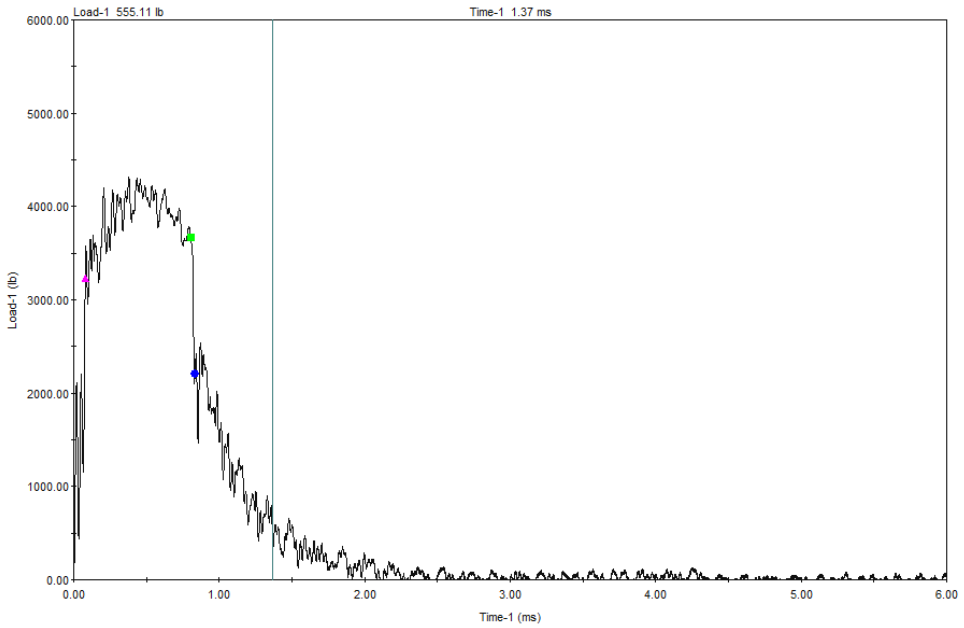

R38: Tested at 375°F

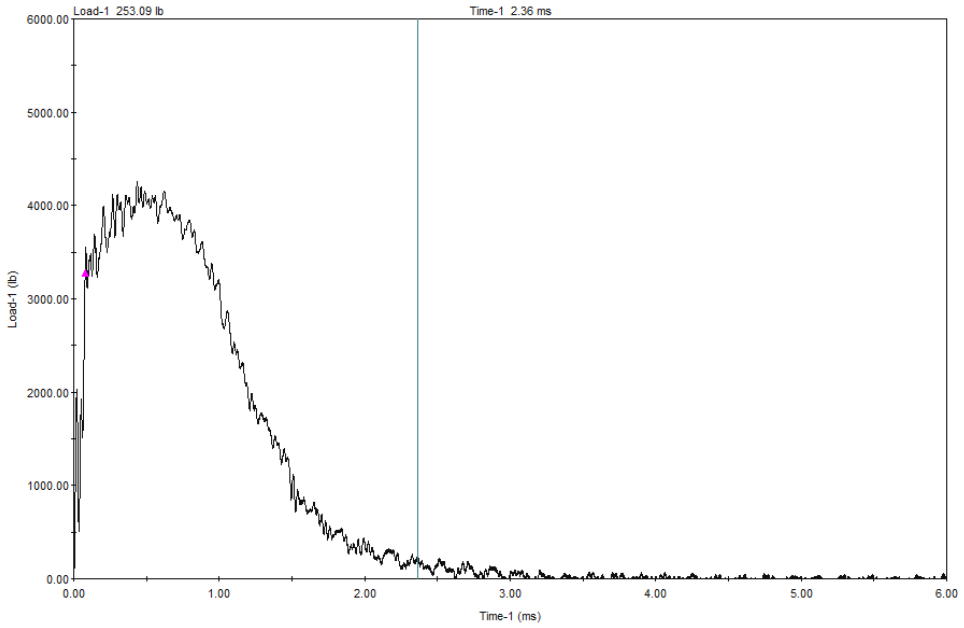

R39: Tested at 425°F

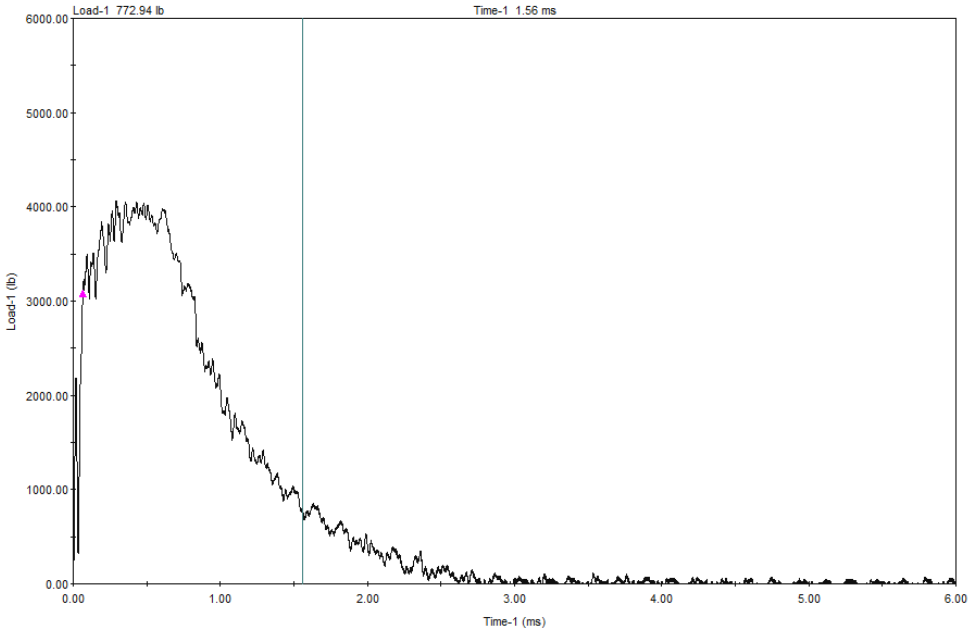

R40: Tested at 450°F